THE STEADY-STATE RESPONSE OF MULTIDEGREE-OF-FREEDOM SYSTEMS WITH A SPATIALLY LOCALIZED NONLINEARITY

Thesis by

Richard Keith Miller

In Partial Fulfillment of the Requirements

for the Degree of

Doctor of Philosophy

California Institute of Technology

Pasadena, California

1976

(Submitted on October 1, 1975)

ACKNOWLEDGMENTS

The author would like to express his gratitude to Professor W. D. Iwan for his invaluable guidance and encouragement throughout this investigation. The assistance of the Faculty of Applied Mechanics is also gratefully acknowledged.

The author would like to express his appreciation to the California Institute of Technology and the National Science Foundation for financial support during his years of graduate study. The partial support of this work under a grant from the National Science Foundation is also acknowledged.

Sincere thanks are due to Miss Sharon Vedrode for her patient and skillful typing of this manuscript.

The author also wishes to express his gratitude to his wife, Beth, for her warm encouragement and constant understanding and patience.

ABSTRACT

This thesis is concerned with the dynamic response of a general multidegree-of-freedom linear system with a one dimensional nonlinear constraint attached between two points. The nonlinear constraint is assumed to consist of rate-independent conservative and hysteretic nonlinearities and may contain a viscous dissipation element. The dynamic equations for general spatial and temporal load distributions are derived for both continuous and discrete systems. The method of equivalent linearization is used to develop equations which govern the approximate steady-state response to generally distributed loads with harmonic time dependence.

The qualitative response behavior of a class of undamped chainlike structures with a nonlinear terminal constraint is investigated. It is shown that the hardening or softening behavior of every resonance curve is similar and is determined by the properties of the constraint. Also examined are the number and location of resonance curves, the boundedness of the forced response, the loci of response extrema, and other characteristics of the response. Particular consideration is given to the dependence of the response characteristics on the properties of the linear system, the nonlinear constraint, and the load distribution.

Numerical examples of the approximate steady-state response of three structural systems are presented. These examples illustrate the application of the formulation and qualitative theory.

It is shown that disconnected response curves and response curves which cross are obtained for base excitation of a uniform shear beam with a cubic spring foundation. Disconnected response curves are also obtained for the steady-state response to a concentrated load of a chainlike structure with a hardening hysteretic constraint. The accuracy of the approximate response curves is investigated.

TABLE OF CONTENTS

Part	Title	Page
Acknowledgments		ii
Abstract		iii
Chapter I	Introduction	1
Chapter II	Formulation and Governing Equations	7
2.1	Formulation	7
2.2	Governing Dynamic Equations for General Excitation	9
2.2.1	Equations of Motion	9
2.2.2	Linear System Force Decomposition	10
2.2.3	Governing Equations	13
2.2.4	General Approach for Solution	15
2.3	Governing Dynamic Equations for Harmonic Excitation	15
2.3.1	General Remarks	15
2.3.2	Generalized Harmonic Excitation	17
2.3.3	Approximate Solution by Way of Equivalent Linearization	20
2.3.4	Assumed Behavior of the Nonlinear Structural Element	28
2.3.5	Governing Equations	30
Chapter III	Qualitative Harmonic Response Behavior of Systems with a Nonlinear Terminal Constraint	35
3.1	Introduction	35
3.2	Steady-State Equations	37
3.3	Qualitative Properties of Stiffness and Damping Functions	39

Part	Title	Page
3.3.1	General Remarks	39
3.3.2	Properties of C(A) and S(A)	39
3.3.3	General Properties of $\kappa_{jj}(\omega)$ and $\gamma_{jj}(\omega)$	42
3.3.4	Properties of $\kappa_{jj}(\omega)$ and $\gamma_{jj}(\omega)$ for Undamped Linear Chainlike Structures	46
3.3.5	Properties of $\kappa_{jj}(\omega)$ and $\gamma_{jj}(\omega)$ for Lightly Damped Linear Chainlike Structures	60
3.4	Qualitative Properties of Load Distribution Functions $p_2(\omega)$ and $q_2(\omega)$	66
3.4.1	General Properties of $p_2(\omega)$ and $q_2(\omega)$	66
3.4.2	$p_2(\omega)$ and $q_2(\omega)$ for a Single Concentrated Load Applied at Attachment Point P	70
3.4.3	Properties of $p_2(\omega)$ and $q_2(\omega)$ for Undamped Linear Chainlike Structures with Base Excitation	71
3.4.4	Properties of $p_2(\omega)$ and $q_2(\omega)$ for Lightly Damped Mass-Terminated Chainlike Structures with Base Excitation	76
3.5	Qualitative Harmonic Response Behavior	77
3.5.1	Free Oscillations of Conservative Systems	77
3.5.2	Forced Oscillations of Conservative Systems with a (Possibly) Dissipative Constraint	82
3.5.3	Forced Oscillations of Generally Dissipative Systems	100
Chapter IV	Numerical Examples of Harmonic Response of Systems with a Nonlinear Terminal Constraint	104
4.1	General Remarks	104
4.2	Steady-State Response to Harmonic Base Excitation of a Uniform Shear Beam with a Cubic Spring Terminal Constraint	105

Part	Title	Page
4.2.1	Application of General Formulation	105
4.2.2	Discussion of Free Oscillations	114
4.2.3	Discussion of Forced Oscillations without Viscous Dissipation	117
4.2.4	Discussion of Forced Oscillations with Viscous Dissipation	120
4.3	Steady-State Response to Harmonic Base Excitation of a Uniform Ten-Mass Chain-like Structure with a Bilinear Softening Terminal Constraint	126
4.3.1	Application of General Formulation	126
4.3.2	Discussion of Free Oscillations	133
4.3.3	Discussion of Forced Oscillations with Viscous Dissipation	134
4.4	Steady-State Response to a Harmonic Concentrated Load of a Uniform Ten-Mass Chainlike Structure with a Terminal Constraint Exhibiting a Form of Limited Slip	136
4.4.1	Application of General Formulation	136
4.4.2	Discussion of Backbone Curves	143
4.4.3	Discussion of Forced Oscillations without Viscous Dissipation	147
4.4.4	Discussion of Forced Oscillations with Viscous Dissipation	151
4.5	Comparison of Exact and Approximate Steady-State Solutions	152
4.5.1	Accuracy of the Approximate Solution for the Continuous System	152
4.5.2	Accuracy of the Approximate Solution for the Discrete System	154
Chapter V	Summary and Conclusions	156

Part	Title	Page
References		163
Appendix A	Transfer Function Characteristics of Undamped Linear Chainlike Structures	169

I. Introduction

In order to describe the response of structures to damaging excitations, consideration must be given to nonlinear structural behavior. Such nonlinear behavior occurs whenever stresses and deformations exceed the elastic limits of any member of the structural system. In the most general case, nonlinear structural behavior occurs simultaneously in many locations throughout the structure. However, in many important applications the nonlinear behavior occurs primarily at a single location, either by intentional design or prevailing circumstances.

Such spatially localized nonlinear behavior frequently occurs in those parts of the structure where sizable discontinuities exist in structural properties. For example, many existing multi-story buildings have a first story which is considerably more flexible than any of the upper stories. In such structures, the first story is typically left "open" (i.e., no shear walls are provided) in order to accommodate a ground-level parking facility or to provide additional window space for architectural reasons. Observations of the earthquake response of such buildings [1-4] clearly indicate that the nonlinear structural behavior occurs primarily in the first story. *An example of such behavior may be observed in Figure* 1.1. Other structures which display localized nonlinear response to strong shaking include many types of mechanical and electrical equipment which frequently sustain damage to structural mountings and isolation systems.

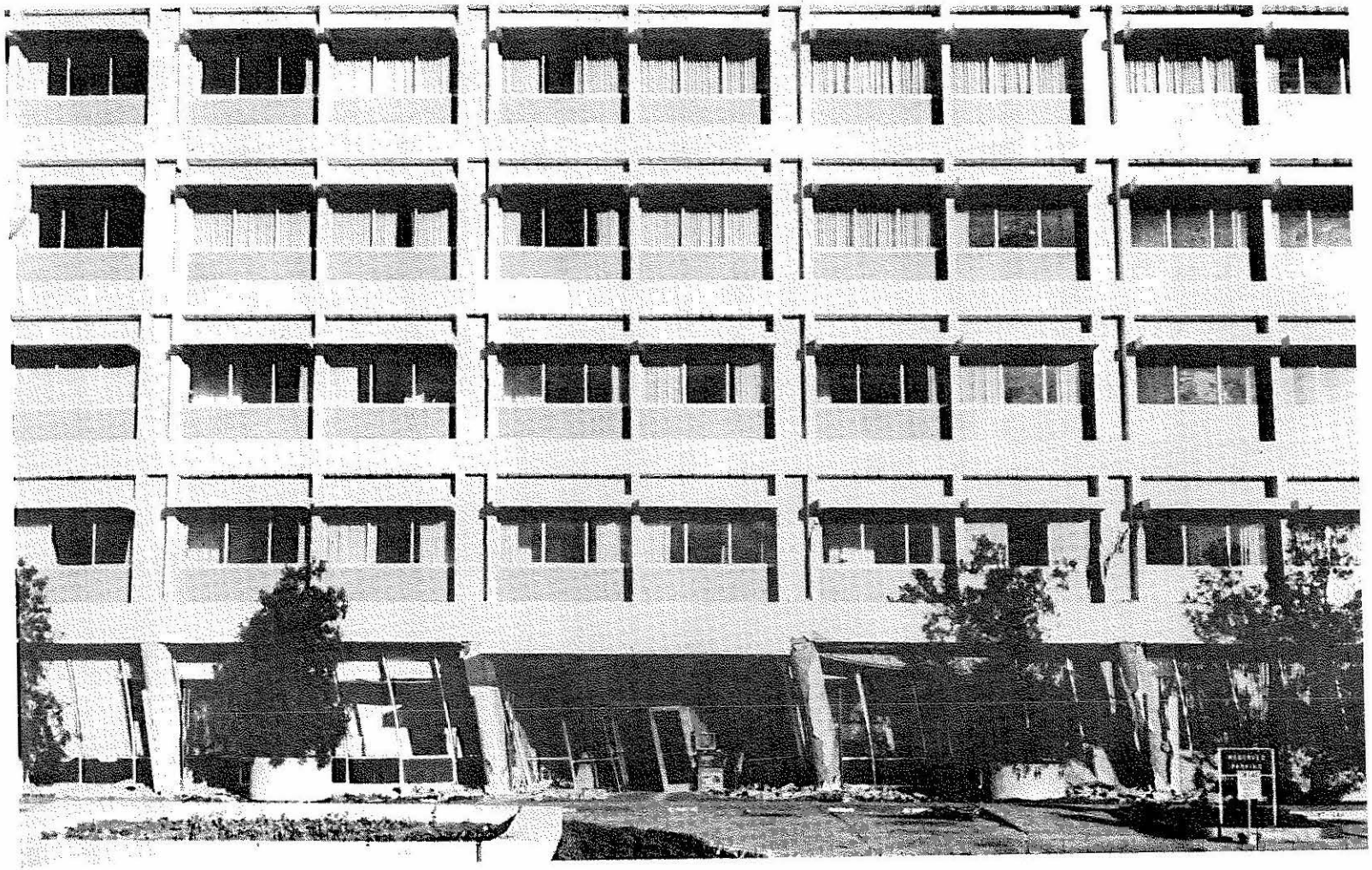

Fig. 1.1 Damage to the First Floor of the Olive View Medical Center after the San Fernando Earthquake of February 9, 1971 [5].

It has long been recognized that a degree of vibration isolation may be provided to a structure which is mounted on flexible supports. Clearly, such a concept forms the basis for the design of most vehicle suspension systems and vibration isolation systems. A proposal to mount an entire building on an intentionally flexible or "soft" first story has been discussed for many years [6-8] but has not received wide acceptance because of problems introduced by large relative story displacements [2, 18]. However, there have been many recent proposals [9-15] to substitute various nonlinear foundation systems for the soft first story in order to achieve a degree of earthquake protection. Such intentionally nonlinear foundations are currently used to control low-level vibrations of some full-scale buildings [16-17].

Recent attempts to predict the dynamic response of systems with a localized nonlinearity have employed numerical or simulation methods [18, 9, 11]. While such methods are very useful for providing detailed information on the response of a specific system to a specific excitation, they are not well suited to more general studies. Numerical methods also tend to be expensive, and as a result they frequently enter the design process only as a check on the final configuration.

Due to the complexities involved, analytical methods for determining the dynamic response of such systems have received much less attention. When applicable, such methods are far more useful for design and theoretical studies. They contribute to the general understanding of the behavior of many systems by providing

direct relationships between the observed response characteristics and the system properties which cause them. Such cause and effect relationships are of primary concern in this study, and consequently an analytical method is employed.

Among the existing analytical methods, none are found which directly apply to problems with transient excitation. The most widely used techniques apply to problems with steady-state harmonic and stationary stochastic excitation. Of these two classes of problems, those with steady-state harmonic excitation are by far the easiest to analyze and are considered in detail in this investigation.

The steady-state response of structures to harmonic excitation is of both direct and indirect importance. Such response is of obvious importance to problems which involve rotating machinery or other sources of steady harmonic excitation. However, it is also important for less obvious reasons to problems involving transient excitation. For instance, it has been observed that the displacement response of many large structures during earthquakes displays nearly harmonic behavior. Furthermore, knowledge of the large amplitude harmonic response is also sometimes used for estimating and interpreting the nonlinear transient response of structures. For instance, the object of many full-scale tests is to determine from harmonic response data the "effective" natural frequencies, damping ratios, and mode shapes for use in estimating the response to earthquake excitation. The concept of effective natural frequencies, damping ratios, and mode shapes has also been used by many

authors [19-26] to interpret the nonlinear response of structures to earthquake and other excitations.

The primary objective of this investigation is to analytically determine the characteristics of the steady-state harmonic response of a general class of systems with a spatially localized nonlinearity. Both the qualitative and quantitative properties of the response are investigated, with particular consideration given to cause and effect relationships which exist. It is intended that this study will provide a basis for further work which will contribute to a better general understanding of the dynamic response of multidegree-of-freedom nonlinear systems.

In Chapter II the dynamic response problem is formulated for a general linear system with a single nonlinear constraint attached between two arbitrarily chosen points. The dynamic equations for general spatial and temporal load distributions are developed. The approximate method of equivalent linearization is used to develop the governing dynamic equations for the steady-state harmonic response of systems with general hysteretic nonlinearities.

In Chapter III the qualitative harmonic response characteristics of linear chainlike systems with a nonlinear terminal constraint are examined in detail. Several theorems are presented which specify the dependence of certain response characteristics on the properties of the linear system, nonlinear constraint, and spatial load distribution. Consideration is given to the response of both conservative and dissipative systems to free and forced oscillations.

In Chapter IV numerical examples of the harmonic response of three different systems are analyzed. The examples include continuous and discrete linear systems, conservative, viscous, and hysteretic nonlinearities, and two load distributions, with primary consideration given to base excitation. A new model for "softening-hardening" hysteresis is presented. Consideration is also given to the accuracy of the approximate steady-state solutions.

II. Formulation and Governing Equations

2.1 Formulation

Depicted in Figure 2.1 is a general structural system with a spatially localized nonlinearity. The system is assembled from two distinct components: (1) an entirely linear structural system (indicated schematically as an irregularly shaped linear solid), and (2) a nonlinear structural element (indicated schematically as a nonlinear spring) which is attached to the linear system at the two points P and Q. The magnitude of relative displacement between these points, labeled "x", represents a measure of deformation in the nonlinear element. The generalized excitations $z_1, z_2, z_3, \ldots$ may represent any compatible combination of prescribed body forces, surface tractions, or displacements applied to the linear system either at discrete points or, in the case of continuous systems, distributed over any portion of the body.

The linear system may represent any continuous or discrete linear structural system for which the principle of superposition is applicable, and for which the standard convolution techniques may be applied. In particular, the linear system may be composed of lumped masses, springs, and dashpots, or it may contain continuous elements such as linear elastic or viscoelastic rods, beams, or plates.

Boundary conditions for the linear system may be provided by regarding the generalized excitations as being composed of two distinct sets. A set of active excitations, $\{z_1, z_2, z_3, \ldots\}$, composed of prescribed time-varying generalized forces and displacements,

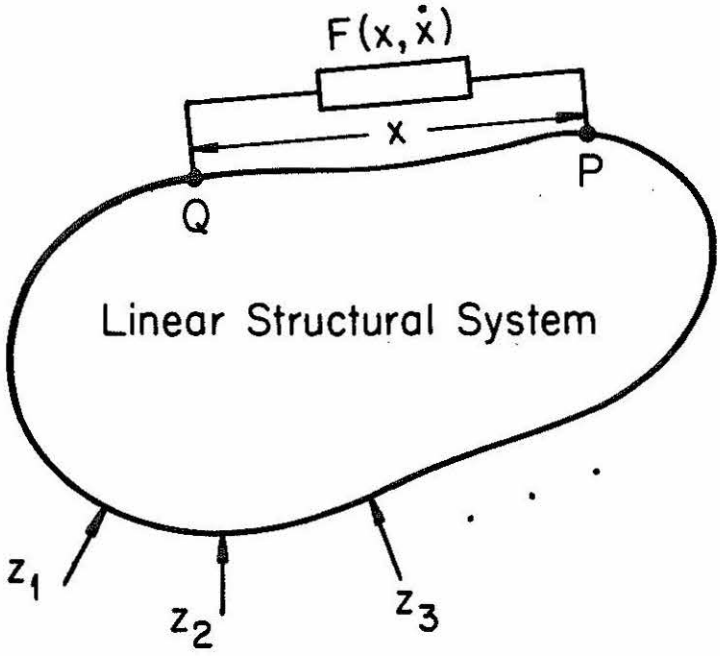

Figure 2.1 - Schematic of a Structural System with a Spatially Localized Nonlinearity

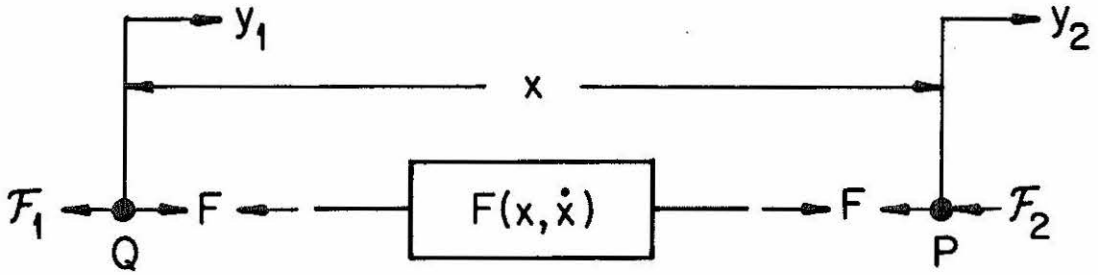

Figure 2.2 - Freebody Diagrams

provides forcing to the system. A set of "null excitations," $\{z_1^*, z_2^*, z_3^*, \ldots\}$, composed of prescribed null forces and displacements, formally provides the boundary conditions to the system. It will hereafter be assumed that the boundary conditions (or null excitations) and the details of the linear system are prescribed together in any given application (e.g., a cantilevered beam, a simply supported plate, etc.). Thus, consideration is given only to active excitations in the following analysis.

The nonlinear structural element may represent any massless, one-dimensional nonlinear structural assemblage whose restoring force magnitude, F, depends only on x and its time derivative $\dot{x}$, and satisfies certain broad assumptions. These assumptions, which are presented later in detail, permit the analysis of the most common engineering models for nonlinear structural behavior, including all rate-independent hysteretic and all conservative hardening and softening nonlinearities. Excluded from consideration are nonlinearities which provide stiffness degrading or other fatigue behavior, and those which contain explicit dependence on the rate $\dot{x}$ (except for a viscous damping term).

2.2 Governing Dynamic Equations for General Excitation

2.2.1 Equations of Motion

Let $\underline{e}$ be a unit vector directed along the line of action of the nonlinear restoring force for the system of Figure 2.1 in its initial state. Assume that displacements within the linear system remain sufficiently small during the ensuing dynamic response that $\underline{e}$ does

not change orientation. Then $\underline{e}$ becomes a convenient direction along which to measure the forces and displacements of the system.

Depicted in Figure 2.2 is a free body diagram of the attachment points P and Q, where all forces and displacements are in the $\underline{e}$ direction. Let y_1 represent the displacement of point Q and y_2 represent the displacement of point P in same direction, as shown. Then

$$x = y_2 - y_1 \tag{2.1}$$

Let $F(x, \dot{x})$ be the magnitude of the restoring force developed in the nonlinear element due to the deformation x. Let $\mathfrak{F}_1$ be the magnitude of the force developed in the linear system at Q due to the displacements y_1 and y_2, and the generalized excitations $z_1, z_2, z_3, \ldots$ Let $\mathfrak{F}_2$ be the magnitude of the similar force developed in the linear system at P. Balancing forces at points P and Q,

$$\left.\begin{aligned} \mathfrak{F}_1 &= F(x, \dot{x}) \\ \mathfrak{F}_2 &= -F(x, \dot{x}) \end{aligned}\right\} \tag{2.2}$$

2.2.2 Linear System Force Decomposition

Clearly by specifying y_1 and y_2, and the generalized excitations $z_1, z_2, z_3, \ldots$, all forces and displacements within the linear system, and in particular $\mathfrak{F}_1$ and $\mathfrak{F}_2$, are completely determined. In this sense, $\mathfrak{F}_1$ and $\mathfrak{F}_2$ may be considered functionally dependent upon y_1, y_2 and $z_1, z_2, z_3, \ldots$ Thus

$$\mathfrak{F}_i = \mathfrak{F}_i(y_1, y_2 ; z_1, z_2, z_3, \dots) ; \qquad i = 1, 2 \tag{2.3}$$

where $\mathfrak{F}_i(\cdot)$ may be interpreted as a linear integral-differential operator.

Applying the principle of superposition to the linear system, the force in equation (2.3) may be decomposed into three component forces as follows

$$\mathfrak{F}_i(y_1, y_2; z_1, z_2, z_3, \dots) = \mathfrak{F}_i(y_1, 0; 0, 0, 0, \dots) + \mathfrak{F}_i(0, y_2; 0, 0, 0, \dots) + \mathfrak{F}_i(0, 0; z_1, z_2, z_3, \dots); \quad i = 1, 2 \tag{2.4}$$

where, for instance

(1) $\mathfrak{F}_1(y_1, 0; 0, 0, 0, \dots)$ represents the magnitude of force developed in the linear system at Q in response to the prescribed displacement time-history y_1 applied at Q, while maintaining null displacements at P (i.e., P is rigidly constrained in the $\underline{e}$ direction) and null excitations $z_1, z_2, z_3, \dots$ (Note that if the generalized excitations involve prescribed displacements, the requirement that $z_1 = z_2 = \cdots = 0$ introduces additional fixity or displacement boundary conditions on the linear system.)

(2) $\mathfrak{F}_1(0, y_2; 0, 0, 0, \dots)$ represents the magnitude of force developed in the linear system at Q in response to the prescribed displacement time-history y_2 applied at P, while maintaining null displacement at Q (i.e., Q is rigidly constrained in the $\underline{e}$ direction), and null excitations $z_1, z_2, z_3, \dots$

(3) $\mathfrak{F}_1(0, 0; z_1, z_2, z_3, \ldots)$ represents the magnitude of force developed in the linear system at Q in response to the prescribed generalized excitations $z_1, z_2, z_3, \ldots$, while maintaining null displacements at both P and Q (i.e., both P and Q are rigidly constrained in the $\underline{e}$ direction).

Thus, the first two terms on the right in (2.4) represent "impedance-like" forces which may be determined directly from y_1 and y_2 and the details of the linear system, without regard to any particular arrangement of generalized excitations. The last term on the right in (2.4) represents an "excitation-like" force which is dependent upon the particular spatial distribution and time-history of the generalized excitations $z_1, z_2, z_3, \ldots$, but which is independent of the motions y_1 and y_2 at points P and Q.

To simplify the notation, consider the definitions

$$\left.\begin{aligned} \mathfrak{F}_{i1}(\cdot) &\equiv \mathfrak{F}_i(\cdot, 0; 0, 0, \ldots) \\ \mathfrak{F}_{i2}(\cdot) &\equiv \mathfrak{F}_i(0, \cdot; 0, 0, \ldots) \end{aligned} \right\} \quad ; \quad i = 1, 2 \qquad (2.5)$$

and noting that, for a given spatial distribution and time-history of excitations $z_1(t), z_2(t), z_3(t), \ldots$, the term $\mathfrak{F}_i(0, 0; z_1, z_2, z_3, \ldots)$ may be evaluated to obtain a known deterministic function of "t", consider the additional definition

$$f_{iEx}(t) \equiv \mathfrak{F}_i(0, 0; z_1(t), z_2(t), z_3(t), \ldots) \qquad (2.6)$$

Combining equations (2.2)-(2.6), the equations of force balance may now be written as follows

$$\left.\begin{aligned} \mathfrak{F}_{11}(y_1) + \mathfrak{F}_{12}(y_2) + f_{1Ex}(t) &= F(x,\dot{x}) \\ \mathfrak{F}_{21}(y_1) + \mathfrak{F}_{22}(y_2) + f_{2Ex}(t) &= -F(x,\dot{x}) \end{aligned}\right\} \quad (2.7)$$

Note from (2.1) that $y_2 = y_1 + x$. Thus, y_2 may be eliminated from (2.7) by another application of the principle of superposition

$$\mathfrak{F}_{ij}(u+v) = \mathfrak{F}_{ij}(u) + \mathfrak{F}_{ij}(v); \quad \forall\, u, v \qquad (2.8)$$

Equations (2.1), (2.7), and (2.8) may be used to obtain

$$\left.\begin{aligned} &\mathfrak{F}_{11}(y_1) + \mathfrak{F}_{12}(y_1) + \mathfrak{F}_{21}(y_1) + \mathfrak{F}_{22}(y_1) + \mathfrak{F}_{22}(x) + \mathfrak{F}_{12}(x) \\ &\qquad = -[f_{1Ex}(t) + f_{2Ex}(t)] \\ &\mathfrak{F}_{22}(y_1) - \mathfrak{F}_{11}(y_1) + \mathfrak{F}_{21}(y_1) - \mathfrak{F}_{12}(y_1) + \mathfrak{F}_{22}(x) - \mathfrak{F}_{12}(x) + 2F(x,\dot{x}) \\ &\qquad = [f_{1Ex}(t) - f_{2Ex}(t)] \end{aligned}\right\} \quad (2.9)$$

Applying the "general reciprocal relation for elastokinetics" [27] to the linear system, it can be shown that

$$\mathfrak{F}_{ij}(\cdot) = \mathfrak{F}_{ji}(\cdot); \quad \forall\, i \neq j \qquad (2.10)$$

2.2.3 Governing Equations

Combining equations (2.9) and (2.10), the governing equations for general excitation are found to be

$$\left.\begin{aligned} &\mathfrak{F}_{11}(y_1) + 2\mathfrak{F}_{12}(y_1) + \mathfrak{F}_{22}(y_1) = -[\mathfrak{F}_{22}(x) + \mathfrak{F}_{12}(x)] - [f_{1Ex}(t) + f_{2Ex}(t)] \\ &\mathfrak{F}_{22}(y_1) - \mathfrak{F}_{11}(y_1) + \mathfrak{F}_{22}(x) - \mathfrak{F}_{12}(x) + 2F(x,\dot{x}) = [f_{1Ex}(t) - f_{2Ex}(t)] \end{aligned}\right\} \quad (2.11)$$

Note that in any given application, equations (2.11) may represent two coupled integral-differential equations which govern x and y_1.

Two interesting observations may be made concerning (2.11). First, observe that since the $\mathfrak{F}_{ij}(\cdot)$ represent linear operators, the first of (2.11) is entirely linear. Thus, there exists some convolution representation of y_1 in terms of x and the known functions $f_{1Ex}(t)$ and $f_{2Ex}(t)$, and in principle y_1 may therefore be eliminated from the second of (2.11) to obtain a single nonlinear dynamic equation for x.

Secondly, if there exists symmetry in the linear system to the extent that

$$\mathfrak{F}_{11}(\cdot) = \mathfrak{F}_{22}(\cdot) \tag{2.12}$$

then from (2.11) the second equation uncouples from the first yielding a single nonlinear differential equation for x which is entirely independent of y_1. In such a case, it is found that the motion of the system is composed of two linearly independent contributions: one which represents "pure rigid body motion" of the nonlinear element, and one which represents "pure deformation" of the nonlinear element. These two component motions are excited independently by combinations of $f_{1Ex}(t)$ and $f_{2Ex}(t)$. For example, if (2.12) holds and if the load distributions and time-histories are such that

$$f_{1Ex}(t) = f_{2Ex}(t) ; \quad \forall\, t \tag{2.13}$$

then it can be shown that only pure rigid body motions of the nonlinear element are possible. Also, if (2.12) holds and if

$$f_{1Ex}(t) = -f_{2Ex}(t) ; \quad \forall\, t \tag{2.14}$$

then it can be shown that only pure deformations of the nonlinear element are possible.

2.2.4 General Approach for Solution

If (2.11) are solved for the time histories $x(t)$ and $y_1(t)$, then $y_2(t)$ may be determined from (2.1). With $y_1(t)$ and $y_2(t)$ both known, the problem of determining the detailed response of all points within the linear system becomes a straightforward application of the techniques of linear elastokinetics. Since this investigation is concerned primarily with the effects of the nonlinearity on the response, and since the techniques of linear elastokinetics for determining the response within the linear system are relatively well understood, consideration will hereafter be limited to determining the time-history $x(t)$ from (2.11).

2.3 Governing Dynamic Equations for Harmonic Excitation

2.3.1 General Remarks

The problem of determining the response of structures to harmonic excitation arises frequently in engineering applications. Most mechanical equipment involves rotating machinery which provides harmonic excitation of various amplitudes. Typical mechanically excited structures of engineering interest are structures and foundations which support large turbine power-generating units,

high-rise buildings which support large roof-mounted air conditioning units, and numerous stationary and portable mechanical units ranging from industrial plant installations to oil exploration equipment. In such systems, nonlinear structural elements are frequently mounted between the source of excitation and the supporting structure in a "vibration isolation system," whose function is to reduce the dynamic forces transmitted by the source.

Harmonic excitation (or near harmonic excitation) also occurs in nature in the form of resonant motion of various kinds. Engineering structures with this type of harmonic excitation include buildings and bridges excited by aero- and hydrodynamic vortex shedding, and structures mounted atop an oscillating massive substructure. In such situations, interest in nonlinear response arises because of the high amplitude forces and displacements which may occur.

Another motivation for studying the nonlinear harmonic response of structures is to gain insight into the response to more complicated earthquake and blast excitations. Such inherently transient and nonlinear response is of obvious engineering importance. However, as yet there exists no straightforward analytical method for interpreting and predicting the nonlinear earthquake response of multidegree-of-freedom structures. All practical analysis is currently accomplished by numerical techniques from which it is difficult to generalize. Considerable insight into such complex response is provided, however, by analytically determining the large-amplitude nonlinear response to harmonic excitation. From

the harmonic response, it is possible to determine the amplitude dependence of the effective natural frequencies, damping ratios, and mode shapes, all of which are parameters of known importance in the understanding of the earthquake response of linear structures. It is also possible to determine the dependence of the amplitude of response on the amplitude of excitation. Such information has been used by many authors [20-26,38,41] to interpret the response of both single- and multidegree-of-freedom nonlinear structures in terms of an "equivalent linear" system. Such practice has gained wide acceptance and is included in many textbooks on vibrations [42, 43]. Furthermore, it has been suggested that, for single-degree-of-freedom systems, such equivalent linear parameters may be used directly to obtain estimates of the earthquake response of the nonlinear system [19].

2.3.2 Generalized Harmonic Excitation

An important class of harmonic excitations is obtained when each of the generalized excitations $z_1(t), z_2(t), z_3(t), \ldots$ has the same harmonic time dependence, $z(t)$

$$z_i(t) = c_i\, z(t)\,; \qquad i = 1, 2, 3, \ldots \tag{2.15}$$

where $\{c_i;\ i = 1, 2, 3, \ldots\}$ is a set of real constants and $z(t)$ is harmonic in t with amplitude z_0 and circular frequency ω:

$$z(t) = z_0 \cos \omega t = z_0 \Re e\{e^{i\omega t}\} \tag{2.16}$$

Then clearly, recalling the definitions in (2.6) and using the properties of linear systems, there exists some transfer function relationship between $f_{jEx}(t)$ $(j = 1, 2)$ and $z(t)$. Thus, let $G_j(i\omega)$ $(j = 1, 2)$ be the complex frequency transfer function defined such that

$$f_{jEx}(t) = G_j(i\omega)z(t) ; \qquad z(t) \equiv e^{i\omega t} \tag{2.17}$$

From (2.17) and (2.6) it is seen that $G_j(i\omega)$ represents the steady-state force developed in the linear system at Q if $j = 1$ or at P if $j = 2$, in response to the generalized excitations with unit harmonic time dependence $e^{i\omega t}$, while maintaining null displacements at both P and Q. Thus, $G_1(i\omega)$ and $G_2(i\omega)$ may both be obtained by solving a single problem in linear elastokinetics using standard techniques for linear systems.

In order to express the relationship (2.17) in a form more convenient for later application, consider the definitions

$$f_{jEx}(t) = p_j(\omega)z(t) + q_j(\omega)\dot{z}(t) ; \qquad z(t) = e^{i\omega t} \tag{2.18}$$

where $p_j(\omega)$ and $q_j(\omega)$ $(j = 1, 2)$ are real valued transfer functions and where it is noted that $\dot{z}(t) = i\omega z(t)$. It is easily shown that (2.18) remains valid for all harmonic $z(t)$ given by (2.16) and that $p_j(\omega)$, $q_j(\omega)$, and $G_j(i\omega)$ are related as follows

$$\left.\begin{aligned} p_j(\omega) &= \Re e\{G_j(i\omega)\} \\ q_j(\omega) &= \frac{1}{\omega}\,\Im m\{G_j(i\omega)\} \end{aligned}\right\} \tag{2.19}$$

Returning to the governing equations (2.11), it is seen that the two forcing terms are linear combinations of $f_{1Ex}(t)$ and $f_{2Ex}(t)$. Therefore, assuming that $z(t)$ is given by (2.16), consider defining $v(\omega)$, $u(\omega)$, $\psi(\omega)$, and $\phi(\omega)$ for convenience such that

$$\left.\begin{aligned} [f_{1Ex}(t) - f_{2Ex}(t)] &= v(\omega)\cos[\omega t - \psi(\omega)] \\ -[f_{1Ex}(t) + f_{2Ex}(t)] &= u(\omega)\cos[\omega t - \psi(\omega) - \phi(\omega)] \end{aligned}\right\} \quad (2.20)$$

Thus, $v(\omega)$ represents the amplitude of the forcing term in the second of (2.11) with $\psi(\omega)$ representing the phase lag relative to $z(t)$, while $u(\omega)$ represents the amplitude of the forcing term in the first of (2.11) with $\phi(\omega)$ representing the phase lag relative to the first term in (2.20).

Then $v(\omega)$, $u(\omega)$, $\psi(\omega)$, and $\phi(\omega)$ are related to $p_1(\omega)$, $q_1(\omega)$, $p_2(\omega)$, $q_2(\omega)$, and the amplitude of generalized excitations, z_0, as follows

$$\left.\begin{aligned} v(\omega) &= z_0\{[p_1(\omega) - p_2(\omega)]^2 + \omega^2[q_1(\omega) - q_2(\omega)]^2\}^{\frac{1}{2}} \\ u(\omega) &= z_0\{[p_1(\omega) + p_2(\omega)]^2 + \omega^2[q_1(\omega) + q_2(\omega)]^2\}^{\frac{1}{2}} \\ \psi(\omega) &= \tan^{-1}\left\{\frac{-\omega[q_1(\omega) - q_2(\omega)]}{[p_1(\omega) - p_2(\omega)]}\right\} \\ \phi(\omega) &= \tan^{-1}\left\{\frac{2\omega[q_1(\omega)p_2(\omega) - q_2(\omega)p_1(\omega)]}{[p_1^2(\omega) - p_2^2(\omega)] + \omega^2[q_1^2(\omega) - q_2^2(\omega)]}\right\} \end{aligned}\right\} \quad (2.21)$$

Substituting (2.20) into (2.11) one finds that the governing equations for the general harmonic response are given by

$$\left.\begin{aligned} &\mathfrak{F}_{11}(y_1) + 2\mathfrak{F}_{12}(y_1) + \mathfrak{F}_{22}(y_1) \\ &\qquad = -[\mathfrak{F}_{22}(x) + \mathfrak{F}_{12}(x)] + u(\omega)\cos[\omega t - \psi(\omega) - \phi(\omega)] \\ &\mathfrak{F}_{22}(y_1) - \mathfrak{F}_{11}(y_1) + \mathfrak{F}_{22}(x) - \mathfrak{F}_{12}(x) + 2F(x,\dot{x}) = v(\omega)\cos[\omega t - \psi(\omega)] \end{aligned}\right\} \quad (2.22)$$

Since steady-state solutions to (2.22) are of primary concern, only relative measures of time and phase are of importance. Therefore, it will be convenient to shift t in (2.22) such that $t \rightarrow t - \psi(\omega)/\omega$. Then (2.16) becomes

$$z(t) = z_0 \cos[\omega t - \psi(\omega)] = z_0 \Re e\left\{e^{i[\omega t - \psi(\omega)]}\right\} \quad (2.23)$$

and (2.22) becomes

$$\left.\begin{aligned} &\mathfrak{F}_{11}(y_1) + 2\mathfrak{F}_{12}(y_1) + \mathfrak{F}_{22}(y_1) \\ &\qquad = -[\mathfrak{F}_{22}(x) + \mathfrak{F}_{12}(x)] + u(\omega)\cos[\omega t - \phi(\omega)] \\ &\mathfrak{F}_{22}(y_1) - \mathfrak{F}_{11}(y_1) + \mathfrak{F}_{22}(x) - \mathfrak{F}_{12}(x) + 2F(x,\dot{x}) = v(\omega)\cos(\omega t) \end{aligned}\right\} \quad (2.24)$$

2.3.3 Approximate Solution by Way of Equivalent Linearization

It is desired to determine the steady-state periodic solutions of the two coupled nonlinear dynamic equations given in (2.24). Such steady-state solutions correspond to steady, forced oscillations of the class of systems shown schematically in Figure 2.1.

In all but the simplest of applications, the linear operators $\mathfrak{F}_{ij}(\cdot)$ and the nonlinear restoring force $F(x,\dot{x})$ take on a sufficiently complex form that, using known techniques, no exact analytical solutions of (2.24) are obtainable. All "exact" solutions must

currently be found by numerically solving the initial value problem obtained by specifying appropriate initial conditions with (2.24). Since steady-state periodic solutions are desired, such techniques are usually very expensive, making a complete study of the response of many systems impractical.

Therefore, one must resort to approximate analytical techniques for most applications. Besides reducing the expense incurred in obtaining a solution, such techniques have the added advantage that, by expressing the solution in an analytic form, the qualitative dependence of the solution upon various properties of the linear system and the nonlinear restoring force may be studied directly, without actually solving any equations. Such qualitative information is particularly useful in understanding the nature of response of an entire class of systems, for both design and theoretical purposes, and is the primary concern of the following chapter.

There exist several approximate analytical techniques which may be applied to (2.24). One of the oldest of these techniques is the perturbation method. Although numerous variations exist, the method is based on the classical perturbation theory of Poincaré [28]. Since this method is not designed to accommodate hysteretic nonlinearities, it is not suitable for the purposes of this investigation.

Other techniques which have been well developed for single-degree-of-freedom systems are the method of slowly varying parameters [29] and the general asymptotic method [30]. These techniques are applicable to systems with hysteretic nonlinearities,

and they are capable of determining the stability and transient behavior, as well as the steady-state response. However, these techniques contain an inherent dependence on the form of the governing differential equations and have been developed for general application to single-degree-of-freedom systems only. Although it is generally possible (depending upon the complexity of the linear operators $\mathfrak{F}_{ij}(\cdot)$, which may involve partial and integral equations) to extend these techniques for application to (2.24), the required modifications will depend on the particular form of the operators $\mathfrak{F}_{ij}(\cdot)$ for any given system. Thus, these techniques are not suitable for the general study of the steady-state harmonic response of all systems governed by dynamic equations of the general form of (2.24).

The techniques of equivalent linearization [31], harmonic balance and energy balance [32] each are applicable to systems with hysteretic nonlinearities. Furthermore, they are all based on averaging methods which are not dependent on the detailed form of the governing dynamic equations. Hence, any of these techniques are suitable for direct application to (2.24). Of these three techniques, the method of equivalent linearization offers the advantages of being directly applicable to the problem of determining the stationary stochastic response. Although such response is not considered in this investigation, the method of equivalent linearization will be used in order to facilitate the future investigation of such response.

With the choice of an approximate method for the solution of (2.24), consideration of the accuracy of the approximate solution is of primary importance. Unfortunately, there currently are no methods for analytically generating useful bounds on the error in the approximate solutions generated by any of the previously mentioned techniques. The problem of determining such bounds has been considered [33, 34], but there is much need for work in this area. Thus, in any given application, the accuracy of the approximate analytical solution must in general be inferred by comparison with a few "exact" numerical solutions. While this appears to be a major disadvantage to the use of such techniques, it has been found in many applications [35-40] that the approximate solutions generated by any of the last five methods are usually quite accurate, even for relatively large excitations of highly nonlinear systems. It is found that the error in the approximate solution generally increases with increasing levels of nonlinearity in the restoring force, and that it varies with the type and nature of the nonlinearity, but that errors less than 1-3 percent are typical, and rarely does the error exceed 12-15 percent for problems of engineering interest. However, most of the checks on the accuracy of such approximate solutions have been carried out for single-degree-of-freedom systems. Therefore, it is one of the goals of this investigation to determine, within practical limitations, the accuracy of the approximate solution for several multidegree-of-freedom nonlinear systems.

In the method of equivalent linearization [31], the nonlinear dynamic equations are replaced with a set of equivalent linear dynamic equations which are then solved by standard techniques. The equivalent linear equations are obtained from the nonlinear equations by replacing each nonlinear term with an equivalent linear term in such a way that the average of the difference between the linear and nonlinear equations is minimized. This minimization takes place over the class of solutions to the linear equations, and generally results in equivalent linear parameters which are dependent upon the solution. Thus, the solution is usually obtained in the form of a transcendental algebraic equation which must be solved iteratively.

Application of this technique to equations (2.24) begins by defining the equivalent linear dynamic equations. Replacing the nonlinear restoring force $F(x, \dot{x})$ by the linear restoring force $kx + c\dot{x}$, one obtains

$$\left.\begin{aligned} &\mathfrak{F}_{11}(y_1) + 2\mathfrak{F}_{12}(y_1) + \mathfrak{F}_{22}(y_1) \\ &\qquad = -[\mathfrak{F}_{22}(x) + \mathfrak{F}_{12}(x)] + u(\omega)\cos[\omega t - \phi(\omega)] \\ &\mathfrak{F}_{22}(y_1) - \mathfrak{F}_{11}(y_1) + \mathfrak{F}_{22}(x) - \mathfrak{F}_{12}(x) + 2(kx + c\dot{x}) = v(\omega)\cos(\omega t) \end{aligned}\right\} \quad (2.25)$$

In order to minimize the mean square equation difference between (2.24) and (2.25), the linear parameters k and c must be chosen such that

$$\left.\begin{aligned} k &= \frac{A[x \cdot F(x,\dot{x})]}{A[x^2]} \\ c &= \frac{A[\dot{x} \cdot F(x,\dot{x})]}{A[\dot{x}^2]} \end{aligned}\right\} \quad (2.26)$$

where $A[\cdot]$ is an appropriate averaging operator defined for all $x, \dot{x}$ within the class of solutions to the linear equations (2.25).

By well known properties of linear systems, all steady-state solutions of (2.25) are harmonic with frequency ω. Hence, let

$$x = A \cos(\omega t - \varphi) \equiv A \cos\theta \quad (2.27)$$

so that

$$\dot{x} = -\omega A \sin(\omega t - \varphi) \equiv -\omega A \sin\theta \quad (2.28)$$

Note that x and $\dot{x}$ are periodic in θ with period 2π. Thus, an appropriate averaging function for use in (2.26) is

$$A[\cdot] \equiv \frac{1}{2\pi}\int_0^{2\pi} (\cdot)\,d\theta \quad (2.29)$$

Substituting (2.27)-(2.29) into (2.26) one finds

$$\left.\begin{aligned} k &= \frac{C(A)}{A} \\ c &= -\frac{S(A)}{\omega A} \end{aligned}\right\} \quad (2.30)$$

where

$$\left.\begin{aligned} C(A) &\equiv \frac{1}{\pi}\int_0^{2\pi} F(A\cos\theta, -\omega A\sin\theta)\cos\theta\, d\theta \\ S(A) &\equiv \frac{1}{\pi}\int_0^{2\pi} F(A\cos\theta, -\omega A\sin\theta)\sin\theta\, d\theta \end{aligned}\right\} \quad (2.31)$$

Thus, the linear parameters k and c are dependent on the unknown approximate solution x, as expected.

Now that the equivalent linear system has been defined, it is appropriate to consider in detail the behavior of the linear operators $\mathfrak{F}_{jk}(\cdot)$ for harmonic arguments. Again using well-known properties of linear systems, there exists some transfer function relationship between each $\mathfrak{F}_{jk}(\cdot)$ and its harmonic argument. Thus, let $H_{jk}(i\omega)$ $(j, k = 1, 2)$ be the complex frequency transfer function defined such that

$$\mathfrak{F}_{jk}[r(t)] = H_{jk}(i\omega)r(t)\,; \qquad r(t) \equiv e^{i\omega t} \quad (2.32)$$

Therefore, recalling the discussion in Section 2.2.2, $H_{11}(i\omega)$ $[H_{22}(i\omega)]$ represents the magnitude of the steady-state force developed in the linear system at Q (at P) in response to the prescribed displacement time-history $e^{i\omega t}$ applied at Q (at P), while maintaining null displacements at P (at Q). Similarly, $H_{12}(i\omega)$ [which equals $H_{21}(i\omega)$ by the reciprocal theorem for elastokinetics] represents the magnitude of the steady-state force developed at Q in response to the prescribed displacement time-history $e^{i\omega t}$

applied at P, while maintaining null displacements at Q (or vice versa).

In order to express the relationship (2.32) in a form more convenient for application, consider the definitions

$$\mathfrak{F}_{jk}[r(t)] = \varkappa_{jk}(\omega)r(t) + \gamma_{jk}(\omega)\dot{r}(t) ; \qquad r(t) = e^{i\omega t} \tag{2.33}$$

where $\varkappa_{jk}(\omega)$ and $\gamma_{jk}(\omega)$ (j, k = 1, 2) are real-valued transfer functions. It is easily shown that (2.33) remains valid for all harmonic r(t) with arbitrary amplitude and phase and that $\varkappa_{jk}(\omega)$, $\gamma_{jk}(\omega)$ and $H_{jk}(\omega)$ are related as follows

$$\left.\begin{aligned} \varkappa_{jk}(\omega) &= \Re e\{H_{jk}(i\omega)\} \\ \gamma_{jk}(\omega) &= \frac{1}{\omega}\,\Im m\{H_{jk}(i\omega)\} \end{aligned}\right\} \tag{2.34}$$

Thus, substituting equations (2.30) and (2.33) into (2.25), the following equations are found to govern the approximate steady-state solution

$$\left.\begin{aligned} &[\varkappa_{11}(\omega)+2\varkappa_{12}(\omega)+\varkappa_{22}(\omega)]y_1 + [\gamma_{11}(\omega)+2\gamma_{12}(\omega)+\gamma_{22}(\omega)]\dot{y}_1 \\ &\quad = -[\varkappa_{22}(\omega)+\varkappa_{12}(\omega)]x - [\gamma_{22}(\omega)+\gamma_{12}(\omega)]\dot{x} + u(\omega)\cos[\omega t - \phi(\omega)] \\ &[\varkappa_{22}(\omega)-\varkappa_{11}(\omega)]y_1 + [\gamma_{22}(\omega)-\gamma_{11}(\omega)]\dot{y}_1 + [\varkappa_{22}(\omega)-\varkappa_{12}(\omega)]x \\ &\quad + [\gamma_{22}(\omega)-\gamma_{12}(\omega)]\dot{x} + 2\,\frac{C(A)}{A}x - 2\,\frac{S(A)}{\omega A}\dot{x} = v(\omega)\cos(\omega t) \end{aligned}\right\} \tag{2.35}$$

where x and y_1 are harmonic, with x given in (2.27).

2.3.4 Assumed Behavior of the Nonlinear Structural Element

Before attempting to obtain solutions to (2.35), it is appropriate to consider conditions on the behavior of the nonlinear restoring force under which steady-state solutions are plausible.

In any structure experiencing periodic motion, the time-histories of all displacements and forces must, by definition, exhibit periodic behavior. Therefore, the dynamic force-displacement relationship for each element of the system (obtained simply by plotting the force time-history as a function of the displacement time-history, with time as a parameter) must exhibit some steady-state configuration which does not change from cycle to cycle. It is this steady-state configuration which determines C(A) and S(A) in equations (2.31).

Not all nonlinearities produce steady-state force-displacement configurations, and therefore must be eliminated from consideration. For example, nonlinearities which model cyclic structural deterioration or other fatigue-like behavior fall under this category and are not considered further. It is observed that, for such nonlinearities, $F(x, \dot{x})$ is not periodic even though x is periodic. Thus, in this case, the definitions of C(A) and S(A) in (2.31) are not defined.

For yielding structural elements, the steady-state configurations are commonly called "hysteresis loops" and are frequently determined experimentally. Often such empirical information must be used in place of an accurate analytical representation for $F(x, \dot{x})$ in practical applications. It is observed, however, that such

information is suitable for the determination of C(A) and S(A) in (2.31) so that analysis of such practical systems causes no unusual difficulty.

There exists a wide variety of possible steady-state configurations, or hysteresis loops, which may be produced by structural nonlinearities. Such configurations may or may not be single-valued, they are usually symmetric about the origin, and are at least piecewise continuous. It will be convenient for later reference to make several formal assumptions on the behavior of the steady-state force-displacement configuration. For example, most experimentally determined hysteresis loops for real structures are found to be independent of the cyclic rate of stress reversal. The following assumption formally limits consideration of nonlinearities to those which display this rate-independence.

Assumption 1 (A1): (Rate-Independent Hysteresis)

It is assumed that the nonlinear restoring force, $F(x, \dot{x})$, produces only steady-state force-displacement configurations which are independent of the cyclic rate of stress reversal.

(Assumption 1 notwithstanding, consideration is later given to nonlinearities which contain rate dependence in the form of a viscous dissipation term.)

Most of the commonly used analytical models for nonlinear structural behavior (e.g., bilinear hysteresis, Ramberg-Osgood models, distributed element models, etc.) produce hysteresis loops which are uniquely determined by the amplitude of deformation, A.

Assumption 2 limits consideration to such nonlinearities, and in so doing eliminates models which display "stiffness degrading" characteristics [44].

Assumption 2 (A2): (Uniqueness of Amplitude Dependence)

It is assumed that the nonlinear restoring force, $F(x, \dot{x})$, produces only steady-state force-displacement configurations which are uniquely dependent on the amplitude of deformation.

Finally, it is found that most nonlinear structural models produce hysteresis loops which display a continuous dependence on changes in the amplitude of deformation. Assumption 3 limits consideration to such nonlinearities.

Assumption 3 (A3): (Continuity of Amplitude Dependence)

It is assumed that the nonlinear restoring force, $F(x, \dot{x})$, produces only steady-state force-displacement configurations with the property that small variations in the amplitude of deformation cause at most correspondingly small variations in the steady-state force-displacement configuration.

More detailed consideration of the properties of the nonlinear restoring force is presented later as it is needed in the analysis.

2.3.5 Governing Equations

Returning to equations (2.35), it is noted that the first equation contains no dependence on the unknown solution. Therefore, y_1 may be determined explicitly as a function of x and the forcing term. Specifically, y_1 may be expressed as

$$y_1(t) = \alpha_1(\omega)x(t) + \alpha_2(\omega)\dot{x}(t) + \beta_1(\omega)\tilde{u}(\omega, t) + \beta_2(\omega)\dot{\tilde{u}}(\omega, t) \qquad (2.36)$$

where

$$\tilde{u}(\omega, t) \equiv u(\omega) \cos [\omega t - \phi(\omega)] \qquad (2.37)$$

Substituting (2.36), (2.37) into (2.35), the following relations for $\alpha_i(\omega)$, $\beta_i(\omega)$ in terms of the $\kappa_{ij}(\omega)$, $\gamma_{ij}(\omega)$ are found [where, for brevity, the abbreviations $\kappa_{ij} \equiv \kappa_{ij}(\omega)$ and $\gamma_{ij} \equiv \gamma_{ij}(\omega)$ are used]

$$\left.\begin{aligned}
\alpha_1(\omega) &= \frac{-[(\kappa_{22}+\kappa_{12})(\kappa_{11}+2\kappa_{12}+\kappa_{22}) + \omega^2(\gamma_{22}+\gamma_{12})(\gamma_{11}+2\gamma_{12}+\gamma_{22})]}{(\kappa_{11}+2\kappa_{12}+\kappa_{22})^2 + \omega^2(\gamma_{11}+2\gamma_{12}+\gamma_{22})^2} \\
\alpha_2(\omega) &= \frac{(\kappa_{22}+\kappa_{12})(\gamma_{11}+2\gamma_{12}+\gamma_{22}) - (\gamma_{22}+\gamma_{12})(\kappa_{11}+2\kappa_{12}+\kappa_{22})}{(\kappa_{11}+2\kappa_{12}+\kappa_{22})^2 + \omega^2(\gamma_{11}+2\gamma_{12}+\gamma_{22})^2} \\
\beta_1(\omega) &= \frac{(\kappa_{11}+2\kappa_{12}+\kappa_{22})}{(\kappa_{11}+2\kappa_{12}+\kappa_{22})^2 + \omega^2(\gamma_{11}+2\gamma_{12}+\gamma_{22})^2} \\
\beta_2(\omega) &= \frac{-(\gamma_{11}+2\gamma_{12}+\gamma_{22})}{(\kappa_{11}+2\kappa_{12}+\kappa_{22})^2 + \omega^2(\gamma_{11}+2\gamma_{12}+\gamma_{22})^2}
\end{aligned}\right\} \qquad (2.38)$$

Let

$$\left.\begin{aligned}
K(\omega) &\equiv \kappa_{22}(\omega) - \kappa_{11}(\omega) \\
\overline{K}(\omega) &\equiv \kappa_{22}(\omega) - \kappa_{12}(\omega) \\
\Gamma(\omega) &\equiv \gamma_{22}(\omega) - \gamma_{11}(\omega) \\
\overline{\Gamma}(\omega) &\equiv \gamma_{22}(\omega) - \gamma_{12}(\omega)
\end{aligned}\right\} \qquad (2.39)$$

Substituting (2.36), (2.37), and (2.39) into the second of (2.35), one obtains the following single equation in x

$$\left.\begin{aligned}
&\left[\overline{K}(\omega) + \alpha_1(\omega)K(\omega) - \omega^2\alpha_2(\omega)\Gamma(\omega) + 2\frac{C(A)}{A}\right]x \\
&\quad + \left[\alpha_2(\omega)K(\omega) + \overline{\Gamma}(\omega) + \alpha_1(\omega)\Gamma(\omega) - 2\frac{S(A)}{\omega A}\right]\dot{x} \\
&\quad = \{v(\omega) - u(\omega)[\beta_1(\omega)K(\omega) - \omega^2\beta_2(\omega)\Gamma(\omega)]\cos\phi(\omega) \\
&\quad - \omega u(\omega)[\beta_2(\omega)K(\omega) + \beta_1(\omega)\Gamma(\omega)]\sin\phi(\omega)\}\cos\omega t \\
&\quad + \{\omega u(\omega)[\beta_2(\omega)K(\omega) + \beta_1(\omega)\Gamma(\omega)]\cos\phi(\omega) \\
&\quad - u(\omega)[\beta_1(\omega)K(\omega) - \omega^2\beta_2(\omega)\Gamma(\omega)]\sin\phi(\omega)\}\sin\omega t
\end{aligned}\right\} \quad (2.40)$$

Substituting from (2.27) and (2.28) for x and $\dot{x}$ into (2.40), the following pair of equations in the amplitude, A, and the phase, φ, are obtained:

$$\left.\begin{aligned}
&A\cos\varphi\left[\overline{K}(\omega) + \alpha_1(\omega)K(\omega) - \omega^2\alpha_2(\omega)\Gamma(\omega) + 2\frac{C(A)}{A}\right] \\
&\quad + \omega A\sin\varphi\left[\alpha_2(\omega)K(\omega) + \overline{\Gamma}(\omega) + \alpha_1(\omega)\Gamma(\omega) - 2\frac{S(A)}{\omega A}\right] \\
&\quad = \{v(\omega) - u(\omega)[\beta_1(\omega)K(\omega) - \omega^2\beta_2(\omega)\Gamma(\omega)]\cos\phi(\omega) \\
&\quad - \omega u(\omega)[\beta_2(\omega)K(\omega) + \beta_1(\omega)\Gamma(\omega)]\sin\phi(\omega)\}
\end{aligned}\right\} \quad (2.41)$$

$$
\left.
\begin{aligned}
&A \sin\varphi \left[\overline{K}(\omega) + \alpha_1(\omega)K(\omega) - \omega^2\alpha_2(\omega)\Gamma(\omega) + 2\frac{C(A)}{A}\right] \\
&\quad - \omega A \cos\varphi\left[\alpha_2(\omega)K(\omega) + \overline{\Gamma}(\omega) + \alpha_1(\omega)\Gamma(\omega) - 2\frac{S(A)}{\omega A}\right] \\
&\quad = \{\omega u(\omega)[\beta_2(\omega)K(\omega) + \beta_1(\omega)\Gamma(\omega)]\cos\Phi(\omega) \\
&\quad - u(\omega)[\beta_1(\omega)K(\omega) - \omega^2\beta_2(\omega)\Gamma(\omega)]\sin\Phi(\omega)\}
\end{aligned}
\right\} \quad (2.41 \text{ cont.})
$$

Finally, squaring and adding the two equations in (2.41), one obtains the following nonlinear algebraic equation which governs the approximate amplitude-frequency behavior of forced oscillations of general systems with a spatially localized nonlinearity

$$
\left.
\begin{aligned}
&A^2\left[\overline{K}(\omega) + \alpha_1(\omega)K(\omega) - \omega^2\alpha_2(\omega)\Gamma(\omega) + 2\frac{C(A)}{A}\right]^2 \\
&\quad + \omega^2A^2\left[\alpha_2(\omega)K(\omega) + \overline{\Gamma}(\omega) + \alpha_1(\omega)\Gamma(\omega) - 2\frac{S(A)}{\omega A}\right]^2 \\
&\quad = \{v(\omega) - u(\omega)[\beta_1(\omega)K(\omega) - \omega^2\beta_2(\omega)\Gamma(\omega)]\cos\Phi(\omega) \\
&\quad - \omega u(\omega)[\beta_2(\omega)K(\omega) + \beta_1(\omega)\Gamma(\omega)]\sin\Phi(\omega)\}^2 \\
&\quad + \{\omega u(\omega)[\beta_2(\omega)K(\omega) + \beta_1(\omega)\Gamma(\omega)]\cos\Phi(\omega) \\
&\quad - u(\omega)[\beta_1(\omega)K(\omega) - \omega^2\beta_2(\omega)\Gamma(\omega)]\sin\Phi(\omega)\}^2
\end{aligned}
\right\} \quad (2.42)
$$

Thus, for purposes of determining the steady-state response, the effect of the linear system enters only through its transfer functions $\kappa_{ij}(\omega)$ and $\gamma_{ij}(\omega)$, the effect of the load distribution enters only through the transfer functions $p_i(\omega)$ and $q_i(\omega)$, and the effect

of the localized nonlinearity enters only through the functions C(A) and S(A).

It is interesting to compare (2.42) with the analogous equation for a single-degree-of-freedom nonlinear oscillator (a special case of the system analyzed herein). Let the equation of motion for such an oscillator be

$$\ddot{x} + 2\zeta\omega_n\dot{x} + \omega_n^2 x + F(x,\dot{x}) = r\cos(\omega t) \qquad (2.43)$$

Then, applying the method of equivalent linearization to (2.43), and using the definitions in (2.27) and (2.31), the steady-state amplitude-frequency equation is found to be

$$A^2\left[\omega_n^2 - \omega^2 + \frac{C(A)}{A}\right]^2 + \omega^2 A^2\left[2\zeta\omega_n - \frac{S(A)}{\omega A}\right]^2 = r^2 \qquad (2.44)$$

Hence, comparing (2.42) with (2.44), it is seen that the basic form of the equations is the same, with the addition of several frequency-dependent terms to each side of (2.44) being the apparent effect of the multidegree-of-freedom system and the spatially distributed loading. This similarity in basic form is capitalized upon in the following chapter to produce some interesting general statements about the response of an important subclass of systems.

III. Qualitative Harmonic Response Behavior of Systems with a Nonlinear Terminal Constraint

3.1 Introduction

Systems with nonlinear terminal constraints are frequently encountered in engineering applications in such areas as vibration isolation, vehicle suspensions, and various rotating machinery problems. The terminal constraint may be intentionally nonlinear to achieve some desired performance, such as the limiting of motion or force in the case of vibration control systems, or it may become nonlinear due to localized large deformations and forces as a result of a particular system configuration. Frequently these localized nonlinearities occur at the attachment points or supports of the system. The dynamic response of such systems has been studied by various authors [9, 18, 45-50], but only in reference to specific applications.

Interest in harmonic response arises frequently when rotating machinery is present, or when forcing is provided by harmonic motion of the supports due, for instance, to resonant motion of a massive substructure. Previous work on harmonic response has concentrated on continuous beams with a supporting cubic spring [45-48]. In an effort to better understand the harmonic response of more general linear structures with a broad class of nonlinear constraints, the qualitative steady-state response behavior of the entire class of systems represented in Fig. 3.1 is investigated in this chapter. Specifically, general theorems are developed which, for certain structures and load distributions, allow the frequency

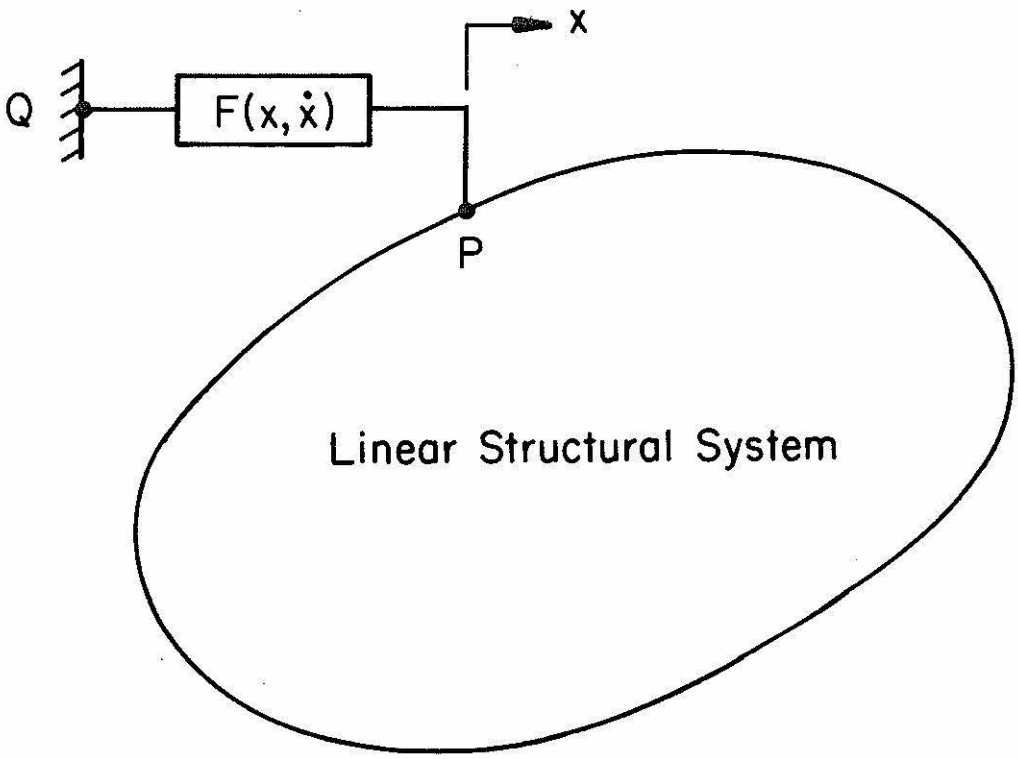

Figure 3.1 - Schematic of a System with a Nonlinear Terminal Constraint

response curve to be sketched qualitatively, without actually solving the governing nonlinear algebraic equation. The effects of rate-independent hysteresis are included, as well as the qualitative effects of viscous damping.

A system with a nonlinear terminal constraint is obtained from the formulation of Chapter II by requiring that $y_1 \equiv 0$. The resulting system, shown schematically in Fig. 3.1, forms the basis for the analysis in this chapter.

3.2 Steady-State Equations

In order that $y_1 = 0$ at all excitation frequencies, let $\varkappa_{11}(\omega) \to \infty$ for all ω. Such would be the case if within the linear system there existed an infinite lumped mass at attachment point Q of Fig. 2.1. Thus, from equations (2.38), (2.39) for large $\varkappa_{11}(\omega)$ one finds

$$\left.\begin{aligned} \alpha_1(\omega) &\sim \frac{-[\varkappa_{22}(\omega) + \varkappa_{12}(\omega)]}{\varkappa_{11}(\omega)} \quad ; \qquad \alpha_2(\omega) \sim \frac{-[\gamma_{22}(\omega) + \gamma_{12}(\omega)]}{\varkappa_{11}(\omega)} \\ \beta_1(\omega) &\sim \frac{1}{\varkappa_{11}(\omega)} \quad ; \qquad \beta_2(\omega) \sim \frac{-[\gamma_{11}(\omega) + 2\gamma_{12}(\omega) + \gamma_{22}(\omega)]}{\varkappa_{11}^2(\omega)} \\ K(\omega) &\sim -\varkappa_{11}(\omega) \end{aligned}\right\} \quad (3.1)$$

Substituting (3.1) into (2.42) and using (2.21) to simplify the result leads to

$$\left[\frac{C(A)}{A} + \varkappa_{22}(\omega)\right]^2 + \omega^2\left[\gamma_{22}(\omega) - \frac{S(A)}{\omega A}\right]^2 = [p_2^2(\omega) + \omega^2 q_2^2(\omega)]\left(\frac{z_0}{A}\right)^2 \qquad (3.2)$$

For the case in which the linear system is a simple rigid body of mass M, it is easily shown that

$$\varkappa_{22}(\omega) = -M\omega^2 ; \quad \gamma_{22}(\omega) = 0 ; \quad p_2^2(\omega) + \omega^2 q_2^2(\omega) = 1$$

in which case (3.2) reduces to

$$\left[\frac{C(A)}{A} - M\omega^2\right]^2 + \omega^2\left[\frac{S(A)}{A\omega}\right]^2 = \left(\frac{z_0}{A}\right)^2$$

which is analogous to the frequency equation of a nonlinear single degree of freedom oscillator, as reported by Iwan [50].

Solving equation (3.2) for $\varkappa_{22}(\omega)$, one obtains

$$-\varkappa_{22}(\omega) = \frac{C(A)}{A} \pm \frac{1}{A}\sqrt{[p_2^2(\omega) + \omega^2 q_2^2(\omega)]z_0^2 - [\omega\gamma_{22}(\omega)A - S(A)]^2} \quad (3.3)$$

Equation (3.3) is the amplitude-frequency equation for a general linear system with a nonlinear terminal constraint, as shown in Fig. 3.1. Note that the effect of the passive linear system is completely specified by $\varkappa_{22}(\omega)$ and $\gamma_{22}(\omega)$, the previously defined effective stiffness and damping frequency transfer functions. The effect of the loading distribution is specified by $p_2(\omega)$ and $q_2(\omega)$, the previously defined frequency dependent load distribution functions. The effect of the nonlinear constraint is specified by the C(A) and S(A) functions, which are related by their definitions to the equivalent linear stiffness and damping, respectively [52]. Recall that the constant z_0 represents the amplitude of generalized harmonic excitation.

3.3 Qualitative Properties of Stiffness and Damping Functions

3.3.1 General Remarks

The purpose of the remainder of this chapter is to determine the qualitative behavior of the steady-state response $A(\omega)$ as determined by equation (3.3). Clearly the details of $A(\omega)$ depend on the qualitative behavior of the stiffness and damping functions C(A), S(A), $\kappa_{22}(\omega)$ and $\gamma_{22}(\omega)$, as well as the load distribution functions $p_2(\omega)$ and $q_2(\omega)$. Thus, consideration is given here to the qualitative behavior of the stiffness and damping functions for structural systems, while in Section 3.4 consideration is given to the qualitative behavior of the load distribution functions.

In order to maximize the generality of nonlinear restoring force for which the results apply, very few restrictions on C(A) and S(A) are imposed. These restrictions affect only sign definiteness, continuity and limiting behavior as $A \to 0$. However, in order to make specific statements about the behavior of $A(\omega)$, consideration of linear systems is restricted to a class of one-dimensional shear structures. In particular, the detailed behavior of $\kappa_{22}(\omega)$ and $\gamma_{22}(\omega)$ for a class of linear chainlike structures is investigated.

3.3.2 Properties of C(A) and S(A)

From their definitions in equations (2.31), it is observed that C(A) and S(A) are weighted integrals of $F(x, \dot{x})$ for a harmonic function having amplitude A and frequency ω. The integration ranges over a complete cycle of the steady-state configuration in the x, F

plane, so that the configuration corresponding to amplitude A is used to evaluate C(A) and S(A).

By assumption (A1), the steady-state configuration in the x, F plane is independent of the rate at which a cycle is traversed, and therefore is independent of ω. Hence, C(A) and S(A) are indeed functions of A only, even though ω appears in the second argument of F in each of the integrands of equations (2.31).

By assumption (A2), the steady-state configurations in the x, F plane are uniquely dependent upon A. Thus, C(A) and S(A) are single-valued functions of A.

By assumption (A3), a small variation in amplitude A produces at most a correspondingly small variation in the steady-state configuration. This is interpreted here to mean that the average of the ascending and descending branches of, and the area enclosed by, the steady-state configuration are both continuous functions of A. It can be shown [53] that S(A) is proportional to the enclosed area and that C(A) is a weighted integral of the average of ascending and descending branches over one cycle. Therefore, C(A) and S(A) are both continuous functions of A.

Assumption 4 (A4): (Infinitesimal Elasticity)

Consideration of nonlinearities $F(x, \dot{x})$ will be limited to include only those for which S(0) = 0. Such will be the case if $F(x, \dot{x})$ is elastic for infinitesimal deformations x.

Assumption 5 (A5): (Passivity of the Nonlinear Restoring Force)

The additional restriction is introduced here that $F(x, \dot{x})$ is

capable only of dissipating a finite amount of energy per cycle of oscillation when driven in the steady-state at finite amplitude and frequency.

Thus, if E_F is the energy dissipated by $F(x, \dot{x})$ per cycle of oscillation

$$E_F \geq 0 \tag{3.4}$$

Under the assumption of harmonic displacement $x = A\cos(\omega t)$, it can be shown, using (2.31), that

$$E_F = -\pi A S(A) \tag{3.5}$$

Thus, (3.4) and (3.5) require that

$$S(A) \leq 0 \ \forall \ A \geq 0 \tag{3.6}$$

In summary, the following properties are assumed to hold throughout the remainder of this thesis:

(1) C(A) and S(A) are single-valued, real continuous functions of A

(2) $S(A) \leq 0 \ \forall \ A \geq 0$

(3) $S(0) = 0$.

It should be noted here that if a viscous damping term $c\dot{x}$ is added to the nonlinear restoring force, the only resulting modification is that a frequency dependent term $-\omega cA$ must be added to S(A) in the above development.

3.3.3 General Properties of $\kappa_{jj}(\omega)$ and $\gamma_{jj}(\omega)$

Recall from equation (2.33) that $\kappa_{jj}(\omega)$ and $\gamma_{jj}(\omega)$ are the effective stiffness and damping of the restoring force produced by the passive linear system when excited at attachment point P by a harmonic displacement of frequency ω. Since the system which generates the restoring force is linear, it follows that $\kappa_{jj}(\omega)$ and $\gamma_{jj}(\omega)$ are single-valued functions of ω.

Assumption 6 (A6):

$\kappa_{jj}(\omega)$ and $\gamma_{jj}(\omega)$ are at least piecewise continuous functions of ω.

Most linear systems of engineering interest satisfy assumption (A6), as will be discussed later in this section. In addition, it can be shown that $\kappa_{jj}(\omega)$ and $\gamma_{jj}(\omega)$ are even functions of ω, using their definitions in terms of $H_{jj}(i\omega)$ in equation (2.34), and noting that $H_{jj}(i\omega)$ represents the Fourier transform of the impulse response of the linear system, which is always a real-valued function of time for physical systems.

Assumption 7 (A7): (Passivity of the Linear System)

The restoring force $\mathfrak{F}_{jj}(x)$ is capable only of dissipating finite energy per cycle of oscillation when driven in the steady state at finite amplitude and frequency.

Thus, if $E_{\mathfrak{F}}$ is the energy dissipated by $\mathfrak{F}_{jj}(x)$ per cycle of oscillation, it is required that

$$E_{\mathfrak{F}} \geq 0 \qquad (3.7)$$

Using (2.33) for $x = A\cos(\omega t)$, it can be shown that

$$E_{\mathcal{F}} = \pi \omega \gamma_{jj}(\omega) A^2 \tag{3.8}$$

Thus, (3.7) and (3.8) together require that

$$\gamma_{jj}(\omega) \geq 0 \ \forall \ \omega \geq 0 \tag{3.9}$$

Definition 1 (D1): (Nondissipative Linear Systems)

All linear systems for which $\gamma_{jj}(\omega) \equiv 0 \ \forall \ \omega$ are said to be nondissipative.

Definition 2 (D2): (Strictly Dissipative Linear Systems)

All linear systems for which $\gamma_{jj}(\omega) > 0 \ \forall \ \omega$ are said to be strictly dissipative.

Note that all undamped linear systems are nondissipative, while all real structural systems are strictly dissipative.

Summarizing the general properties of $\kappa_{jj}(\omega)$ and $\gamma_{jj}(\omega)$ which will henceforth be assumed:

(1) $\kappa_{jj}(\omega)$ and $\gamma_{jj}(\omega)$ are real, single-valued, and at least piecewise continuous functions of ω

(2) $\kappa_{jj}(\omega)$ and $\gamma_{jj}(\omega)$ are even functions of ω

(3) $\gamma_{jj}(\omega) \geq 0 \ \forall \ \omega$

Definition 3 (D3): [Zeros of $H_{jj}(i\omega)$]

The set of all frequencies $\{\omega_{zk} \mid k = 1, 2, \ldots\}$ such that $|H_{jj}(i\omega_{zk})| = 0$ for nontrivial displacements y_j is defined as the set of zeros of $H_{jj}(i\omega)$.

Definition 4 (D4): [Poles of $H_{jj}(i\omega)$]

The set of all frequencies $\{\omega_{pk} | k = 1, 2, \ldots\}$ such that $|H_{jj}(i\omega_{pk})|$ is unbounded for bounded y_j is defined as the set poles of $H_{jj}(i\omega)$.

Definition 5 (D5): (Unconstrained Linear System)

The linear system obtained by setting to zero all generalized excitations and by requiring that attachment point P (see Fig. 3.1) be force-free is defined as the unconstrained linear system.

Definition 6 (D6): (Rigidly Constrained Linear System)

The linear system obtained by setting to zero all generalized excitations and by requiring that attachment point P be fixed against motion is defined as the rigidly constrained linear system.

Note from equation (2.32) that the zeros of $H_{jj}(i\omega)$ must correspond to the frequencies of free vibration of the unconstrained linear system. Note similarly that the poles of $H_{jj}(i\omega)$ must correspond to frequencies of free vibration of the rigidly constrained linear system.

Since free vibrations cannot exist at any frequency for strictly dissipative linear systems, the complex frequency transfer function for such systems can have no real poles or zeros. Therefore, $\kappa_{jj}(\omega)$ and $\gamma_{jj}(\omega)$ are bounded for all frequencies, and do not simultaneously vanish for such systems.

Since $\gamma_{jj}(\omega) = 0 \; \forall \; \omega$ for all nondissipative linear systems, the poles and zeros of $H_{jj}(i\omega)$ and $\kappa_{jj}(\omega)$ are identical for this case.

Form of $\kappa_{jj}(\omega)$ and $\gamma_{jj}(\omega)$ for Continuous and Discrete Linear Systems

The dynamic behavior of the most general continuous (distributed parameter) linear system is determined by a general linear partial differential operator involving several spatial variables and time, and containing time and spatially dependent coefficients. For such general systems, it is not generally possible to obtain a closed form analytic representation for the transfer function $H_{jj}(i\omega)$. In fact, if the system is unbounded in at least one spatial variable, or if the operator contains cross derivatives involving both space and time, then it is possible that, in addition to poles, $H_{jj}(i\omega$ will contain essential singularities in the finite $i\omega$ plane. Thus, for general continuous linear systems, very little can be said about the general form of $H_{jj}(i\omega)$, and hence also $\kappa_{jj}(\omega)$ and $\gamma_{jj}(\omega)$.

However, engineering applications are frequently concerned with finite continuous linear systems whose partial differential operators involve only one spatial variable and contain only constant coefficients. For a general class of such systems, it can be shown [54] that the only singularities of $H_{jj}(i\omega)$ in the finite $i\omega$ plane are poles [i.e., $H_{jj}(i\omega)$ is a "meramorphic" function], and that $H_{jj}(i\omega)$ may be represented as the ratio of two functions, each of which is analytic in the finite $i\omega$ plane (i.e., ratio of two "entire" functions). Thus, $H_{jj}(i\omega)$, and hence also $\kappa_{jj}(\omega)$ and $\gamma_{jj}(\omega)$, may be expressed as the ratio of two power series in ω, each of which is convergent everywhere in the finite $i\omega$ plane.

The dynamic behavior of the most general discrete (lumped parameter) linear systems is determined by a general kth order

linear ordinary differential operator involving k system coordinates and time, and containing time dependent coefficients. As in the case of continuous systems, it is not generally possible to obtain a closed-form analytic representation for $H_{jj}(i\omega)$, and very little can be said about its general form.

However, engineering applications are frequently concerned with discrete linear systems whose differential operators involve only real constant coefficients. It can be shown [55] that the transfer function $H_{jj}(i\omega)$ for such systems always admits a closed form representation as a ratio of polynomial functions of ω. Furthermore the denominator polynomial in $i\omega$ has only real coefficients and is the kth order characteristic polynomial of the rigidly constrained linear system. Since the numerator polynomial in $i\omega$ also has only real coefficients, it is seen that $\kappa_{jj}(\omega)$ and $\gamma_{jj}(\omega)$ each admit a closed-form representation as a ratio of real polynomial functions of ω, whose roots are either purely imaginary or occur in pairs with real parts of opposite sign.

3.3.4 Properties of $\kappa_{jj}(\omega)$ and $\gamma_{jj}(\omega)$ for Undamped Linear Chainlike Structures

One of the frequently encountered mechanical models for structural systems is that of the "undamped linear chainlike structure," an example of which is shown in Fig. 3.2. The structure is composed alternately of lumped masses and linear springs which are connected only to the nearest element on either side, and the motion is confined to be unidirectional. The number of elements

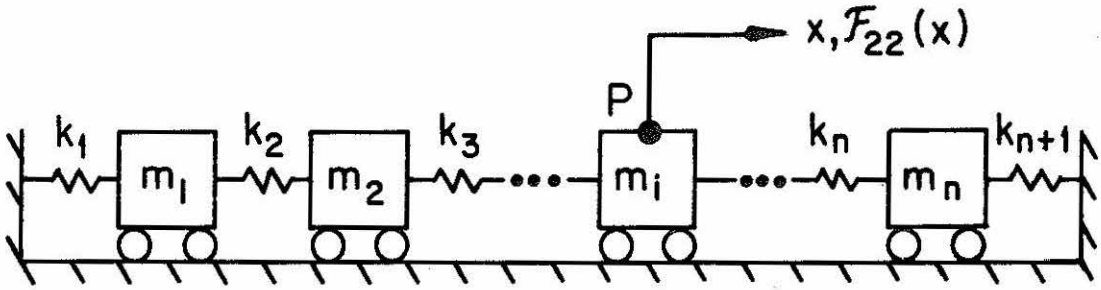

Figure 3.2 - Schematic of an Undamped n-Mass Linear Chainlike Structure

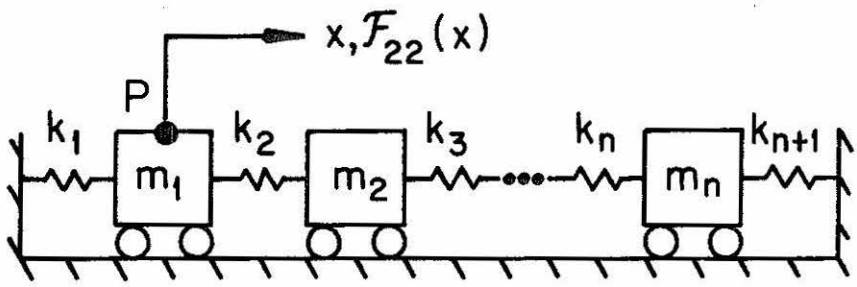

Figure 3.3 - Schematic of a Chainlike System with Attachment Point P Located at Mass m_1

is arbitrary as long as the chainlike structure is maintained. This simplified system has been used to model the dynamic behavior of such structures as tall buildings of frame construction, various pieces of mechanical equipment, and as a discretized model for one-dimensional motion in a continuum.

The structure may be terminated at either end with a spring (as shown) or a mass (accomplished by setting $k_1 = 0$ and/or $k_{n+1} = 0$). The attachment point P is shown at the ith mass, where $1 \leq i \leq n$, and n is the total number of masses in the system. Note that P may be specified anywhere within the chainlike structure by choosing "i" appropriately and by allowing $m_i \equiv 0$.

Since the system contains no viscous damping elements, it is nondissipative. Hence,

$$\nu_{jj}(\omega) = 0 \quad \forall \quad \omega \tag{3.10}$$

and $\kappa_{jj}(\omega)$ and $H_{jj}(i\omega)$ are identical.

Clearly the behavior of $\kappa_{jj}(\omega)$ depends on the location of attachment point P within the structure. It is convenient to consider first the case in which P is located at one end of the structure (i.e., P is attached to mass m_1 or m_n). Without loss of generality, assume that P is located at mass m_1, as shown in Fig. 3.3.

$\kappa_{jj}(\omega)$ is the amplitude of force $\mathfrak{F}_{jj}(x)$ required to maintain unit harmonic motion $x = e^{i\omega t}$ at attachment point P. That is

$$\mathfrak{F}_{jj}(e^{i\omega t}) = \kappa_{jj}(\omega) e^{i\omega t} \tag{3.11}$$

According to the previous discussion on discrete linear systems with constant coefficients, $\kappa_{jj}(\omega)$ admits representation as a ratio of real polynomials $p_N(\omega)$ and $p_D(\omega)$

$$\kappa_{jj}(\omega) = \frac{p_N(\omega)}{p_D(\omega)} \tag{3.12}$$

But it is well known that any polynomial function may be written as a product of terms as follows

$$p(\omega) = c \prod_{\ell=1}^{n} (\omega - \omega_\ell) \tag{3.13}$$

where c is a real constant, $\{\omega_\ell | \ = 1, 2, \ldots, n\}$ is the set of roots of $p(\omega) = 0$, and n is the order of the polynomial. Hence, $\kappa_{jj}(\omega)$ admits the following representation

$$\kappa_{jj}(\omega) = \kappa_0 \frac{\prod_{i=1}^{\ell} (\omega - \omega_{zi})}{\prod_{j=1}^{m} (\omega - \omega_{pj})} \tag{3.14}$$

where κ_0 is a real constant, $\{\omega_{zi} | \, i = 1, 2, \ldots, \ell\}$ is the set of roots of the ℓth order polynomial $p_N(\omega)$, and $\{\omega_{pj} | \, j = 1, 2, \ldots, m\}$ is the set of roots of the mth order polynomial $p_D(\omega)$. Note that $\kappa_{jj}(\omega)$ is therefore completely specified by determining κ_0, ℓ, m, $\{\omega_{zi} | \, i = 1, 2, \ldots, \ell\}$ and $\{\omega_{pj} | \, j = 1, 2, \ldots, m\}$.

As previously noted, the poles and zeros of $\kappa_{jj}(\omega)$ may be determined by considering the free vibrations of the system in

Fig. 3.3 with appropriate constraints on attachment point P. Specifically, the poles of $\kappa_{jj}(\omega)$ are the natural frequencies of the rigidly constrained linear system, and the zeros of $\kappa_{jj}(\omega)$ are the natural frequencies of the unconstrained linear system.

Writing the equations of motion for the rigidly constrained linear system, one finds that the poles of $\kappa_{jj}(\omega)$ are those frequencies ω such that

$$\det\left|\Omega_p^2 - \omega^2 I\right| = 0 \tag{3.15}$$

where

$$\Omega_p^2 \equiv \begin{bmatrix} \frac{(k_2+k_3)}{m_2} & \frac{-k_3}{(m_2m_3)^{\frac{1}{2}}} & & & 0 \\ \frac{-k_3}{(m_2m_3)^{\frac{1}{2}}} & \frac{(k_3+k_4)}{m_3} & & & \\ & & & & \frac{-k_n}{(m_{n-1}m_n)^{\frac{1}{2}}} \\ & & & & \\ 0 & & \frac{-k_n}{(m_{n-1}m_n)^{\frac{1}{2}}} & & \frac{(k_n+k_{n+1})}{m_n} \end{bmatrix} \tag{3.16}$$

Since the $(n-1)\times(n-1)$ matrix Ω_p^2 is symmetric and positive definite, well-known theorems in matrix theory guarantee that all eigenvalues of Ω_p^2 are real and positive. Hence, there are $(2n-2)$ poles of $\kappa_{jj}(\omega)$ which occur in $(n-1)$ pairs of real, nonzero frequencies with opposite sign.

Writing the equations of motion for the unconstrained linear system, one finds that the zeros of $\kappa_{jj}(\omega)$ are those frequencies ω such that

$$\det|\Omega_z^2 - \omega^2 I| = 0 \tag{3.17}$$

where

$$\Omega_z^2 \equiv \begin{bmatrix} \frac{(k_1+k_2)}{m_1} & \frac{-k_2}{(m_1m_2)^{\frac{1}{2}}} & & & 0 \\ \frac{-k_2}{(m_1m_2)^{\frac{1}{2}}} & \frac{(k_2+k_3)}{m_2} & & & \\ & & & & \frac{-k_n}{(m_{n-1}m_n)^{\frac{1}{2}}} \\ & & & & \\ 0 & & & \frac{-k_n}{(m_{n-1}m_n)^{\frac{1}{2}}} & \frac{(k_n+k_{n+1})}{m_n} \end{bmatrix} \tag{3.18}$$

Since the $n \times n$ matrix Ω_z^2 is symmetric and positive definite (semi-definite if $k_{n+1} = 0$ and $k_1 = 0$), well-known theorems in matrix theory guarantee that all eigenvalues of Ω_z^2 are real and positive (non-negative). Hence, there are $2n$ zeros of $\kappa_{jj}(\omega)$ which occur in n pairs of real frequencies with opposite sign.

From the above discussion, it is seen that $\kappa_{jj}(\omega)$ admits the representation

$$\kappa_{jj}(\omega) = \kappa_0 \frac{\prod_{i=1}^{n} (\omega^2 - \omega_{zi}^2)}{\prod_{i=1}^{(n-1)} (\omega^2 - \omega_{pi}^2)} \tag{3.19}$$

The constant κ_0 may be determined by noting from (3.19) that

$$\kappa_{jj}(\omega) \sim \kappa_0 \omega^2 \qquad \text{as } \omega \to \infty \tag{3.20}$$

Considering once again the system shown in Fig. 3.3 and the definition of $\kappa_{jj}(\omega)$ as the amplitude of force $\mathfrak{F}_{jj}(\omega)$ required to maintain unit harmonic motion of mass m_1, it is observed on physical grounds that

$$\kappa_{jj}(\omega) \sim -m_1 \omega^2 \qquad \text{as } \omega \to \infty \tag{3.21}$$

Comparing equations (3.20) and (3.21), it is clear that

$$\kappa_0 = -m_1 \tag{3.22}$$

Thus, combining equations (3.19) and (3.22), $\kappa_{jj}(\omega)$ may be expressed as

$$\kappa_{jj}(\omega) = -m_1 \frac{\prod_{i=1}^{n} (\omega^2 - \omega_{zi}^2)}{\prod_{i=1}^{n-1} (\omega^2 - \omega_{pi}^2)} \tag{3.23}$$

Using the tribanded structure of each of Ω_p^2 and Ω_z^2, and the fact that $k_2, k_3, \ldots, k_n$ are always nonzero, it is shown in Appendix A by applying techniques in matrix theory that

$$\omega_{z1}^2 < \omega_{p1}^2 < \omega_{z2}^2 < \cdots < \omega_{p,n-1}^2 < \omega_{zn}^2 \tag{3.24}$$

It is further shown that for all positive (negative) ω, $\kappa_{jj}(\omega)$ is a strictly decreasing (increasing) function of ω which ranges from $\kappa_{jj}(0) \geq 0$ to $-\infty$ for $\omega \in [0, \omega_{p1})$, and from $+\infty$ to $-\infty$ for $\omega \in (\omega_{p1}, \omega_{p2})$, $\omega \in (\omega_{p2}, \omega_{p3}), \ldots, \omega \in (\omega_{p,n-1}, \infty)$. The resulting qualitative behavior of $\kappa_{jj}(\omega)$ is sketched in Fig. 3.4.

Clearly the form of $\kappa_{jj}(\omega)$ presented in (3.23) is intended to apply only when $m_1 \neq 0$. The case in which $m_1 \equiv 0$ is handled in a manner completely analogous to the above, with the only modification being that the matrix Ω_z^2 of equation (3.18) now becomes an $(n-1) \times (n-1)$ matrix which does not involve m_1. The resulting form for $\kappa_{jj}(\omega)$ in this case is

$$\kappa_{jj}(\omega) = (k_1 + k_2) \prod_{i=1}^{(n-1)} \frac{(\omega^2 - \omega_{zi}^2)}{(\omega^2 - \omega_{pi}^2)} \tag{3.25}$$

where it is shown in Appendix A that

$$\omega_{z1}^2 < \omega_{p1}^2 < \omega_{z2}^2 < \cdots < \omega_{zn-1}^2 < \omega_{pn-1}^2 \tag{3.26}$$

In this case, the qualitative behavior of $\kappa_{jj}(\omega)$ is similar to that

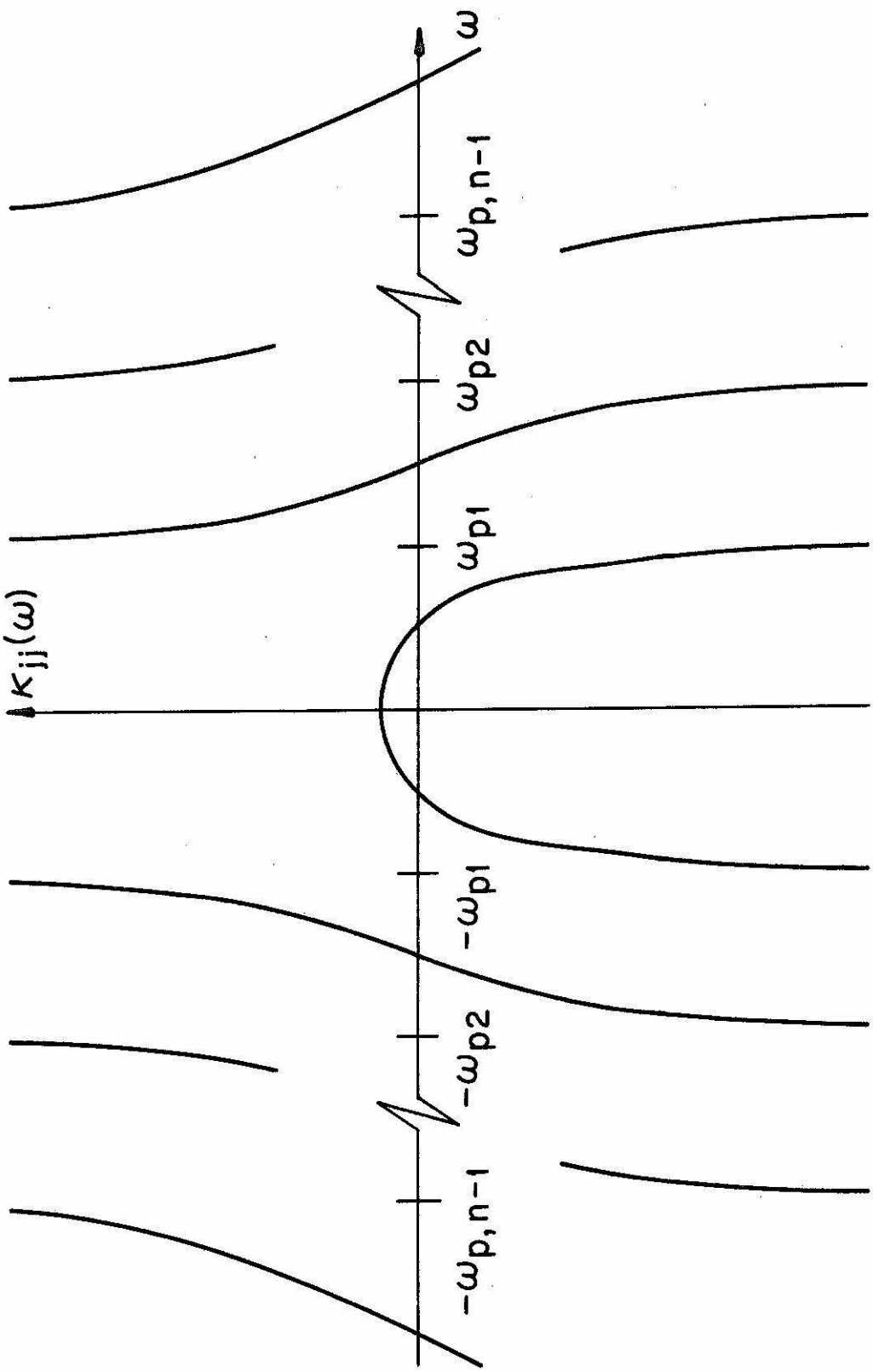

Figure 3.4 - Qualitative Behavior of $\kappa_{jj}(\omega)$ for an Undamped Linear Chainlike Structure with Attachment "P" at One End

shown in Fig. 3.4, except that as $\omega \to \pm\infty$, $\kappa_{jj}(\omega) \to (k_1 + k_2)$ rather than $-\infty$.

In order to determine the qualitative properties of $\kappa_{jj}(\omega)$ for the case in which attachment point P is located at mass m_i internal to the chainlike structure, it is convenient to consider the freebody diagram of Fig. 3.5, which isolates mass m_i from the remainder of the structure. The resulting equilibrium equation is

$$\mathfrak{F}_{jj}(x) = m_i\ddot{x} + f_\ell(x) + f_r(x) \tag{3.27}$$

where f_ℓ and f_r are the forces transmitted from those portions of the structure to the left and right of mass m_i, respectively, as shown in Fig. 3.6.

Letting $x = e^{i\omega t}$ in (3.27) and defining $\kappa_\ell(\omega)$ and $\kappa_r(\omega)$ as follows

$$\left.\begin{aligned} f_\ell(e^{i\omega t}) &= \kappa_\ell(\omega)\, e^{i\omega t} \\ f_r(e^{i\omega t}) &= \kappa_r(\omega)\, e^{i\omega t} \end{aligned}\right\} \tag{3.28}$$

one obtains

$$\kappa_{jj}(\omega) = -\omega^2 m_i + \kappa_\ell(\omega) + \kappa_r(\omega) \tag{3.29}$$

Clearly the properties of $\kappa_{jj}(\omega)$ in this case depend on the behavior of $\kappa_\ell(\omega)$ and $\kappa_r(\omega)$. However, by their definition in equation (3.28) and Fig. 3.6, it is noted that $\kappa_\ell(\omega)$ and $\kappa_r(\omega)$ are each analogous to $\kappa_{jj}(\omega)$ in the previously discussed case in which

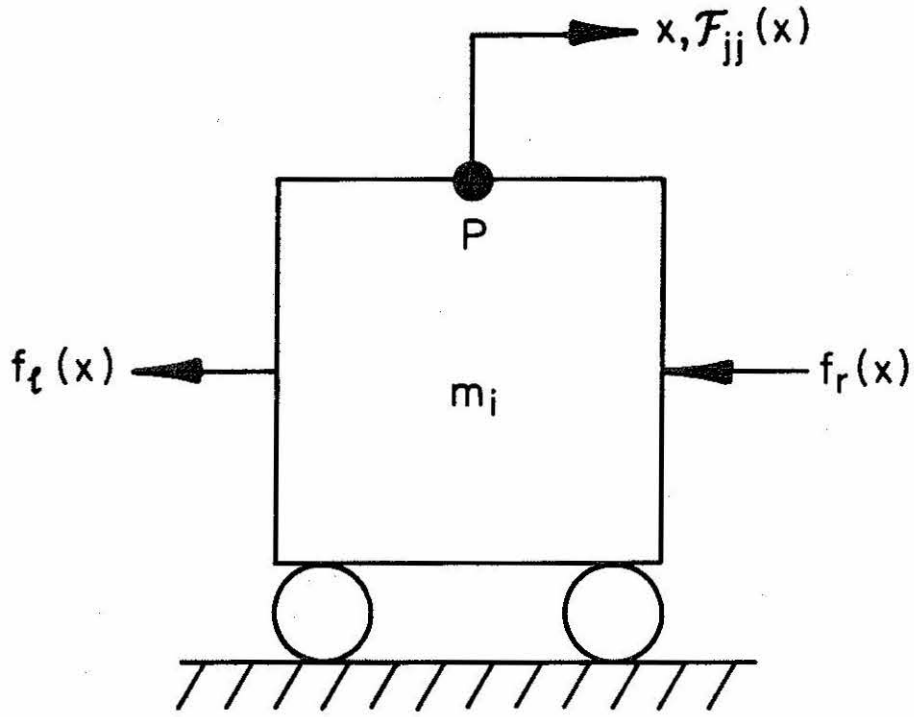

Figure 3.5 - Freebody Diagram of Mass m_i

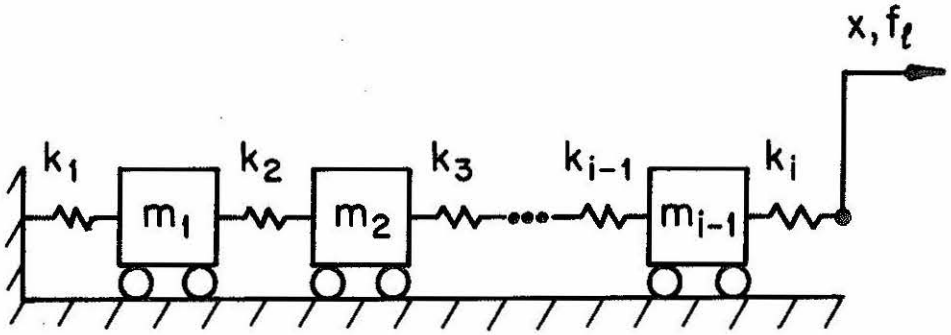

(a)

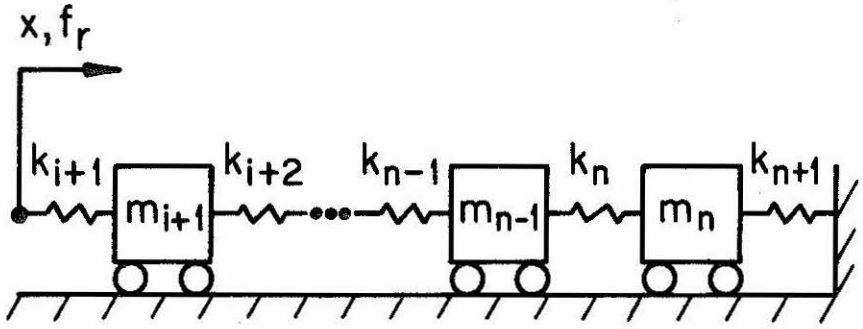

(b)

Figure 3.6 - Transmitted Forces f_ℓ, From Left Portion of Chainlike Structure (a), and f_r, From Right Portion (b)

attachment point P is massless and located at one end of a chain-like structure. Thus

$$\left.\begin{aligned} \kappa_{\ell}(\omega) &= k_i \prod_{j=1}^{(i-1)} \frac{(\omega^2 - \omega_{\ell z j}^2)}{(\omega^2 - \omega_{\ell p j}^2)} \\ \kappa_r(\omega) &= k_{i+1} \prod_{j=1}^{(n-i)} \frac{(\omega^2 - \omega_{r z j}^2)}{(\omega^2 - \omega_{r p j}^2)} \end{aligned}\right\} \quad (3.30)$$

where k_i and k_{i+1} are the spring stiffnesses shown in Fig. 3.6, and all poles and zeros are determined as in the previous discussion.

Since $\kappa_{\ell}(\omega)$, $\kappa_r(\omega)$, and $-\omega^2 m_i$ are each strictly decreasing functions for positive ω, it may be concluded that $\kappa_{jj}(\omega)$ remains a strictly decreasing function for positive ω in the case where attachment point P is located within the chainlike structure.

Consider the set Λ consisting of the union of poles of $\kappa_{\ell}(\omega)$ and $\kappa_r(\omega)$

$$\Lambda \equiv \{\omega_{\ell p j}^2 \mid j = 1, 2, \ldots, i-1\} \cup \{\omega_{r p j}^2 \mid j = 1, 2, \ldots, n-i\} \quad (3.31)$$

Then, clearly there exists two distinct possibilities: (1) each of the elements of Λ is distinct, (2) there exists one or more pairs of identical elements in Λ.

If all the elements of Λ are distinct, then $\kappa_{jj}(\omega)$ will have (n-1) poles on the positive ω-axis, one corresponding to each of the distinct poles of $\kappa_{\ell}(\omega)$ and $\kappa_r(\omega)$. It can be shown that such

will be the case if attachment point P does not correspond to a nodal point at any frequency for the free vibrations of the unconstrained linear system.

However, if there exists ℓ identical pairs of elements in Λ, then $\kappa_{jj}(\omega)$ will have exactly $(n-\ell-1)$ poles on the positive ω-axis, one corresponding to each of the $(n-\ell-1)$ distinct elements of Λ. It can be shown that such will be the case if attachment point P corresponds to a nodal point at exactly ℓ frequencies of free vibration of the unconstrained linear system.

Except for the possibility of the exclusion of some poles due to the placement of P at an interior node, the qualitative properties of $\kappa_{jj}(\omega)$ for P located within the chainlike structure are the same as those for P located at one end of the structure.

Thus, the important properties of $\kappa_{jj}(\omega)$ may be summarized as follows:

(1) If the chainlike structure has $(n-1)$ masses excluding attachment point P, and if there exists ℓ natural frequencies of the unconstrained linear system for which P corresponds to a nodal point, then $\kappa_{jj}(\omega)$ has $(n-\ell-1)$ distinct positive poles which divide the positive ω-axis into $(n-\ell)$ regions in which $\kappa_{jj}(\omega)$ is a continuous single-valued, strictly-decreasing function of ω.

(2) $\kappa_{jj}(\omega)$ ranges from:

(a) $\kappa_{jj}(0) \geq 0$ to $-\infty$ for $\omega \in [0, \omega_{p1})$

(b) $+\infty$ to $-\infty$ for $\omega \in (\omega_{p1}, \omega_{p2}), \ldots, (\omega_{p,n-\ell-2}, \omega_{p,n-\ell-1})$

(c) $+\infty$ to $-\infty$ for $\omega \in (\omega_{p,n-\ell-1}, \infty)$ if $m_i \neq 0$

(d) $+\infty$ to $(k_i + k_{i+1})$ for $\omega \in (\omega_{p,n-\ell-1}, \infty)$ if $m_i = 0$.

With a minor qualification, it is easily shown that the above transfer function properties are also obtained in the case of a uniform continuous shear beam, which is the continuous analogy of a uniform chainlike structure. The qualification is simply that conditions (2c) and (2d) must be disregarded in the continuous case since there are an infinite number of transfer function poles.

Although it is not easily proven, a strong argument can be made that similar transfer function properties should hold for nonuniform continuous shear beams provided that the nonuniformity is sufficiently well behaved.

3.3.5 Properties of $\kappa_{jj}(\omega)$ and $\gamma_{jj}(\omega)$ for Lightly Damped Linear Chainlike Structures

Since all structural systems are dissipative, it is of interest to determine the effect on $\kappa_{jj}(\omega)$ and $\gamma_{jj}(\omega)$ of the addition of a small amount of viscous damping.

Commonly in structural engineering practice, linear structural systems are initially modeled as being nondissipative in order to determine the resonant frequencies, corresponding mode shapes, and uncoupled generalized coordinates (each of which is governed by the equation of a simple undamped oscillator). Then, to account for small structural dissipation, a small viscous damping term is added independently to each of the uncoupled equations for the generalized coordinates. In order to determine the effect of such a

procedure on $\kappa_{jj}(\omega)$ and $\gamma_{jj}(\omega)$, a different transfer function representation than that of the previous section is required.

Consider once again the system shown in Fig. 3.2. Let x_ℓ and x_r represent the displacements of masses m_{i-1} and m_{i+1} respectively (positive to the right). Then, from Fig. 3.6

$$\left.\begin{aligned} f_\ell(x) &= k_i[x - x_\ell(x)] \\ f_r(x) &= k_{i+1}[x - x_r(x)] \end{aligned}\right\} \quad (3.32)$$

where it is noted that $x_\ell(x)$ and $x_r(x)$ are considered as system responses to the input motion x.

Substituting (3.32) into (3.27), one obtains

$$\mathfrak{F}_{jj}(x) = m_i\ddot{x} + (k_i + k_{i+1})x - k_i x_\ell(x) - k_{i+1}x_r(x) \qquad (3.33)$$

Note from Fig. 3.6 that $x_\ell(x)$ is determined from the left portion of the chainlike structure, which has (i-1) masses, and that $x_r(x)$ is determined from the right portion of the chainlike structure, which has (n-i) masses. Since each portion of the structure is undamped, there exists (i-1) normal modes and generalized coordinates which contribute to the response $x_\ell(x)$, and there exists (n-i) normal modes and coordinates which contribute to the response $x_r(x)$. Thus, $x_\ell(x)$ and $x_r(x)$ may each be expanded in terms of their respective generalized coordinates $\{z_{\ell j}(t) \mid j = 1, 2, \ldots, i-1\}$ and $\{z_{rj}(t) \mid j = 1, 2, \ldots, n-i\}$, as follows

$$\left.\begin{aligned} x_\ell(t) &= \sum_{j=1}^{i-1} a_{\ell j} z_{\ell j}(t) \\ x_r(t) &= \sum_{j=1}^{n-i} a_{rj} z_{rj}(t) \end{aligned}\right\} \quad (3.34)$$

where, for the undamped structure,

$$\left.\begin{aligned} \ddot{z}_{\ell j}(t) + \omega^2_{\ell pj} z_{\ell j}(t) &= b_{\ell j} x(t) ; \qquad j = 1, 2, \ldots, i-1 \\ \ddot{z}_{rj}(t) + \omega^2_{rpj} z_{rj}(t) &= b_{rj} x(t) ; \qquad j = 1, 2, \ldots, n-i \end{aligned}\right\} \quad (3.35)$$

and where $\{\omega^2_{\ell pj} | j = 1, 2, \ldots, i-1\}$ and $\{\omega^2_{rpj} | j = 1, 2, \ldots, n-i\}$ are the elements of the set Λ in equation (3.31) which determine the poles of $\kappa_{jj}(\omega)$. Furthermore, it can be shown by using properties of the mode shapes derived from the results of Appendix A, that all of the real constants $a_{\ell j}, b_{\ell j}$ $(j = 1, 2, \ldots, i-1)$ and a_{rj}, b_{rj} $(j = 1, 2, \ldots, n-i)$ are nonzero.

At this point viscous damping may be added to the system by including a small independent damping term in each of (3.35) to obtain

$$\left.\begin{aligned} \ddot{z}_{\ell j}(t) + 2\zeta_{\ell j}\omega_{\ell pj}\dot{z}_{\ell j}(t) + \omega^2_{\ell pj} z_{\ell j}(t) &= b_{\ell j} x(t) ; \qquad j = 1, 2, \ldots, i-1 \\ \ddot{z}_{rj}(t) + 2\zeta_{rj}\omega_{rpj}\dot{z}_{rj}(t) + \omega^2_{rpj} z_{rj}(t) &= b_{rj} x(t) ; \qquad j = 1, 2, \ldots, n-i \end{aligned}\right\} \quad (3.36)$$

where $\{\zeta_{\ell j} | j = 1, 2, \ldots, i-1\}$ and $\{\zeta_{rj} | j = 1, 2, \ldots, n-i\}$ are small

damping coefficients which individually prescribe the fraction of critical damping in the respective modes of the left and right portions of the chainlike structure.

To obtain a representation for $H_{jj}(i\omega)$, let $x = e^{i\omega t}$ in (3.33), and define $Z_{\ell j}(i\omega)$ and $Z_{rj}(i\omega)$ as follows

$$\left.\begin{aligned} z_{\ell j}(t) &= Z_{\ell j}(i\omega)e^{i\omega t}\ ; \qquad j = 1, 2, \ldots, i-1 \\ z_{rj}(t) &= Z_{rj}(i\omega)e^{i\omega t}\ ; \qquad j = 1, 2, \ldots, n-i \end{aligned}\right\} \quad (3.37)$$

Thus, from (2.32), (3.33), (3.34), and (3.37) one obtains

$$H_{jj}(i\omega) = k_i + k_{i-1} - \omega^2 m_i - k_i \sum_{j=1}^{i-1} a_{\ell j} Z_{\ell j}(i\omega) - k_{i+1} \sum_{j=1}^{n-i} a_{rj} Z_{rj}(i\omega) \qquad (3.38)$$

Substituting $x = e^{i\omega t}$ into (3.36) the following expressions for $Z_{\ell j}(i\omega)$ and $Z_{rj}(i\omega)$ are obtained

$$\left.\begin{aligned} Z_{\ell j}(i\omega) &= -b_{\ell j} \frac{(\omega^2 - \omega_{\ell pj}^2) + i\omega 2\zeta_{\ell j}\omega_{\ell pj}}{(\omega^2 - \omega_{\ell pj}^2)^2 + 4\zeta_{\ell j}^2\omega^2\omega_{\ell pj}^2}\ ; \qquad j = 1, 2, \ldots, i-1 \\ Z_{rj}(i\omega) &= -b_{rj} \frac{(\omega^2 - \omega_{rpj}^2) + i\omega 2\zeta_{rj}\omega_{rpj}}{(\omega^2 - \omega_{rpj}^2)^2 + 4\zeta_{rj}^2\omega^2\omega_{rpj}^2}\ ; \qquad j = 1, 2, \ldots, n-i \end{aligned}\right\} \quad (3.39)$$

Substituting (3.39) into (3.38), the following representation is obtained for $H_{jj}(i\omega)$

$$H_{jj}(i\omega) = k_i + k_{i-1} - \omega^2 m_i + k_i \sum_{j=1}^{i-1} a_{\ell j} b_{\ell j} \frac{(\omega^2 - \omega_{\ell pj}^2) + i\omega 2\zeta_{\ell j}\omega_{\ell pj}}{(\omega^2 - \omega_{\ell pj}^2)^2 + 4\zeta_{\ell j}^2\omega^2\omega_{\ell pj}^2}$$

$$+ k_{i+1} \sum_{j=1}^{n-i} a_{rj} b_{rj} \frac{(\omega^2 - \omega_{rpj}^2) + i\omega 2\zeta_{rj}\omega_{rpj}}{(\omega^2 - \omega_{rpj}^2)^2 + 4\zeta_{rj}^2\omega^2\omega_{rpj}^2} \tag{3.40}$$

From (3.40), $\nu_{jj}(i\omega)$ and $\gamma_{jj}(\omega)$ are readily identified

$$\left.\begin{aligned} \nu_{jj}(\omega) \equiv \mathrm{Re}[H_{jj}(i\omega)] &= k_i + k_{i-1} - \omega^2 m_i + k_i \sum_{j=1}^{i-1} a_{\ell j} b_{\ell j} \frac{(\omega^2 - \omega_{\ell pj}^2)}{(\omega^2 - \omega_{\ell pj}^2)^2 + 4\zeta_{\ell j}^2\omega^2\omega_{\ell pj}^2} \\ &+ k_{i+1} \sum_{j=1}^{n-i} a_{rj} b_{rj} \frac{(\omega^2 - \omega_{rpj}^2)}{(\omega^2 - \omega_{rpj}^2)^1 + 4\zeta_{rj}^2\omega^2\omega_{rpj}^2} \\ \gamma_{jj}(\omega) \equiv \frac{1}{\omega}\mathrm{Im}[H_{jj}(i\omega)] &= 2k_i \sum_{j=1}^{i-1} \frac{\zeta_{\ell j}\omega_{\ell pj} a_{\ell j} b_{\ell j}}{(\omega^2 - \omega_{\ell pj}^2)^2 + 4\zeta_{\ell j}^2\omega^2\omega_{\ell pj}^2} \\ &+ 2k_{i+1} \sum_{j=1}^{n-i} \frac{\zeta_{rj}\omega_{rpj} a_{rj} b_{rj}}{(\omega^2 - \omega_{rpj}^2)^2 + 4\zeta_{rj}^2\omega^2\omega_{rpj}^2} \end{aligned}\right\} \tag{3.41}$$

From (3.41) it can be shown that for sufficiently small $\{\zeta_{\ell j} | j = 1, 2, \ldots, i-1\}$ and $\{\zeta_{rj} | j = 1, 2, \ldots, n-i\}$, $\nu_{jj}(\omega)$ and $\gamma_{jj}(\omega)$ are arbitrarily close to the undamped transfer functions for all frequencies which are not near the undamped poles specified by the distinct elements of Λ in (3.31). Thus, the addition of small modal damping does not change the qualitative properties of $\nu_{jj}(\omega)$ and

$\gamma_{jj}(\omega)$ in those frequency ranges which are not close to the undamped poles of $\kappa_{jj}(\omega)$.

In order to investigate the behavior of $\kappa_{jj}(\omega)$ and $\gamma_{jj}(\omega)$ near the undamped poles, it is convenient to rewrite (3.41) in terms of the distinct elements of Λ in (3.31). Recall that Λ contains $(n-\ell-1)$ distinct elements [which are the undamped positive poles of $\kappa_{jj}(\omega)$] where ℓ is the number of identical pairs in the sets $\{\omega_{lpj}^2 | j = 1, 2, \ldots, i-1\}$ and $\{\omega_{rpj}^2 | j = 1, 2, \ldots, n-i\}$. Let $\{\omega_{pj}^2 | j = 1, 2, \ldots, n-\ell-1\}$ be the set of distinct elements of Λ. Then (3.41) may be written as follows

$$\left.\begin{aligned} \kappa_{jj}(\omega) &= k_i + k_{i+1} - \omega^2 m_i + \sum_{j=1}^{n-\ell-1} c_j \frac{(\omega^2 - \omega_{pj}^2)}{(\omega^2 - \omega_{pj}^2)^2 + 4\zeta_j^2 \omega^2 \omega_{pj}^2} \\ \gamma_{jj}(\omega) &= 2 \sum_{j=1}^{n-\ell-1} c_j \frac{\zeta_j \omega_{pj}}{(\omega^2 - \omega_{pj}^2)^2 + 4\zeta_j^2 \omega^2 \omega_{pj}^2} \end{aligned}\right\} \quad (3.42)$$

where $c_j \neq 0$ $(j = 1, 2, \ldots, n-\ell-1)$ are linear combinations of $a_{\ell j}$, $b_{\ell j}$, a_{rj}, b_{rj}, k_i, and k_{i+1}, and where $\{\zeta_j | j = 1, 2, \ldots, n-\ell-1\}$ is the set of small damping coefficients obtained from $\{\zeta_{\ell j} | j = 1, 2, \ldots, i-1\}$ and $\{\zeta_{rj} | j = 1, 2, \ldots, n-i\}$ by adding terms when appropriate.

Near the undamped poles, $\kappa_{jj}(\omega)$ and $\gamma_{jj}(\omega)$ may be written as follows, for sufficiently small damping coefficients

$$\kappa_{jj}(\omega) \cong c_k \frac{(\omega^2 - \omega_{pk}^2)}{(\omega^2 - \omega_{pk}^2)^2 + 4\zeta_k^2\omega^2\omega_{pk}^2} + \left[k_i + k_{i+1} - \omega_{pk}^2 m_i + \sum_{\substack{j=1 \\ j\neq k}}^{n-\ell-1} \frac{c_j}{(\omega_{pk}^2 - \omega_{pj}^2)} \right]$$

$$\gamma_{jj}(\omega) \cong 2c_k \frac{\zeta_k\omega_{pk}}{(\omega^2 - \omega_{pk}^2)^2 + 4\zeta_k^2\omega^2\omega_{pk}^2} + \left[2 \sum_{\substack{j=1 \\ j\neq k}}^{n-\ell-1} \frac{c_k\zeta_k\omega_{pj}}{(\omega_{pk}^2 - \omega_{pj}^2)^2} \right] \qquad (3.43)$$

for $\omega \cong \omega_{pk}$, $(k = 1, 2, \ldots, n-\ell-1)$. Note in (3.43) that only the first term in each expression contains a dependence on ω, while the remaining terms sum to a constant. Furthermore, it is seen that the ω-dependent terms take the form respectively of $\kappa(\omega)$ and $\gamma(\omega)$ transfer functions for a single-degree-of-freedom damped oscillator.

From (3.43) and the above discussion, the qualitative effects on $\kappa_{jj}(\omega)$ and $\gamma(\omega)$ of adding a small amount of viscous damping are demonstrated in Fig. 3.7, which shows typical undamped and corresponding lightly damped transfer functions.

3.4 Qualitative Properties of Load Distribution Functions $p_2(\omega)$ and $q_2(\omega)$

3.4.1 General Properties of $p_2(\omega)$ and $q_2(\omega)$

Recall from equation (2.18) that $p_2(\omega)$ and $q_2(\omega)$ are the in-phase and quadrature components of the reaction force $f_{2Ex}(t)$ developed at attachment point P, when P is fixed against motion (relative to point Q in Fig. 3.1) and the generalized loads z_1, z_2, $z_3, \ldots$, each with harmonic time dependence $z(t)$, are applied as indicated in Fig. 3.8. Since the system which generates the

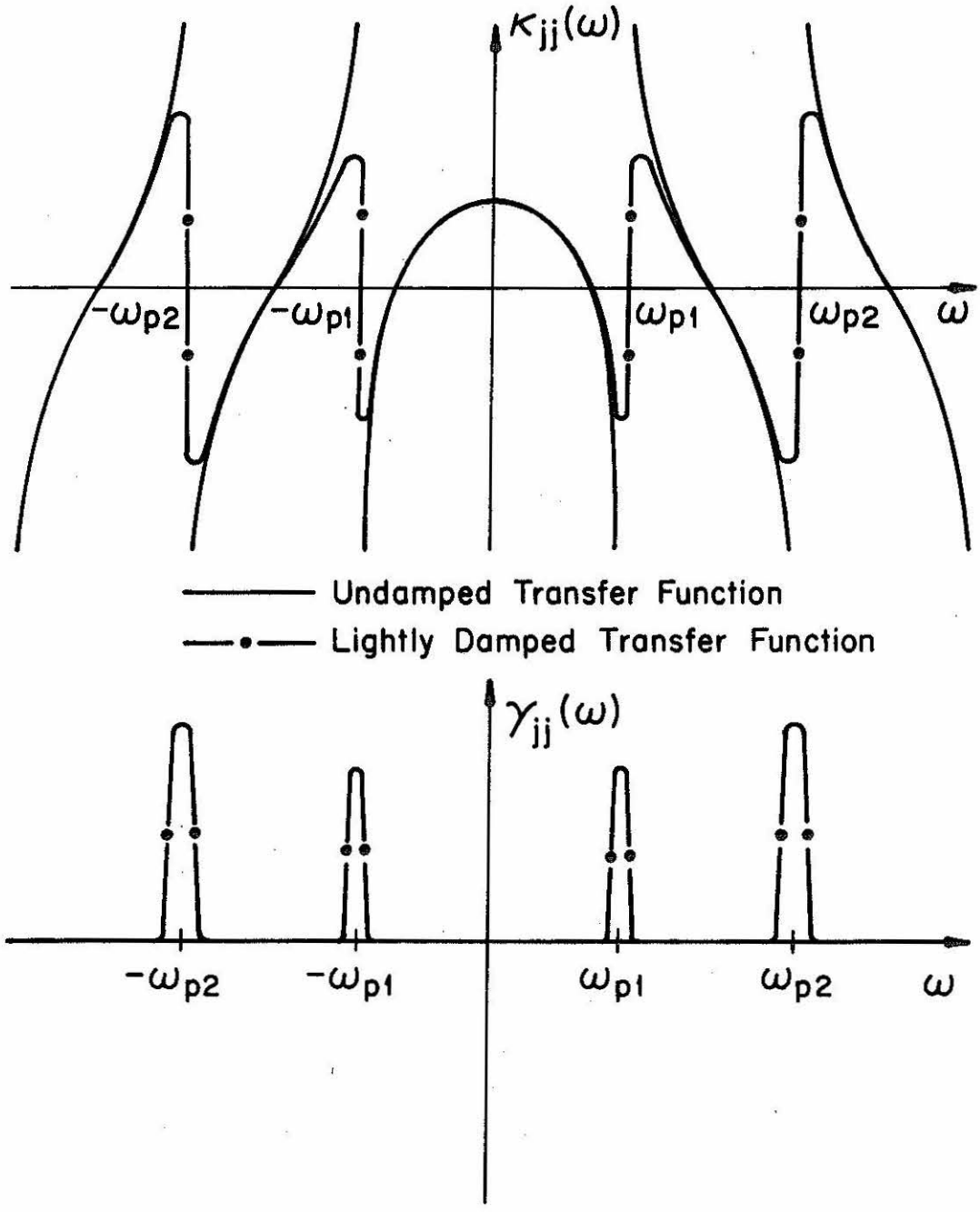

Figure 3.7 - Typical Undamped and Lightly Damped Transfer Functions for Linear Chainlike Structures

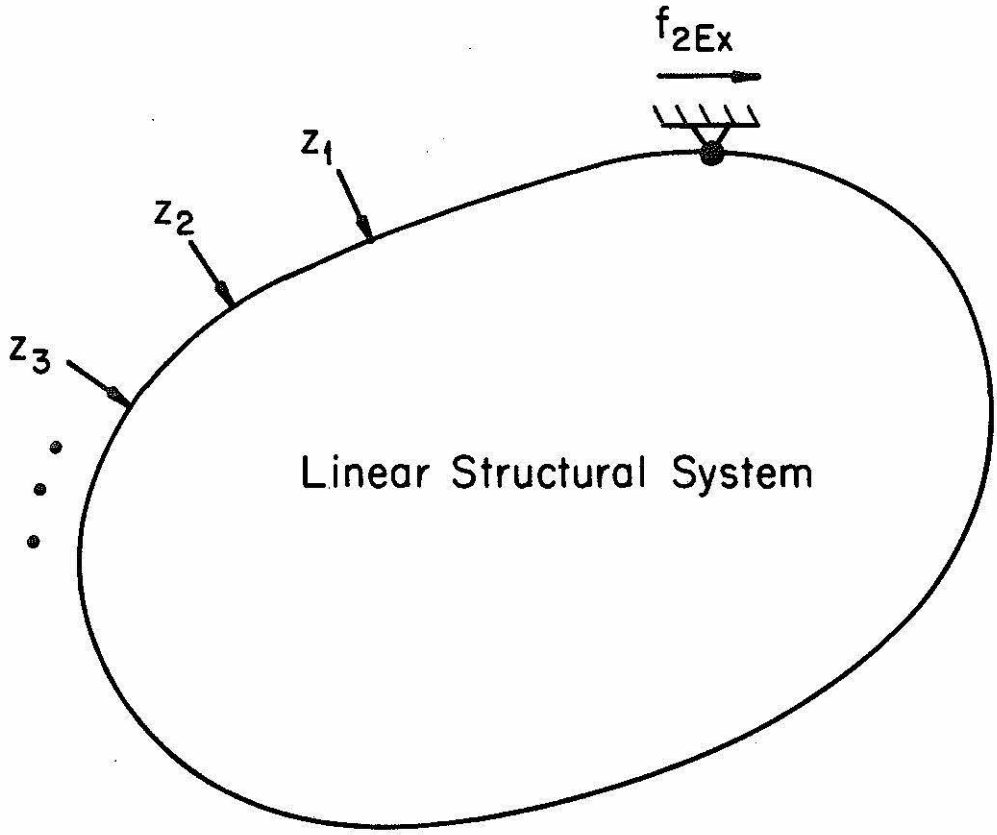

Figure 3.8 - System Configuration for the Determination of Load Distribution Functions $p_2(\omega)$ and $q_2(\omega)$

reaction force is linear, it follows that $p_2(\omega)$ and $q_2(\omega)$ are single-valued functions of ω.

Assumption 8 (A8):

$p_2(\omega)$ and $q_2(\omega)$ are at least piecewise continuous functions of ω.

Most linear systems of engineering interest satisfy assumption (A8), as will be discussed later in this section. In addition, it can be shown that $p_2(\omega)$ and $q_2(\omega)$ are even functions of ω, using their definitions in terms of $G_2(i\omega)$ in equation (2.17) and noting that $G_2(i\omega)$ represents the Fourier transform of the impulse response of the linear system, which is always a real valued function of time for physical systems.

Definition 5 (D5): [Zeros of $G_2(i\omega)$]

The set $\{\lambda_{zk} | k = 1, 2, \ldots\}$ of all frequencies such that $|G_2(i\omega)| = 0$ for the forced system with nonzero loads is defined as the set of zeros of $G_2(i\omega)$.

Note that the zeros of $G_2(i\omega)$ correspond to the frequencies of forced vibration of the linear system for which attachment point P corresponds to a nodal point, since at these frequencies no reaction force f_{2Ex} is required to maintain zero displacement at P. Generally, the set of zeros of $G_2(i\omega)$ is highly dependent upon the particular load distribution.

Definition 8 (D8): [Poles of $G_2(i\omega)$]

The set $\{\lambda_{pk} | k = 1, 2, \ldots\}$ of all frequencies such that $|G_2(i\omega)|$ is unbounded is defined as the set of poles of $G_2(i\omega)$.

Note that the set of poles of $G_2(i\omega)$ must correspond to frequencies of free vibration of the rigidly constrained linear system.

For strictly dissipative linear systems, free vibrations cannot exist at any frequency. Hence, for such systems, $G_2(i\omega)$ can have no real poles. Therefore, $p_2(\omega)$ and $q_2(\omega)$ remain bounded at all frequencies.

For nondissipative systems, the motion of all points within the linear system is exactly in-phase with $z(t)$ (or exactly 180° out of phase). Thus, for nondissipative systems,

$$q_2(\omega) \equiv 0 \quad \forall \quad \omega \tag{3.44}$$

and the poles and zeros of $G_2(i\omega)$ and $p_2(\omega)$ are identical.

The comments in Section 3.3.3 on the form of $\kappa_{jj}(\omega)$ and $\gamma_{jj}(\omega)$ for continuous and discrete linear systems also apply to $p_2(\omega)$ and $q_2(\omega)$.

3.4.2 $p_2(\omega)$ and $q_2(\omega)$ for a Single Concentrated Load Applied at Attachment Point P

The simplest possible loading configuration for the determination of $p_2(\omega)$ and $q_2(\omega)$ is that in which a single concentrated load is applied at attachment point P, with no other loading applied to the system. Such a configuration may prove to be a convenient

experimental arrangement for the identification of an unknown nonlinear restoring force $F(x, \dot{x})$.

In this case, it is clear that

$$\left.\begin{aligned} p_2(\omega) &= 1 \quad \forall \ \omega \\ q_2(\omega) &= 0 \quad \forall \ \omega \end{aligned}\right\} \tag{3.45}$$

3.4.3 Properties of $p_2(\omega)$ and $q_2(\omega)$ for Undamped Linear Chain-Like Structures with Base Excitation

A discussion of undamped linear chainlike structures is contained in Section 3.3.4, and an example is shown in Fig. 3.2.

In the case of base excitation, the generalized harmonic loading, $z(t)$, is the displacement of the base of the structure with respect to an inertial reference frame. In order to determine the load distribution functions $p_2(\omega)$ and $q_2(\omega)$ for base excitation, attachment point P is required to move with the base so that there is no relative motion between P and the base, and the reaction force $f_{2Ex}(t)$ thereby developed at point P is determined. Fig. 3.9 shows such a configuration for an undamped linear chainlike structure.

Since the system in Fig. 3.9 is linear, the reaction force $f_{2Ex}(t)$ admits representation as the superposition of two forces $\mathfrak{F}_{22}(z)$ and $\hat{\mathfrak{F}}_{2Ex}(z)$, which are determined from the systems and loading shown in Figs. 3.10(a) and (b), respectively. Thus,

$$f_{2Ex}(t) = \mathfrak{F}_{22}[z(t)] + \hat{\mathfrak{F}}_{2Ex}[z(t)] \tag{3.46}$$

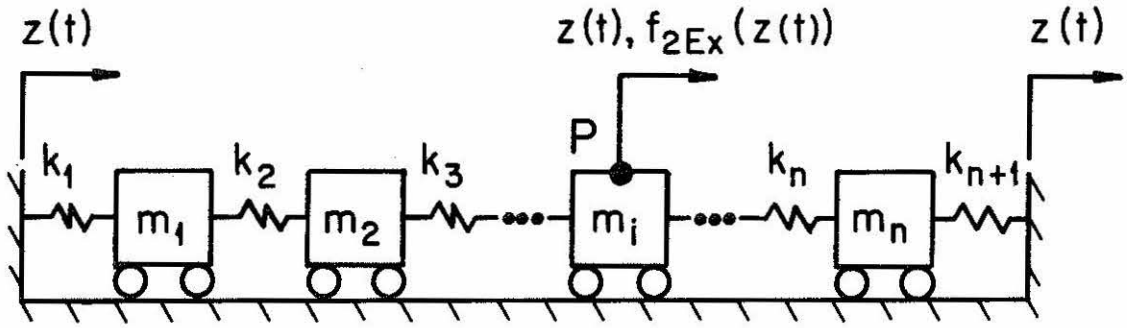

Figure 3.9 - Base Excitation of an Undamped Linear Chainlike Structure with Fixed Attachment Point P

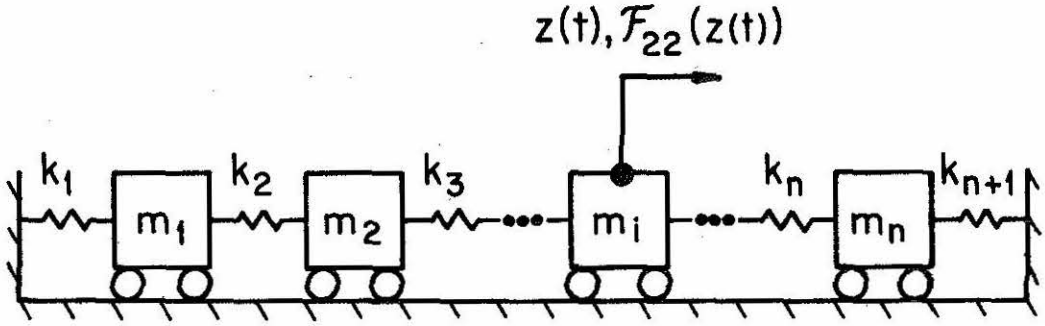

(a)

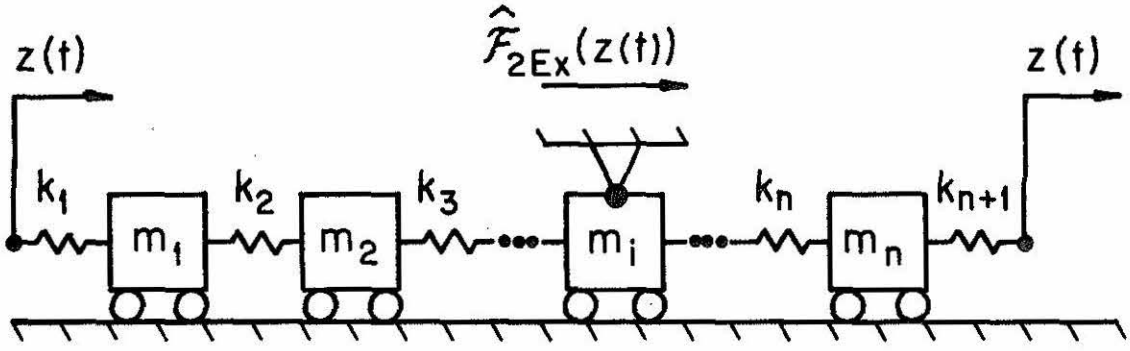

(b)

Figure 3.10 - Decomposition of Base Excitation of an Undamped Linear Chainlike Structure

By comparing Figs. 3.2 and 3.10(a) it is clear that

$$\mathcal{F}_{22}(e^{i\omega t}) = H_{22}(i\omega)\, e^{i\omega t}$$

where $H_{22}(i\omega)$ has the properties discussed in Section 3.3.4.

Define $\hat{G}_2(i\omega)$ such that

$$\hat{\mathcal{F}}_{2\,Ex}(e^{i\omega t}) = \hat{G}_2(i\omega)\, e^{i\omega t} \tag{3.47}$$

Then, from (3.46) one obtains

$$G_2(i\omega) = H_{22}(i\omega) + \hat{G}_2(i\omega) \tag{3.48}$$

Since the system contains no viscous damping elements, it is nondissipative. Hence

$$q_2(\omega) = 0 \quad \text{and} \quad \gamma_{22}(\omega) = 0 \;\forall\; \omega \tag{3.49}$$

and if $\hat{p}_2(\omega)$ and $\hat{q}_2(\omega)$ are defined such that

$$\left.\begin{aligned} \hat{p}_2(\omega) &= \Re e\{\hat{G}_2(i\omega)\} \\ \hat{q}_2(\omega) &= \frac{1}{\omega}\, \Im m\{\hat{G}_2(i\omega)\} \end{aligned}\right\} \tag{3.50}$$

then

$$\hat{q}_2(\omega) = 0 \;\forall\; \omega \tag{3.51}$$

Combining (3.48), (3.49), and (3.51) one finds that

$$p_2(\omega) = \varkappa_{22}(\omega) + \hat{p}_2(\omega) \tag{3.52}$$

From Fig. 3.10(b) it is clear that $\hat{\mathfrak{F}}_{2Ex}[z(t)] = 0$ for all $z(t)$ [and thus also $\hat{p}_2(\omega) \equiv 0$], if $k_1 = 0$ and $k_{n+1} = 0$.

Definition 9 (D9): (Mass-Terminated Chainlike Structure)

Any undamped linear chainlike structure which has the property that $k_1 \equiv 0$ and $k_{n+1} \equiv 0$ is defined as a mass-terminated chainlike structure.

Hence, for base excitation of all mass-terminated chainlike structures

$$\left.\begin{aligned} G_2(i\omega) &= H_{22}(i\omega) \quad \forall \ \omega \\ p_2(\omega) &= \varkappa_{22}(\omega) \quad \forall \ \omega \end{aligned}\right\} \tag{3.53}$$

The properties of $\varkappa_{22}(\omega)$ for undamped linear chainlike structures are discussed in Section 3.3.4.

Consider now the properties of $\hat{p}_2(\omega)$. Clearly $\hat{p}_2(\omega)$ admits representation as a ratio of real polynomials $\hat{p}_N(\omega)$ and $\hat{p}_D(\omega)$

$$\hat{p}_2(\omega) = \frac{\hat{p}_N(\omega)}{\hat{p}_D(\omega)} \tag{3.54}$$

But it is well known that any polynomial function may be written as a product of terms indicated in equation (3.13). Hence, $\hat{p}_2(\omega)$ admits the following representation

$$\hat{p}_2(\omega) = \hat{p}_0 \frac{\prod_{i=1}^{\ell} (\omega - \mu_{zi})}{\prod_{j=1}^{m} (\omega - \mu_{pj})} \tag{3.55}$$

where $\hat{p}_0$ is a real constant, $\{\mu_{zi} | i = 1, 2, \ldots, \ell\}$ is the set of roots of the ℓth order polynomial $\hat{p}_N(\omega)$ and $\{\mu_{pj} | j = 1, 2, \ldots, m\}$ is the set of roots of the mth order polynomial $\hat{p}_D(\omega)$.

By considering Fig. 3.10(b) and the discussion in Section 3.3.4, it is clear that the poles of $\hat{p}_2(\omega)$ must correspond to the natural frequencies of the rigidly constrained linear system, and thus $\{\mu_{pj}^2 | j = 1, 2, \ldots\}$ is a subset of the set Λ of equation (3.31). Therefore, the poles of $\hat{p}_2(\omega)$ are derived from the same set Λ as those of $\kappa_{22}(\omega)$. Thus, from (3.52), it is seen that $p_2(\omega)$ can have at most the same number of poles as $\kappa_{22}(\omega)$ and can have no poles which are different from those of $\kappa_{22}(\omega)$.

3.4.4 Properties of $p_2(\omega)$ and $q_2(\omega)$ for Lightly Damped Mass-Terminated Chainlike Structures with Base Excitation

Since all structural systems are dissipative, it is of interest to determine the effect on $p_2(\omega)$ and $q_2(\omega)$ of the addition of a small amount of viscous damping. Note from equation (3.48) and definition (D9) that for all mass-terminated chainlike structures with base excitation

$$G_2(i\omega) = H_{22}(i\omega) \tag{3.56}$$

Thus, it may be concluded that

$$\left.\begin{aligned} p_2(\omega) &= \varkappa_{22}(\omega) \quad \forall \ \omega \\ q_2(\omega) &= \gamma_{22}(\omega) \quad \forall \ \omega \end{aligned}\right\} \tag{3.57}$$

Therefore, the results of Section 3.3.5 apply directly to $p_2(\omega)$ and $q_2(\omega)$ for mass-terminated chainlike structures with base excitation.

3.5 Qualitative Harmonic Response Behavior

3.5.1 Free Oscillations of Conservative Systems

By free oscillations it is meant that the amplitude of all generalized excitations is identically zero. That is

$$z_0 = 0 \tag{3.58}$$

Substituting (3.58) into (3.3), one obtains the following amplitude-frequency equation for free oscillations

$$-\varkappa_{22}(\omega) = \frac{C(A)}{A} \pm \frac{1}{A}\sqrt{-[\omega\gamma_{22}(\omega)A - S(A)]^2} \tag{3.59}$$

Since all variables in (3.59) are strictly real-valued, (3.59) can have solutions only if

$$\omega\gamma_{22}(\omega)A = S(A) \tag{3.60}$$

Note from (3.6) and (3.9) that (3.60) may be satisfied for nontrivial response amplitudes A only if

$$\left.\begin{aligned} \omega\gamma_{22}(\omega) &= 0 \\ S(A) &= 0 \end{aligned}\right\} \quad (3.61)$$

Clearly equations (3.61) are satisfied for nondissipative linear systems and conservative structural nonlinearities.

Substituting (3.60) into (3.59) one obtains

$$-\kappa_{22}(\omega) = \frac{C(A)}{A} \quad (3.62)$$

Thus, equation (3.62) is the resulting amplitude-frequency equation which governs free oscillations.

By way of verification of (3.62), note that if there is no nonlinear constraint present, then $C(A) = 0 \ \forall \ A$ and (3.62) then requires that the free oscillations occur at the zeros of $\kappa_{22}(\omega)$, independent of amplitude, as required. On the other hand, if the constraint is rigid, then $C(A) \to \infty \ \forall \ A$ and (3.62) requires that the free vibrations occur at the poles of $\kappa_{22}(\omega)$, independent of amplitude, as required. It should be recalled, though, that the poles and zeros of $\kappa_{22}(\omega)$ do not include those frequencies of free vibration for which attachment point P corresponds to a nodal point. Clearly those frequencies are not affected by the presence of the nonlinear constraint since motion at those frequencies cannot contribute to the motion of point P.

Definition 10 (D10): [Backbone Curve(s)]

The backbone curve(s) are defined in the A, ω plane as the loci of all solutions $A(\omega)$ of equation (3.62).

A nonlinear system is said to be "softening" if the backbone curve leans to the left in the A, ω plane (i.e., if the natural frequency decreases for increasing amplitude), and is said to be "hardening" if the backbone curve leans to the right (i.e., if the natural frequency increases for increasing amplitude). Theorem 1 states that for all undamped linear chainlike structures, each of the backbone curves exhibits the same hardening or softening behavior.

Theorem 1: (Hardening or Softening Behavior)

If (1) $\kappa_{22}(\omega)$ is the transfer function of an undamped linear chainlike structure

(2) $C(A)/A \in C^1[0, \infty)$

then every backbone curve has the same hardening or softening behavior, which is determined by the algebraic sign of

$$\frac{d}{dA}\left[\frac{C(A)}{A}\right]$$

proof:

Differentiating (3.62) with respect to A and solving for $d\omega/dA$ one finds

$$\frac{d\omega}{dA} = \frac{\frac{d}{dA}\left[\frac{C(A)}{A}\right]}{-\frac{d\kappa_{22}(\omega)}{d\omega}}$$

By hypothesis (1), $d\kappa_{22}(\omega)/d\omega$ exists and is negative for all positive ω [except at the poles of $\kappa_{22}(\omega)$, which cannot belong to any backbone curves]. Hence, the sign of $d\omega/dA$ is the same as the sign

of $\frac{d}{dA}\left[C(A)/A\right]$, independent of ω. Thus, it is consluded that:

$$\frac{d}{dA}\left[\frac{C(A)}{A}\right] > 0 \Rightarrow \text{hardening behavior}$$

$$\frac{d}{dA}\left[\frac{C(A)}{A}\right] < 0 \Rightarrow \text{softening behavior}$$

for all backbone curves. Q. E. D.

In the special case of the single-degree-of-freedom oscillator, it is well known that there exists only one backbone curve, which represents the amplitude dependence of the frequency of free vibration. However, in the more general multidegree-of-freedom case, there exists many such backbone curves in the A, ω plane. Knowing how many such curves exist and their approximate location is of prime importance in engineering applications. Theorem 2 provides this information for the frequently encountered class of chainlike structures.

Theorem 2: (Number and Location of Backbone Curves)

If (1) $\kappa_{22}(\omega)$ is the transfer function of an undamped linear chainlike structure with poles at $\{0 < \omega_{p1} < \omega_{p2} < \ldots < \omega_{p,n-\ell-1}\}$

(2) $C(A)/A \geq 0$ for all $A \geq 0$

then: (a) if attachment point P has nonzero mass, there exists exactly $(n-\ell)$ distinct backbone curves in the A, ω plane, which are separated by the $(n-\ell-1)$ poles of $\kappa_{22}(\omega)$.

(b) if attachment point P is massless, there exists exactly

$(n-\ell-1)$ distinct backbone curves in the A, ω plane, one contained in each of the intervals $(0, \omega_{p1})$, $(\omega_{p1}, \omega_{p2}), \ldots,$ $[\omega_{p,\,n-\ell-2}, \omega_{p,\,n-\ell-1}]$.

proof:

Observe in (3.62) that for any fixed value of $A \geq 0$, the right hand side is a fixed non-negative constant.

By hypothesis (1) it is known that $\kappa_{22}(\omega)$ is a strictly decreasing function of ω for all $\omega \geq 0$. Furthermore, $\kappa_{22}(\omega)$ ranges from $+\infty$ to $-\infty$ in each of the $(n-\ell-2)$ intervals $(\omega_{p1}, \omega_{p2}), \ldots, (\omega_{p,\,n-\ell-2}, \omega_{p,\,n-\ell-1})$. Hence, in each of these intervals, there exists exactly one frequency ω corresponding to each fixed amplitude A in (3.62). Thus, each of these intervals contains exactly one backbone curve.

In the interval $[0, \omega_{p1})$, $\kappa_{22}(\omega)$ ranges from $\kappa_{22}(0) \geq 0$ to $-\infty$, and is strictly decreasing. Thus, by hypothesis (2), there exists exactly one frequency ω corresponding to each fixed amplitude A in (3.62). Hence, there exists exactly one backbone curve in this interval as well.

In the interval $(\omega_{p,\,n-\ell-1}, \infty)$, there exist two possibilities depending on the mass at attachment point P. If the attachment point has nonzero mass, then $\kappa_{22}(\omega)$ ranges from $+\infty$ to $-\infty$ in this interval and is strictly decreasing. Hence, in this case, there is exactly one backbone curve in this interval.

However, if the attachment point is massless, then $\kappa_{22}(\omega)$ ranges from $+\infty$ to $(k_i + k_{i+1}) > 0$. Thus, in this case, $-\kappa_{22}(\omega) < 0$

and by hypothesis (2) there does not exist a backbone curve in this interval. Q. E. D.

Theorems 1 and 2 thus provide sufficient qualitative information to sketch the free vibration backbone curves for a nondissipative linear chainlike structure with a conservative nonlinear constraint. The number and general location of backbone or resonance curves is determined by the natural frequencies of the rigidly constrained linear system, and the location of the attachment point. The hardening or softening behavior is determined by the C(A) function for the nonlinearity. In Fig. 3.11, typical backbone curves for such a system with a hardening elastic constraint are sketched.

It should be noted that the major results of theorems 1 and 2 hold for any linear system whose transfer function $\kappa_{22}(\omega)$ has distinct poles and is strictly decreasing for all positive ω. Since the uniform shear beam has these transfer function properties, the theorems also apply in that case, with minor modification. The modification is simply that there are an infinite number of transfer function poles, with each consecutive pair enclosing exactly one backbone curve.

3.5.2 Forced Oscillations of Conservative Systems with a (Possibly) Dissipative Constraint

In this section, the forced oscillations of a nondissipative linear system with a general nonlinear terminal constraint are considered. The nonlinear constraint may be conservative or it may be viscously and hysteretically dissipative.

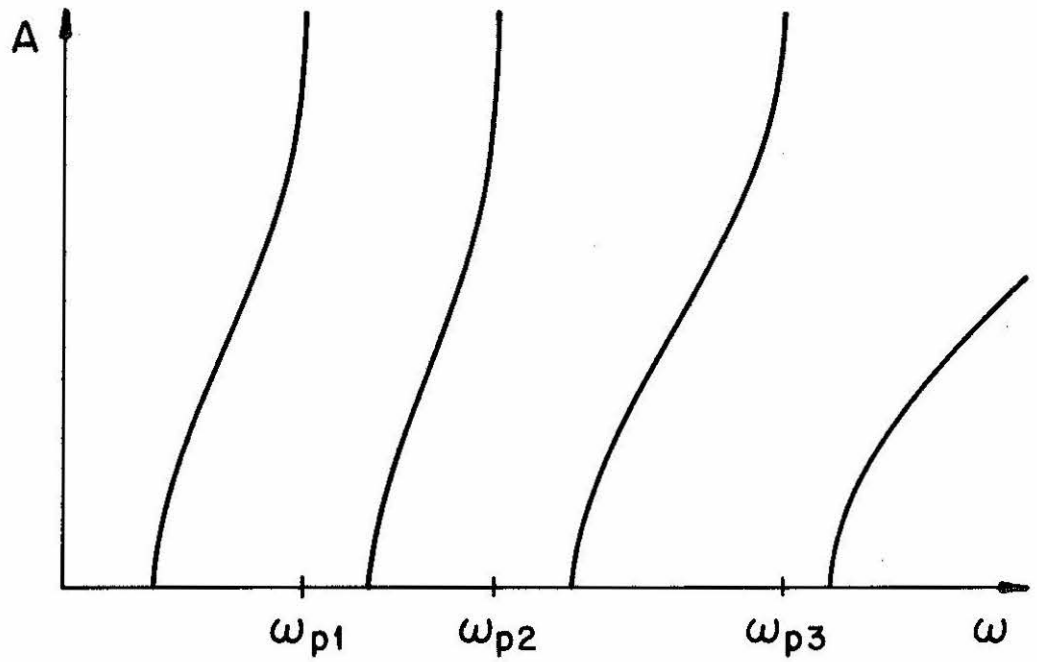

Figure 3.11 - Typical Backbone Curves for a Nondissipative Chainlike Structure with a Hardening Elastic Constraint

Recall that for nondissipative linear systems it follows that $\gamma_{22}(\omega)$ and $q_2(\omega)$ are identically zero. Thus, equation (3.3) becomes

$$-\kappa_{22}(\omega) = \frac{C(A)}{A} \pm \frac{1}{A}\sqrt{p_2^2(\omega)z_0^2 - S^2(A)} \tag{3.63}$$

Recall that if the nonlinear restoring force $F(x, \dot{x})$ contains a viscous dissipation term $c\dot{x}$, then a frequency dependent term $-\omega cA$ must be added to S(A) throughout.

The similarity of the general form of (3.63) with that of the analogous equation for a single-degree-of-freedom oscillator has already been pointed out. In the single-degree-of-freedom case, it has been shown [56] that there exist certain conditions on the nonlinear restoring force and the excitation which govern the qualitative nature of the response $A(\omega)$. Thus, the form of (3.63) suggests that similar conditions may exist for the present multidegree-of-freedom case.

For example, it is well known that by sufficiently increasing the level of excitation, unbounded response is produced in a class of undamped hysteretic single-degree-of-freedom oscillators. This class of oscillators includes the commonly used bilinear hysteretic oscillator, and the dependence of the critical excitation level on the parameters of the hysteresis loop are well known [35].

In the following theorem it is shown that an analogous result holds in the multidegree-of-freedom case. The effects of the additional degrees of freedom are to introduce a dependence of the critical level of excitation on the loading distribution and to

introduce the possibility of unbounded response at more than one excitation frequency.

Theorem 3: (Conditions for Unbounded Response)

If (1) $\kappa_{22}(\omega)$ ranges from $+\infty$ to $-\infty$ for finite $\omega \geq 0$

(2) $\lim_{A \to \infty} S(A) = M$ where $|M| < \infty$

(3) $\lim_{A \to \infty} \frac{C(A)}{A} = k_\infty$ where $|k_\infty| < \infty$

(4) $\{\tilde{\omega}_i \mid i = 1, 2, 3, \ldots\}$ is the set of all frequencies such that: $-\kappa_{22}(\tilde{\omega}_i) = k_\infty$

then, there exists unbounded response amplitude A at one or more of the frequencies $\tilde{\omega}_i$, whenever $z_0 \geq z_0^*$ where:

$$z_0^* \equiv \min \{z_{01}, z_{02}, \ldots\} \quad \text{and} \quad z_{0i} \equiv |M/p_2(\tilde{\omega}_i)| \; ; \quad i = 1, 2, 3, \ldots$$

proof:

For ω such that $p_2(\omega)$ is bounded, it is seen that there are two steady-state solution loci, one determined from each of the equations

$$-\kappa_{22}(\omega) = \frac{C(A)}{A} + \frac{1}{A}\sqrt{p_2^2(\omega)z_0^2 - S^2(A)}$$

$$-\kappa_{22}(\omega) = \frac{C(A)}{A} - \frac{1}{A}\sqrt{p_2^2(\omega)z_0^2 - S^2(A)}$$

Consider the limiting behavior of the above equations as $A \to \infty$. Assuming that the system and excitation are such that $p_2^2(\omega)z_0^2 \geq M^2$, the two solution loci converge since the difference between the

above equations vanishes as $A \to \infty$. Thus, the frequencies $\{\tilde{\omega}_i \mid i = 1, 2, \ldots\}$ at which unbounded resonance occurs are determined by

$$-\varkappa_{22}(\omega) = k_\infty \quad \text{and} \quad p_2^2(\tilde{\omega}_i) z_0^2 \geq M^2 ; \quad i = 1, 2, 3, \ldots$$

By hypothesis (1) there always exists at least one frequency ω which satisfies the first condition. By hypothesis (3), this frequency does not correspond to a pole of $\varkappa_{22}(\omega)$ or $p_2(\omega)$.

Note that corresponding to each $\tilde{\omega}_i$ there exists a z_0 sufficiently large that the second condition is also satisfied unless $p_2(\tilde{\omega}_i) \equiv 0$.

Therefore, the minimum level of excitation z_0^* at which unbounded resonance occurs is determined by

$$z_0^* \equiv \min \{z_{01}, z_{02}, \ldots\} \quad \text{where} \quad z_{0i} \equiv |M/p_2(\tilde{\omega}_i)| ; \quad i = 1, 2, 3, \ldots$$

Q. E. D.

Note that if the nonlinear restoring force contains viscous damping, $|M| \to \infty$ in Theorem 3, for all $\omega > 0$. Thus, all response amplitudes for finite excitation levels are bounded in this case.

The limited slip nonlinearity, introduced by Iwan [58], is useful in models of riveted and bolted structural connections. For this nonlinearity, $|M| = 0$ in Theorem 3. (It can be shown that any hysteretic nonlinearity has this property if the area enclosed by the hysteresis loop is bounded by A^m as $A \to \infty$, where $m < 1$.) Thus, unbounded response exists for all excitation levels and load distributions such that at least one $\tilde{\omega}_i$ does not correspond to a zero of $p_2(\omega)$.

Of considerable practical interest in problems of the forced harmonic response of structures is the location of amplitude extrema in the A, ω plane. It is generally desirable to be aware of the excitation frequencies at which amplitude peaks occur in order to avoid structural damage caused by forced resonance. Except for zeros of response associated with $p_2(\omega) \equiv 0$, the local response extrema occur on the locus of horizontal tangency. It is well known that in the case of undamped hysteretic single-degree-of-freedom oscillators, the response extrema occur on the backbone curve. Thus, the locus of horizontal tangency and the backbone curve coincide in that case.

It is shown below that for multidegree-of-freedom systems, the above statement is no longer true in general. The effect of the additional degrees of freedom is to introduce a dependence on the load distribution which may cause the response extrema to occur on either side of the backbone curves.

Differentiating (3.63) with respect to ω and requiring that $dA/d\omega \equiv 0$, one finds that the locus of horizontal tangency is given by

$$-\varkappa_{22}(\omega) = \frac{C(A)}{A} - \left(\frac{z_0}{A}\right)^2 p_2(\omega) \left(\frac{dp_2(\omega)/d\omega}{d\varkappa_{22}(\omega)/d\omega}\right) \qquad (3.64)$$

By comparing (3.64) and (3.62), it is clear that the locus of horizontal tangency does not coincide with any of the backbone curves unless the last term on the right in (3.64) is identically zero. Furthermore, since the algebraic sign of this term may be either

positive or negative depending on $p_2(\omega)$, the local response extrema may occur on either side of the backbone curves. However, it is seen that for large amplitudes A the magnitude of this term is small, so that the local response extrema occur very nearly on the backbone curves.

Using (3.64) together with (3.63), it can be shown that the local response extrema occur at the intersections of the loci of horizontal tangency and the loci of solutions of

$$z_0^2 p_2^2(\omega)\left[1 - \left(\frac{z_0}{A}\right)^2 \left(\frac{dp_2(\omega)/d\omega}{d\kappa_{22}(\omega)/d\omega}\right)^2\right] = S^2(A) \qquad (3.65a)$$

Note that for large amplitudes, (3.65a) becomes asymptotic to

$$z_0^2 p_2^2(\omega) = S^2(A) \qquad (3.65b)$$

Thus, an approximate method for estimating the location of large amplitude response extrema consists of determining the simultaneous solutions of the backbone curves and the loci of solutions of (3.65b). [It should be noted from (3.63) that steady-state solutions may exist only within the region defined by: $z_0^2 p_2^2(\omega) \geq S^2(A)$, so that (3.65b) represents the boundary of this region.] Clearly, these approximate extrema will yield lower bounds on all amplitude maxima and upper bounds on all amplitude minima. The corresponding estimated frequencies will either be upper or lower bounds depending upon the location of the loci of horizontal tangency. Since the approximate

extrema also represent the locations at which the solutions of (3.63) cross the backbone curves, it is seen that if there are no intersections, then unbounded response exists.

Furthermore, another approximate method for estimating the response extrema is sometimes useful. This method consists of determining the simultaneous solutions (when they exist) of the loci of horizontal tangency and the loci of solutions of (3.65b). By providing an upper bound on response maxima and a lower bound on response minima, the estimated amplitude extrema obtained by this method complement the estimates obtained by the previous method. However, no simple general relationship exists between the corresponding estimated and exact frequencies.

The usefulness of both of these approximate methods is limited by their simplicity and accuracy. In many applications, it is much easier to determine the required solution loci of the less complicated equations involved in the approximate methods than it is to find the solution loci of (3.63). The accuracy of the estimates depends upon two factors: (1) the proximity of loci of horizontal tangency and the backbone curves in the neighborhood of the extrema, and (2) the slope of the curves determined by (3.65b) in the neighborhood of the intersections with the backbone curves. Clearly if the loci of horizontal tangency and the backbone curves are well separated, or if the slope of curves determined by (3.65b) is very steep in the neighborhood of the intersections with the backbone curves, then the approximate methods may yield bounds which are not useful.

If the nonlinear restoring force $F(x, \dot{x})$ contains a viscous damping term $c\dot{x}$, then the equivalent of equations (3.64) and (3.65a) become considerably more complicated. In particular, the loci of horizontal tangency are then determined by

$$-\varkappa_{22}(\omega) = \frac{C(A)}{A} - \left(\frac{z_0}{A}\right)^2 p_2(\omega)\left(\frac{dp_2(\omega)/d\omega}{d\varkappa_{22}(\omega)/d\omega}\right) + \frac{\omega c^2}{(d\varkappa_{22}/d\omega)} - \frac{cS(A)}{A(d\varkappa_{22}(\omega)/d\omega)} \tag{3.66}$$

However, the approximate methods may still provide useful bounds if (3.66) is used in place of (3.64) and if a viscous damping term $-\omega cA$ is added to $S(A)$ in (3.65b). The previous comments concerning the accuracy of the estimates remain applicable, but it will be noted that since (3.66) is more complicated than (3.64), some of the advantages of simplicity have been lost.

In the theory of vibration isolation in linear structures, it is well known that for excitation frequencies which coincide with a resonant frequency of a single component within a complex structure, the resonant component acts as a vibration absorber for the remainder of the structure. This "vibration absorber effect" is frequently used in the design of practical vibration isolation systems. Since the linear system considered here is undamped, a vibration absorber effect exists and is the subject of the following theorem.

Theorem 4: (Vibration Absorber Effect)

If (1) $\kappa_{22}(\omega)$ has first order poles at the frequencies

$\{\omega_{p1}, \omega_{p2}, \cdots\}$

(2) $p_2(\omega)$ has first order poles at the frequencies

$\{\overline{\omega}_{p1}, \overline{\omega}_{p2}, \cdots\}$ where $\forall$ i = 1, 2, ... there exists a

j = 1, 2, ... such that $\overline{\omega}_{pi} = \omega_{pj}$

(3) C(A) and S(A) remain bounded $\forall$ non-negative A

then, as $\omega \to \omega_{pi}$, i = 1, 2, ..., the response amplitude A(ω) as determined by (3.63) approaches a bounded constant value, independent of C(A) and S(A). In particular, as $\omega \to \omega_{pi}$,

$$A \to 0, \text{ if } \omega_{pi} \notin \{\overline{\omega}_{p1}, \overline{\omega}_{p2}, \cdots\}$$

$$A \to \left| \frac{p_2(\omega_{pi})}{\kappa_{22}(\omega_{pi})} \right| z_o, \text{ if } \omega_{pi} \in \{\overline{\omega}_{p1}, \overline{\omega}_{p2}, \cdots\}$$

proof:

Multiplying both sides of (3.63) by A one obtains

$$-A\kappa_{22}(\omega) = C(A) \pm \sqrt{p_2^2(\omega) z_0^2 - S^2(A)} \qquad (3.67)$$

Consider the above equation as $\omega \to \omega_{pi}$, i = 1, 2, ... Two distinct possibilities exist: either $\kappa_{22}(\omega)$ becomes unbounded while $p_2(\omega)$ remains bounded, or both $\kappa_{22}(\omega)$ and $p_2(\omega)$ simultaneously become unbounded.

If $\omega_{pi} \notin \{\overline{\omega}_{p1}, \overline{\omega}_{p2}, \cdots\}$, then as $\omega \to \omega_{pi}$ the right hand side of (3.67) remains bounded, while $\kappa_{22}(\omega)$ becomes unbounded. Clearly,

there exists a solution $A(\omega)$ in this case only if the left hand side simultaneously remains bounded. Thus, it must be that $A \to 0$ as $\omega \to \omega_{pi}$ in this case.

If $\omega_{pi} \in \{\overline{\omega}_{p1}, \overline{\omega}_{p2}, \dots\}$, then as $\omega \to \omega_{pi}$, (3.67) becomes

$$-A\varkappa_{22}(\omega) \cong \pm|p_2(\omega)|z_0$$

Or, noting that A must be non-negative,

$$A \to \left|\frac{p_2(\omega_{pi})}{\varkappa_{22}(\omega_{pi})}\right| z_0$$

where $p_2(\omega_{pi})/\varkappa_{22}(\omega_{pi})$ is bounded, by hypotheses (1) and (2). Q. E. D.

As previously discussed, the load distribution function $p_2(\omega)$ will have zeros at each frequency for which the attachment point corresponds to a node. These zeros of $p_2(\omega)$ are highly dependent upon the details of the spatial distribution of the generalized loads, and may occur in general at any non-negative frequency other than the poles of $p_2(\omega)$. Theorem 5 states that for excitation frequencies corresponding to one of these zeros, the response amplitude must vanish, or lie on one of the backbone curves (for conservative non-linearities).

Theorem 5: [Response at Zeros of $p_2(\omega)$]

If $p_2(\overline{\omega}) = 0$ for some $\overline{\omega}$, then as $\omega \to \overline{\omega}$ either $A(\overline{\omega}) \to 0$ or $A(\overline{\omega}) \to \overline{A}$ where $\overline{A}$ is determined by

$$-\varkappa_{22}(\overline{\omega}) = \frac{C(\overline{A})}{\overline{A}} \quad \text{and} \quad S(\overline{A}) = 0$$

proof:

Eliminating the radical term in (3.63) and solving for $p_2^2(\omega)z_0^2$, one finds

$$A^2\left[\kappa_{22}(\omega) + \frac{C(A)}{A}\right]^2 + S^2(A) = p_2^2(\omega)z_0^2$$

Then, since $p_2(\overline{\omega}) = 0$, $A(\overline{\omega})$ is determined by

$$A^2(\overline{\omega})\left[\kappa_{22}(\overline{\omega}) + \frac{C[A(\overline{\omega})]}{A(\overline{\omega})}\right]^2 + S^2[A(\overline{\omega})] = 0$$

Thus,

$$S[A(\overline{\omega})] = 0$$

and either

$$A(\overline{\omega}) = 0 \quad \text{or} \quad -\kappa_{22}(\overline{\omega}) = \frac{C[A(\overline{\omega})]}{A(\overline{\omega})}$$

Recalling that $S(0) \equiv 0$, it follows that $A(\overline{\omega}) = 0$ or $A(\overline{\omega}) = \overline{A}$ where

$$S(\overline{A}) = 0 \quad \text{and} \quad -\kappa_{22}(\overline{\omega}) = \frac{C(\overline{A})}{\overline{A}} \qquad \text{Q. E. D.}$$

A more detailed description of the response is not easily obtained without restriction to some special applications. In particular, by requiring the load distribution function $p_2(\omega)$ to be constant for all ω, the effects on the response of the linear system and nonlinear constraint are easily separated from those of the load distribution.

In Section 3.4.2 it was shown that $p_2(\omega) = 1$ for all ω if the loading consists only of a single concentrated load applied at the attachment point. Due to the special results which are available in this case, this loading condition may prove to be a convenient experimental arrangement for the identification of an unknown nonlinear constraint force $F(x, \dot{x})$.

Substituting $p_2(\omega) = 1 \ \forall \ \omega$ into (3.63), one finds

$$-\kappa_{22}(\omega) = \frac{C(A)}{A} \pm \frac{1}{A} \sqrt{z_0^2 - S^2(A)} \tag{3.68}$$

where it is noted that the left hand side is independent of amplitude A, while the right hand side is independent of frequency ω. Using this observation it is possible to prove several special results.

From equation (3.65) in this special case, it is clear that the extrema of admissible amplitudes A are determined by

$$z_0^2 = S^2(A) \tag{3.69}$$

independent of frequency and of the linear system. For each response extremum A* determined from (3.69), the corresponding frequencies ω* are determined by the backbone curve frequencies corresponding to amplitude A*. (If $z_0^2 > \sup[S^2(A)]$, when such supremum exists, then there exists unbounded forced response at each backbone curve.)

Also, since equation (3.69) is identical to the analogous equation for a single-degree-of-freedom nonlinear oscillator [57], it can be shown that the condition for the existence of disconnected

response curves is also unchanged. In particular, there exists disconnected response behavior centered on each backbone curve of a chainlike system if $S^2(A)$ exhibits at least one relative maximum. {$S^2(A)$ exhibits exactly one relative maximum in the case of the limited slip nonlinearity [56].}

For the case in which $p_2(\omega) \equiv 1$, several specific statements can be made concerning the qualitative behavior of the entire response curve $A(\omega)$. In the following theorem, sufficient information is developed to sketch such a curve.

Theorem 6: [Qualitative Response Behavior for $p_2(\omega) = 1$]

If (1) $\kappa_{22}(\omega)$ is the transfer function of an undamped linear chainlike structure with poles at $\{\omega_{p1}, \omega_{p2}, \ldots, \omega_{pn}\}$

(2) Attachment point P has non-zero mass

(3) $p_2^2(\omega) = 1 \; \forall \; \omega$

(4) $C(A)/A \geq 0 \; \forall \; A \geq 0$, and $\lim_{A \to \infty} C(A)/A$ exists

(5) A is restricted to those regions where $z_0^2 > S^2(A)$ (i.e., excluding amplitude extrema)

then (a) there exists exactly two frequencies ω in each of the n intervals $(\omega_{p1}, \omega_{p2}), \ldots, (\omega_{pn}, \infty)$ which satisfy (3.68) for a given amplitude A

(b) in the interval $[0, \omega_{p1})$, there exists exactly two frequencies ω which satisfy (3.68) for each amplitude A such that

$$A^2\left[\frac{C(A)}{A} + \kappa_{22}(0)\right]^2 + S^2(A) \geq z_0^2$$

and exactly one frequency ω for each amplitude A such that

$$A^2\left[\frac{C(A)}{A} + \kappa_{22}(0)\right]^2 + S^2(A) < z_0^2$$

(c) within any of the above frequency intervals, each pair of frequencies corresponding to the same amplitude A are separated by the backbone curve frequency at that amplitude.

proof:

By hypothesis (5) and (3.68), the steady-state response is determined by the loci of all solutions $A(\omega)$ of each of the equations

$$-\kappa_{22}(\omega) = \frac{C(A)}{A} + \frac{1}{A}\sqrt{z_0^2 - S^2(A)} \qquad (3.70)$$

$$-\kappa_{22}(\omega) = \frac{C(A)}{A} - \frac{1}{A}\sqrt{z_0^2 - S^2(A)}$$

By hypotheses (1) and (2), the left hand side of each of (3.70) is a strictly increasing function of ω, ranging from $-\infty$ to $+\infty$ in each of the n intervals $(\omega_{p1}, \omega_{p2}), \ldots, (\omega_{pn}, \infty)$. Hence, in each of these intervals there exists exactly one frequency satisfying each of (3.70) for a given amplitude A. Furthermore, by comparing (3.62) with (3.70) and using the property that the left hand side of each is strictly increasing, it is seen that within each interval, each pair of frequencies ω satisfying (3.70) for a given amplitude A are

distinct and separated by the backbone curve frequency satisfying (3.62) for the same amplitude A.

In the interval $[0, \omega_{p1})$, the left hand side of each of (3.53) is strictly increasing, ranging from $-\kappa_{22}(0)$ to $+\infty$, by hypothesis (1). Thus, by hypothesis (4), there exists exactly one frequency ω satisfying the first of (3.70) for any non-negative amplitude A which satisfies hypothesis (5). However, there exists exactly one frequency ω satisfying the second of (3.70) only for those amplitudes A such that

$$\frac{C(A)}{A} - \frac{1}{A}\sqrt{z_0^2 - S^2(A)} \geq \min_{\omega \in [0, \omega_{p1})} [-\kappa_{22}(\omega)]$$

or

$$A^2\left[\frac{C(A)}{A} + \kappa_{22}(0)\right]^2 + S^2(A) \geq z_0^2 \qquad (3.71)$$

and such that hypothesis (5) is satisfied. Note by solving (3.68) for z_0^2 that equality in (3.71) represents the condition for "static" solutions. [It should be recalled that (3.68) and hence (3.71) are subject to the approximations discussed in Chapter II, so that static solutions determined from (3.71) are only approximate.] Clearly as $A \to 0$, the inequality in (3.71) is violated, so that there always exists a region of amplitudes for which the second of (3.70) poses no solution for $\omega \in [0, \omega_{p1})$.

Finally, for $\omega \in [0, \omega_{p1})$ and for amplitudes A such that there exists a unique frequency satisfying each of (3.70), these two

frequencies are distinct and separated by the backbone curve frequency satisfying (3.62) for the same amplitude A, by hypothesis (1). Q. E. D.

It can be shown graphically that increasing (decreasing) z_0^2 in (3.69) can only increase (decrease) the response extrema which correspond to maxima and decrease (increase) those extrema which correspond to minima. Similarly, it can be shown for fixed amplitude A that increasing (decreasing) z_0^2 in (3.68) can only increase (decrease) the width of the response curves about the locus of horizontal tangency. Based on these results and the previous theorems, sufficient information has been developed at this point to sketch the qualitative behavior of $A(\omega)$ for various excitation levels. Figure 3.12 shows a typical response curve $A(\omega)$ for a chainlike system with loading such that $p_2(\omega) \equiv 1$ for all ω.

The previous theorems provide useful information on certain general features of the response $A(\omega)$, and on the way in which these features may be affected by various alterations in the linear system, nonlinear constraint, and loading distribution. In particular, it was shown that in the A, ω plane, the response is separated by the poles of $\varkappa_{22}(\omega)$ into distinct regions which contain a single backbone curve. The backbone curves represent undamped free vibrations (for conservative systems) and have similar hardening and softening behavior (for chainlike systems). The number and general location of backbone curves was shown to be determined by the passive linear system, with the hardening or softening behavior

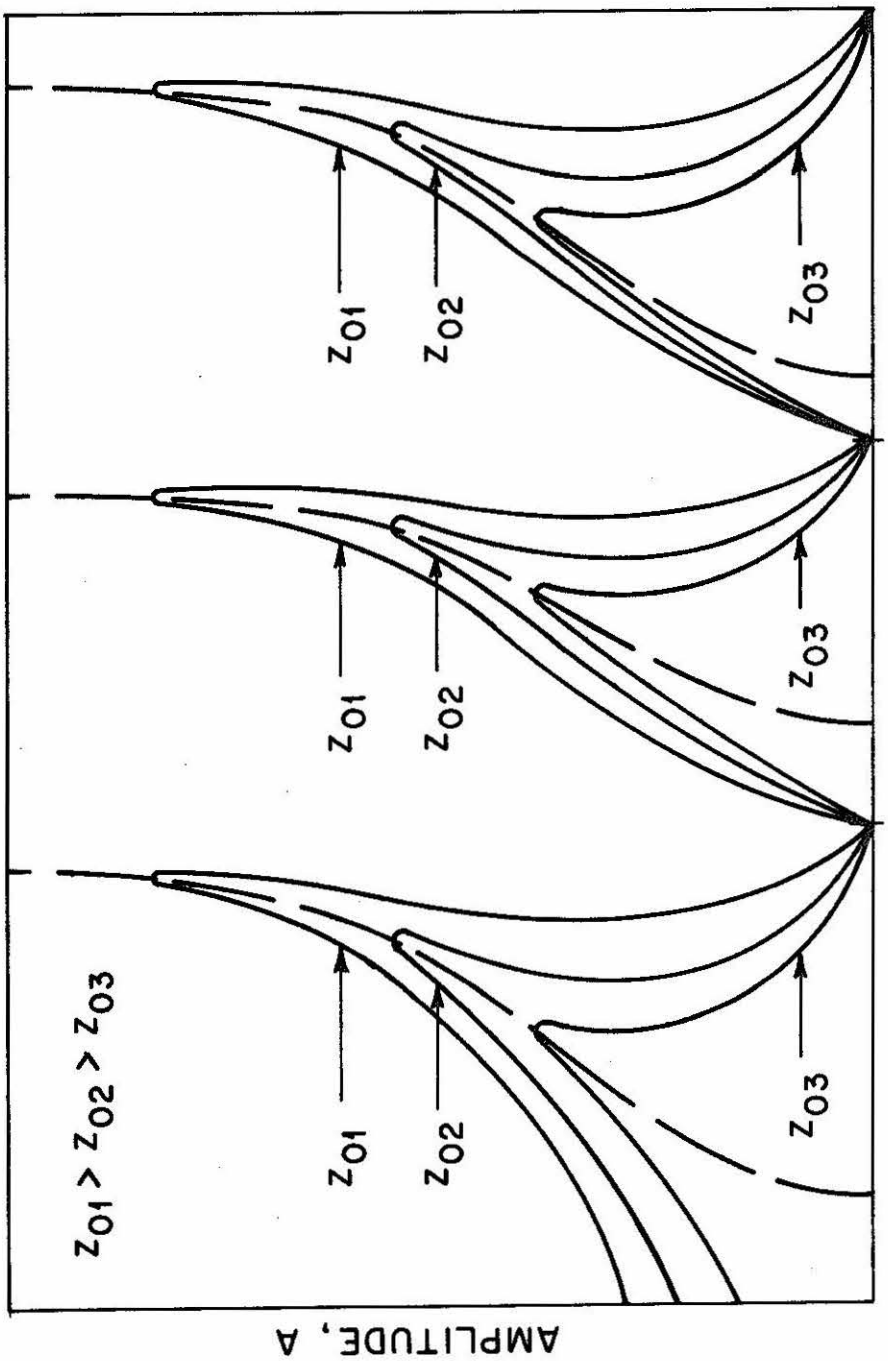

Figure 3.12 - Qualitative Dependence of A(ω) on Excitation Level for an Undamped Chainlike System with Loading such that $p_2(\omega) = 1$

determined by the nonlinear constraint force $F(x, \dot{x})$. The loading distribution has no effect on this basic structure of the response diagram $A(\omega)$.

It was also shown that as the excitation frequency makes the transition from one of these distinct regions to another, the response $A(\omega)$ is single-valued and passes through a bounded constant whose value is determined by the passive linear system and the loading distribution, independent of the nonlinear constraint. It was also shown that unbounded forced response may occur only in special circumstances depending on all three factors, and that for strictly dissipative nonlinearities the response $A(\omega)$ vanishes at the zeros of the load distribution function.

Finally, it was also shown that depending on the load distribution, the local response extrema may occur on either side of the backbone curves, and approximate methods for estimating the location of response extrema were presented.

3.5.3 Forced Oscillations of Generally Dissipative Systems

In this section, consideration is given to the forced oscillations of a strictly dissipative linear system with a general nonlinear terminal constraint. Consideration of strictly dissipative linear systems is important, since all real structures are strictly dissipative. The nonlinear constraint may be conservative, or it may be viscously and hysteretically dissipative.

Recall that for strictly dissipative linear systems, $Y_{22}(\omega)$ is strictly positive for all non-zero ω. Thus, the amplitude response

$A(\omega)$ is determined by equation (3.3) with this restriction on $\gamma_{22}(\omega)$.

Since (3.3) applies to a rather broad class of systems, nonlinearities, and load distributions, relatively few similarities in the details of the response can reasonably be anticipated. Thus, it is difficult to make general statements concerning the qualitative behavior of the response, as evidenced by the complexity of equation (3.3). However, the restriction of $\gamma_{22}(\omega)$ to positive values is sufficient to provide the following boundedness theorem. In addition, by neglecting the energy dissipated in the nonlinear constraint, the theorem provides a bound on the maximum amplitude which is independent of the nonlinearity.

Theorem 7: (Boundedness of Damped Response)

If the linear system is strictly dissipative, then all steady state response amplitudes $A(\omega)$ are bounded from above by $[p_2^2(\omega) + \omega^2 q_2^2(\omega)]^{\frac{1}{2}} z_0/\omega\gamma_{22}(\omega)$, $\forall\ \omega > 0$.

proof:

Observe that the left hand side of (3.3) is a real valued function of ω. Note that the right hand side is also real valued only for those values of A and ω such that

$$[p_2^2(\omega) + \omega^2 q_2^2(\omega)]z_0^2 \geq [\omega\gamma_{22}(\omega)A - S(A)]^2 \qquad (3.72)$$

Hence, (3.72) represents a restricted region in the A, ω plane outside of which solutions $A(\omega)$ to (3.3) cannot exist. Clearly the

boundaries of this region (which represent extrema of admissible response at any given frequency) are determined by equality in (3.72)

$$[p_2^2(\omega) + \omega^2 q_2^2(\omega)]z_0^2 = [\omega \gamma_{22}(\omega)A - S(A)]^2 \qquad (3.73)$$

But since $F(x, \dot{x})$ is passive, equation (3.6) requires that

$$\omega \gamma_{22}(\omega)A - S(A) \geq \omega \gamma_{22}(\omega)A \geq 0 \quad \forall\, A, \omega \geq 0 \qquad (3.74)$$

so that an upper bound $A^*(\omega)$ on the response maximum is obtained from (3.73) by using (3.74) to obtain

$$A^*(\omega) = \frac{[p_2^2(\omega) + \omega^2 q_2^2(\omega)]^{\frac{1}{2}} z_0}{\omega \gamma_{22}(\omega)} \qquad (3.75)$$

As noted in Section 3.4.1, $p_2(\omega)$ and $q_2(\omega)$ are bounded $\forall\, \omega$ for strictly dissipative systems, so that $A^*(\omega)$ is bounded $\forall\, \omega > 0$.

Therefore, since $A^*(\omega)$ is bounded for all $\omega > 0$, all response amplitudes $A(\omega)$ determined from (3.3) are also bounded for strictly dissipative systems. Q.E.D.

Since a considerable variation in response behavior is expected when comparing the damped response of different systems, it is more reasonable to compare the damped and undamped response of the same system. In particular, for base excitation of mass-terminated chainlike structures with light viscous damping, the transfer function properties given in Sections 3.3.5 and 3.4.3 help to provide some insight into the effect of damping on the

response. In such a case, the effect on the response of both the load distribution and the linear system are determined by $\kappa_{22}(\omega)$ and $\gamma_{22}(\omega)$. As previously shown, the transfer functions $\kappa_{22}(\omega)$ and $\gamma_{22}(\omega)$ for lightly damped systems are very closely approximated by the corresponding undamped transfer functions for all frequencies which are not near the undamped poles of $\kappa_{22}(\omega)$. Thus, the lightly damped response will generally be closely approximated by the undamped response for all such frequencies. However, for excitation frequencies which are near the undamped poles of $\kappa_{22}(\omega)$, the damped transfer functions $\kappa_{22}(\omega)$ and $\gamma_{22}(\omega)$ differ markedly from the undamped functions, as shown in Figure 3.7. It is therefore expected that major qualitative differences between the damped and undamped response may occur near these undamped poles. Unfortunately, it is difficult to predict the nature of these qualitative differences without restricting consideration to a particular nonlinearity.

For the single-degree-of-freedom nonlinear oscillator, it has been shown [56] that the effects of increasing the level of viscous damping are: (1) to decrease the value of all response maxima, (2) to increase the value of all response minima, and (3) for fixed response amplitude, to cause the corresponding excitation frequency to move nearer to the frequency corresponding to the same fixed amplitude on the locus of horizontal tangency. Although it is not easily proven, similar results are expected for increasing levels of viscous damping in the multidegree-of-freedom case.

IV. Numerical Examples of Harmonic Response of Systems with a Nonlinear Terminal Constraint

4.1 General Remarks

Presented in this chapter are quantitative examples of the harmonic response of three different structural systems. These examples demonstrate the application of the general formulation of Chapter II to both continuous and discrete linear systems, with different generalized excitations, and with nonlinearities ranging from conservative hardening and softening to hysteretic.

In addition to providing examples of the general theory of the previous chapters, the present investigation includes consideration of a model for nonlinear structural behavior which has not been previously presented. The structural model, which is assembled from linear elastic springs and a Coulomb friction slider, produces hysteresis loops whose limiting behavior approaches that of the elastoplastic, the bilinear hysteretic, or the so-called "limited slip" [58] models for various parameter values.

Consideration is also given to the accuracy of the approximate solution. A comparison is made between the approximate and exact solutions (obtained by numerical integration of the equations of motion) for three different systems and various excitation frequencies.

4.2 Steady-State Response to Harmonic Base Excitation of a Uniform Shear Beam with a Cubic Spring Terminal Constraint

4.2.1 Application of General Formulation

Depicted in Figure 4.1 is an idealized model for the physical system under consideration. The system consists of a uniform shear beam (shown vertically erect) with one end stress free and the other constrained by a one-dimensional nonlinear structural element. Excitation is provided by an impressed harmonic displacement of the rigid base of the system, to which one end of the nonlinear element is attached. In this case, x (which represents the deformation in the nonlinear element) measures the relative displacement between the end of the shear beam and the base of the system. Such a system might be used to model the behavior of a tall building mounted on a nonlinear foundation, or a soil profile bonded nonlinearly to a rigid substructure.

The nonlinear structural element is assumed to have a restoring force given by

$$F(x, \dot{x}) = kx(1 + \epsilon x^2) + c\dot{x} \qquad (4.1)$$

where k is a linear spring constant, c is a viscous damping coefficient, and ϵ is a (small) nonlinearity parameter, which produces hardening behavior when positive and softening behavior when negative. Thus, the nonlinear structural element consists of a parallel combination of a linear spring, a cubic spring, and a viscous dashpot.

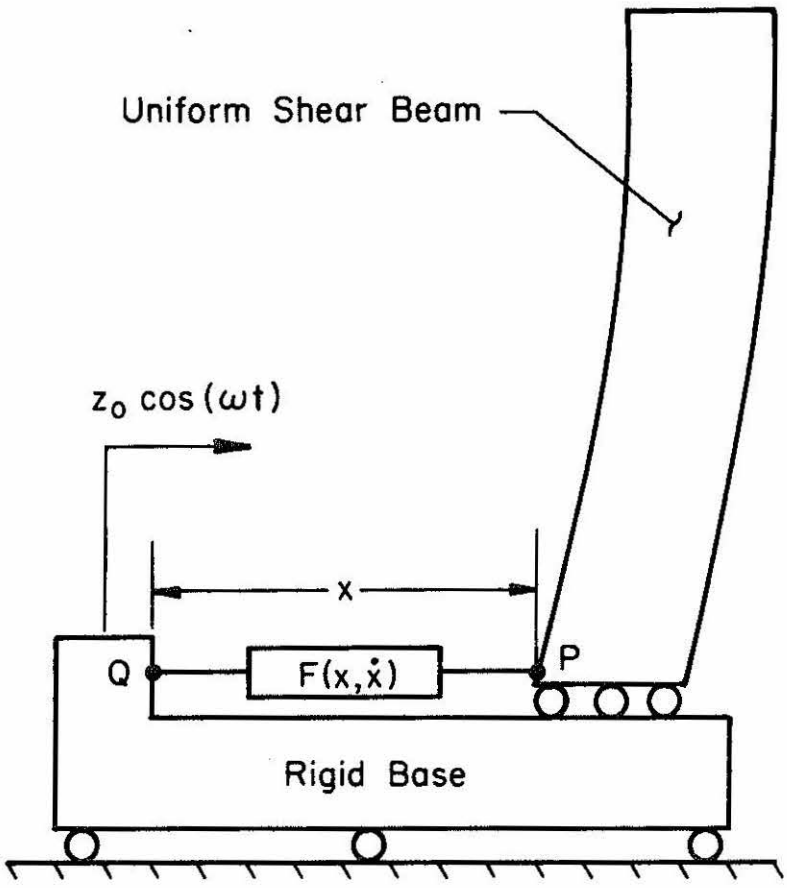

Figure 4.1 - Base Excitation of a Uniform Shear Beam with a Nonlinear Terminal Constraint

Substituting (4.1) into (2.31), and using (2.27), one finds that the "equivalent linear stiffness" of such a nonlinearity is given by

$$\frac{C(A)}{A} = k(1 + \tfrac{3}{4}\epsilon A^2) \tag{4.2}$$

and that the "equivalent linear damping coefficient" is simply the viscous damping coefficient, c. Thus,

$$-\frac{S(A)}{\omega A} = c \tag{4.3}$$

The linear system takes the form of a uniform free-free shear beam, with attachment point P taken at one end. The complex frequency transfer function $H_{22}(i\omega)$ is the force developed in the shear beam at P, in response to an impressed displacement time-history $e^{i\omega t}$ applied at P. The force is positive when in the same direction as positive displacement.

If ℓ is the length of the shear beam, a is the cross-sectional shear area, G is the shear modulus of the material, and ρ is the mass density, then one finds that

$$H_{22}(i\omega) = -\left(\frac{Ga}{\ell}\right)\left(\frac{\omega\ell}{V}\right)\tan\left(\frac{\omega\ell}{V}\right) \tag{4.4}$$

where

$$V \equiv (G/\rho)^{\frac{1}{2}} \tag{4.5}$$

is the velocity of shear waves in the beam. Thus, from (2.34), one finds that

$$\left.\begin{aligned} \varkappa_{22}(i\omega) &= -\left(\frac{Ga}{\ell}\right)\left(\frac{\omega\ell}{V}\right)\tan\left(\frac{\omega\ell}{V}\right) \\ \gamma_{22}(\omega) &= 0 \end{aligned}\right\} \quad (4.6)$$

It is easily verified that $\varkappa_{22}(\omega)$ is strictly decreasing for all positive ω and ranges monotonically from $+\infty$ to $-\infty$ for all ω between consecutive poles of $\tan \frac{\omega\ell}{V}$. Hence, the behavior of $\varkappa_{22}(\omega)$ is qualitatively identical to that of a linear chainlike structure, as discussed in Section 3.3.4, except that there exist infinitely many poles and zeros.

Since the linear system corresponds to a shear beam with both ends free, it is analogous to a mass-terminated linear chainlike structure, as described in definition (D9). Therefore, equations (3.53) remain valid, so that

$$\left.\begin{aligned} p_2(\omega) &= -\left(\frac{Ga}{\ell}\right)\left(\frac{\omega\ell}{V}\right)\tan\left(\frac{\omega\ell}{V}\right) \\ q_2(\omega) &= 0 \end{aligned}\right\} \quad (4.7)$$

Thus, $p_2(\omega)$ and $\varkappa_{22}(\omega)$ are identical and share the same poles and zeros.

For convenience, let

$$\left.\begin{aligned} \frac{Ga}{\ell} &= \frac{2}{\pi} \\ \frac{\ell}{V} &= \frac{\pi}{2} \end{aligned}\right\} \quad (4.8)$$

Then, it is easily shown that the poles of $\varkappa_{22}(\omega)$ and $p_2(\omega)$ occur at

$\omega = 1, 3, 5, \ldots$ and that the zeros occur at $\omega = 0, 2, 4, 6, \ldots$ Furthermore, let

$$k = \frac{Ga}{\ell} = \frac{2}{\pi} \tag{4.9}$$

Substituting (4.2), (4.3), (4.6)-(4.9) into (3.3) and (3.62), it is found that the approximate steady-state solutions for forced oscillations are governed by the transcendental equation

$$\omega \tan\left(\frac{\pi\omega}{2}\right) = \frac{2}{\pi}\left(1 + \tfrac{3}{4}\epsilon A^2\right) \pm \frac{1}{A}\sqrt{z_0^2\omega^2\tan^2\left(\frac{\pi\omega}{2}\right) - \omega^2 c^2 A^2} \tag{4.10}$$

The backbone curves (which represent the approximate steady-state solution for free oscillations) are governed by

$$\omega \tan\left(\frac{\pi\omega}{2}\right) = \frac{2}{\pi}\left(1 + \tfrac{3}{4}\epsilon A^2\right) \tag{4.11}$$

Equations (4.10) and (4.11) were solved iteratively by digital computation, and the resulting loci of solutions are shown in Figs. 4.2-5. The solid lines represent the approximate solution for forced oscillations, as determined by (4.10), the broken lines represent the approximate solution for free oscillations (for $c = 0$), as determined by (4.11), and the data points represent "exact" solutions, which are discussed at the end of this chapter.

Depicted in Figure 4.2 are the loci of approximate steady-state solutions for the first five "modes" of the system with no viscous dissipation (i.e., $c = 0$). The nonlinearity parameter is

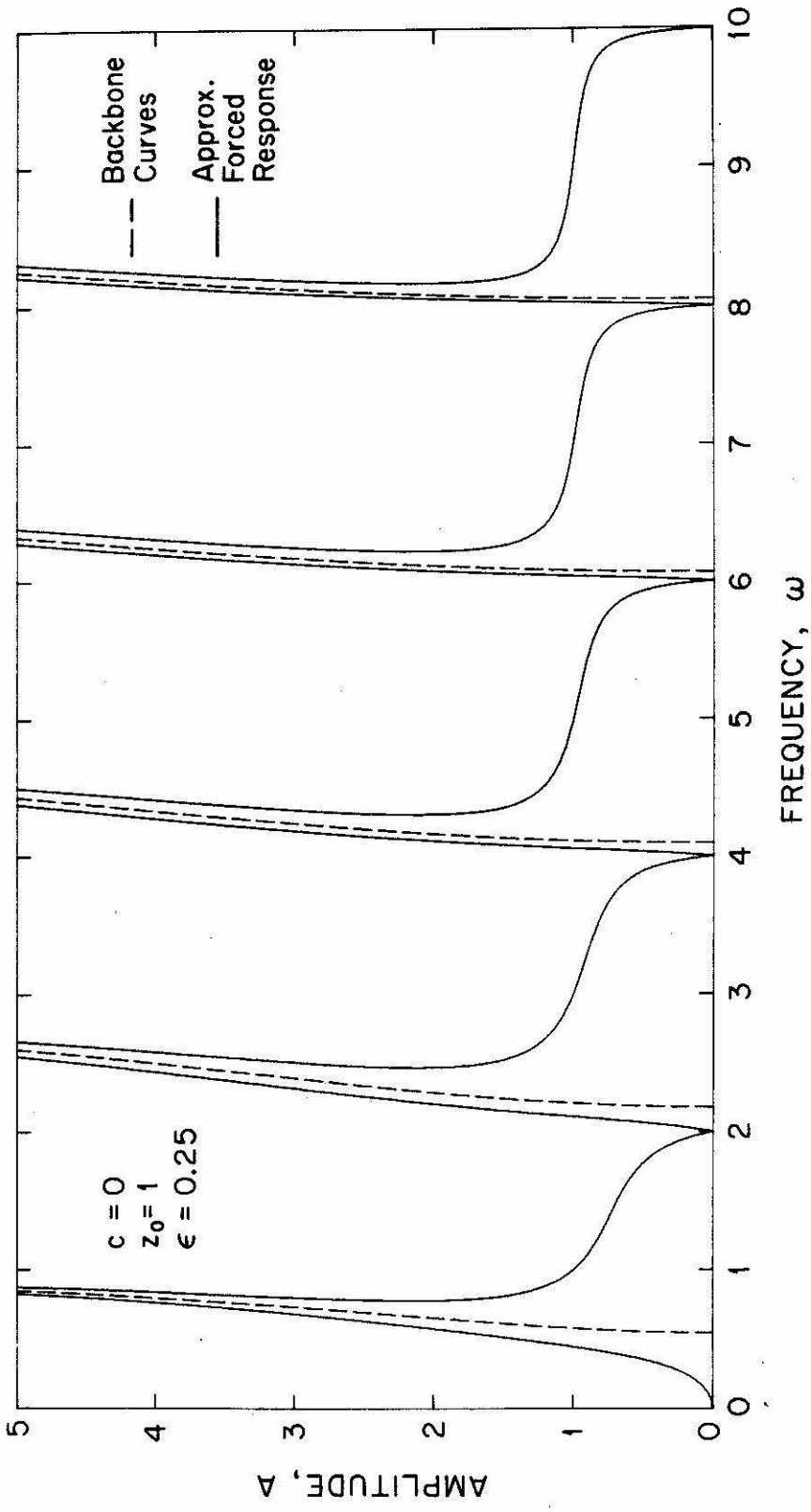

Figure 4.2 - Approximate Steady-State Response for Free and Forced Oscillations of the Undamped Cubic Hardening System

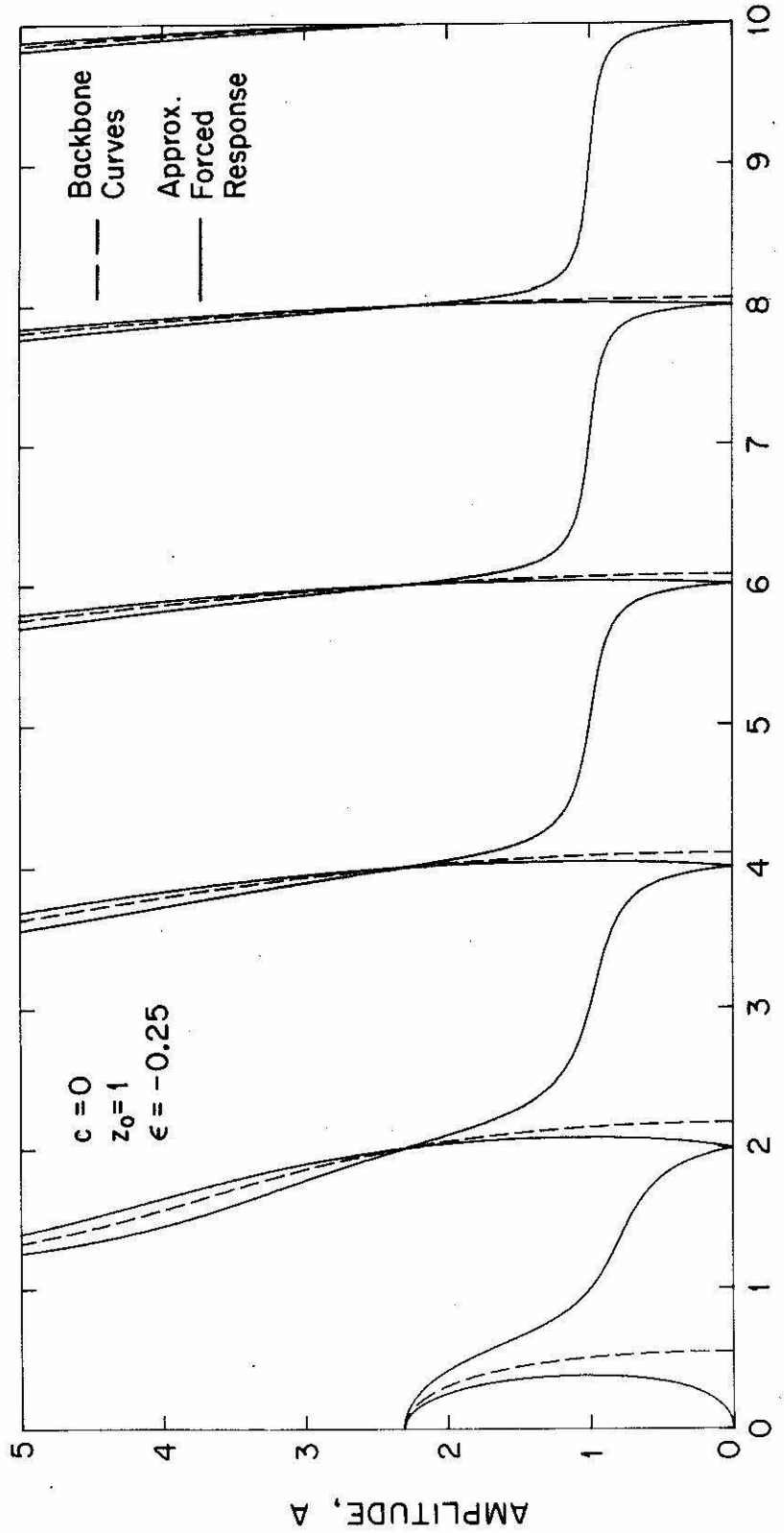

Figure 4.3 - Approximate Steady-State Response for Free and Forced Oscillations of the Undamped Cubic Softening System

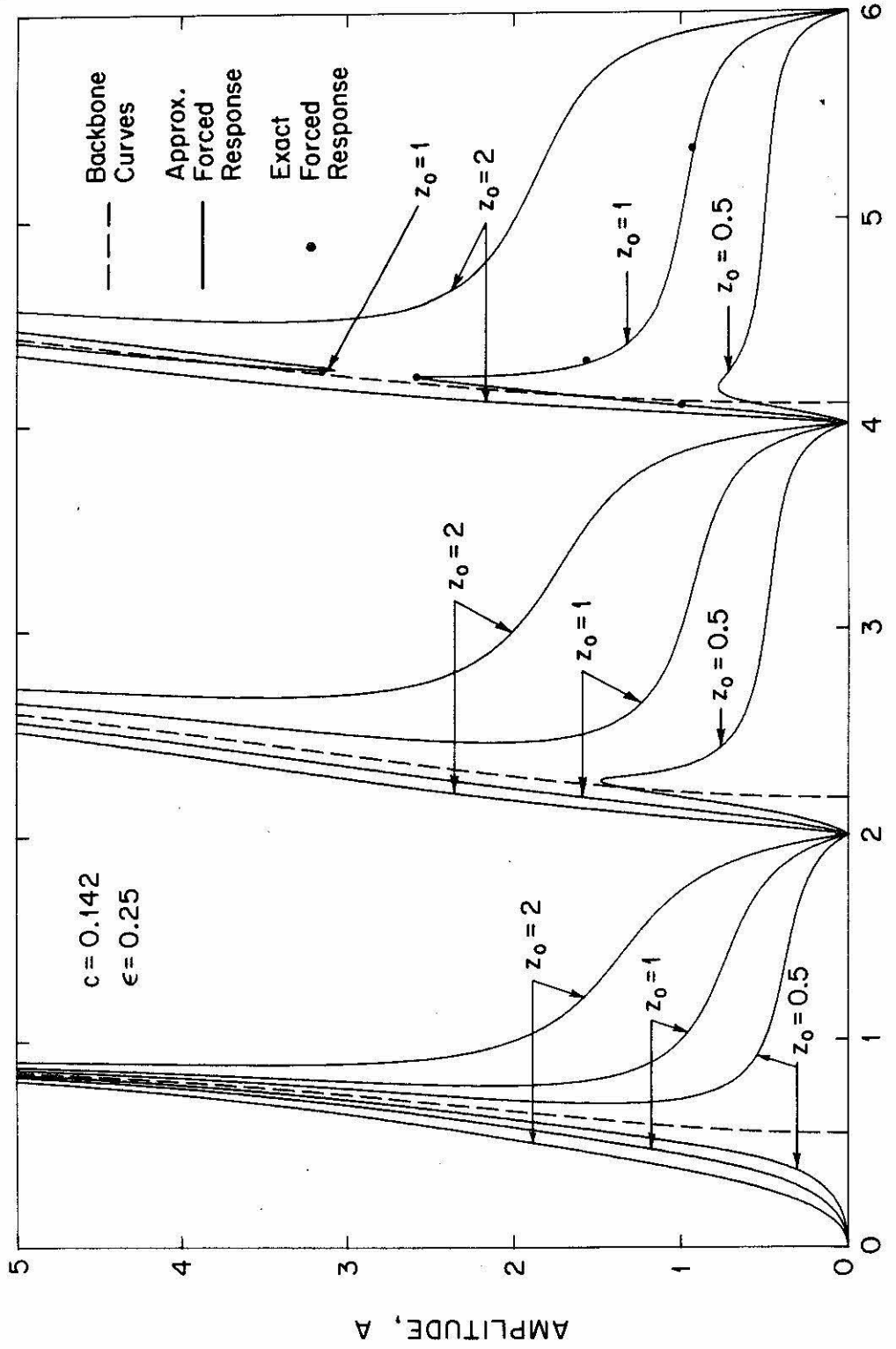

Figure 4.4 - Approximate Steady-State Response for Forced Oscillations of the Damped (c = 0.142) Cubic Hardening System for Three Excitation Levels

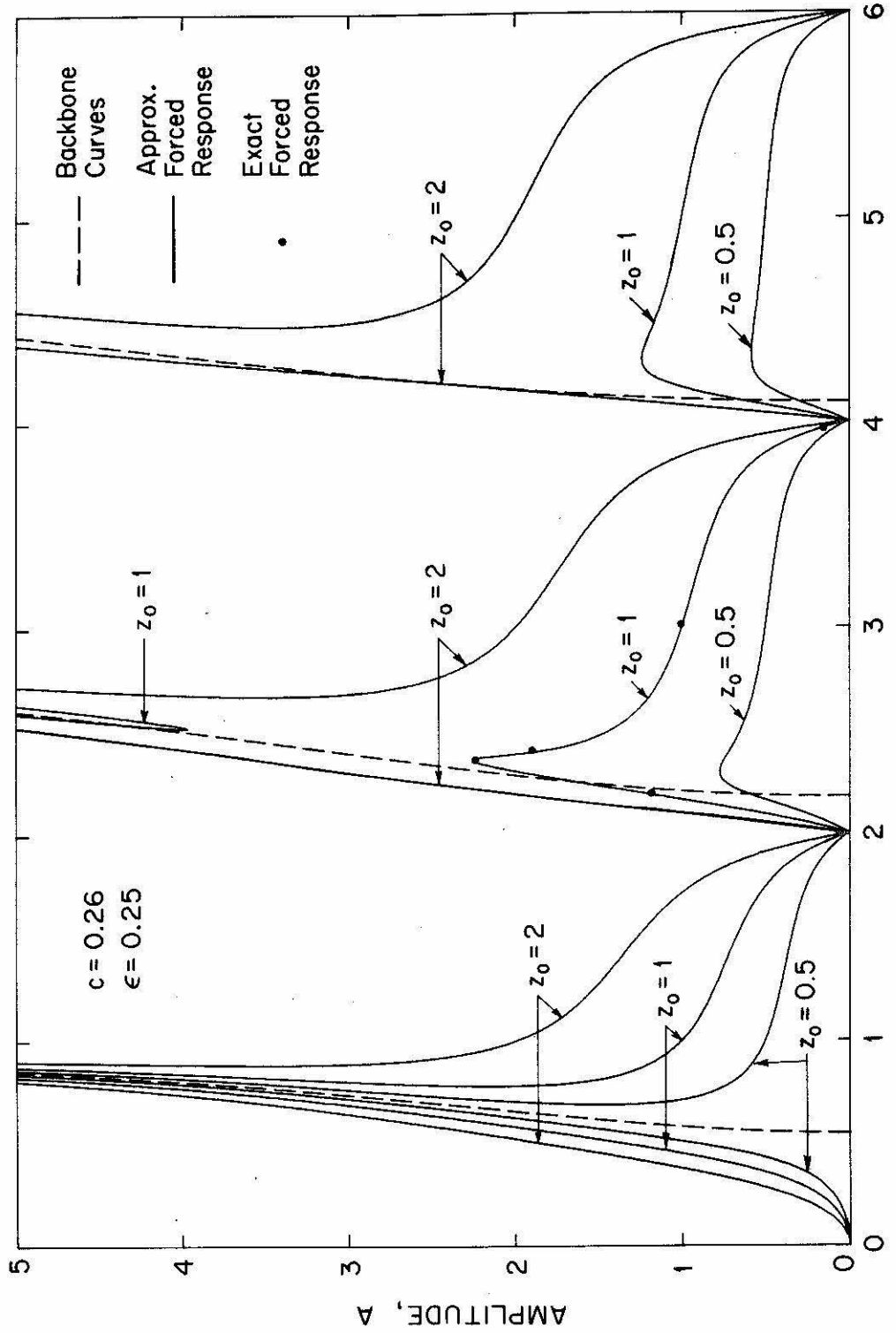

Figure 4.5 - Approximate Steady-State Response for Forced Oscillations of the Damped (c = 0.26) Cubic Hardening System for Three Excitation Levels

quite large ($\epsilon = +0.25$) and represents a cubic hardening spring. The level of excitation is $z_0 = 1$.

Shown in Figure 4.3 are similar solutions for a cubic softening system, with $\epsilon = -0.25$. The system is again nondissipative ($c = 0$), and the level of excitation is again $z_0 = 1$.

Shown in Figure 4.4 are the approximate steady-state solutions for the first three modes of the system, for three different excitation levels: $z_0 = 0.5,\ 1.0,\ 2.0$. The system is hardening ($\epsilon = +-.25$) and dissipative ($c = 0.142$). Shown in Figure 4.5 are similar solutions for a system with more viscous dissipation ($c = 0.260$). All other parameters are the same as in Figure 4.4.

4.2.2 Discussion of Free Oscillations

The approximate solutions for steady-state free oscillations are best studied in Figures 4.2 and 4.3, where they are shown as broken lines. It is observed from Figure 4.2 that, for the cubic hardening system, each backbone curve exhibits similar hardening behavior. Similarly, it is observed from Figure 4.3 that, for the cubic softening system, each backbone curve exhibits similar softening behavior. These observations agree with the predictions in Theorem 1 of Chapter III, since, for $C(A)/A$ as given in (4.2), the derivative $\frac{d}{dA}[C(A)/A]$ is positive for positive ϵ and negative for negative ϵ.

It is further observed that, in each of Figures 4.2 and 4.3, exactly one backbone curve exists in each of the frequency intervals $[0, 1)$, $(1, 3)$, $(3, 5)$, etc., where it will be recalled that the odd

positive integers are poles of $\alpha_{22}(\omega)$, as given in (4.6) and (4.8). These observations agree with the predictions in Theorem 2 of Chapter III.

Referring to Figure 4.2, it is seen that, for small amplitude oscillations, the backbone curve frequencies approach the natural frequencies of the system with linear spring constraint only. However, as the amplitude increases, the nonlinear constraint monotonically becomes stiffer, until, as the amplitude becomes unbounded, the constraint becomes effectively rigid. Such an interpretation is justified by examining equation (4.2), which determines the effective stiffness of the nonlinear constraint. Thus, for large amplitude oscillations, each of the backbone curves assymptotically approaches one of the natural frequencies of the rigidly constrained system [i.e., the poles of $\alpha_{22}(\omega)$].

Clearly, the effect of increasing (decreasing) the linear spring constant k in (4.1) is to increase (decrease) each of the backbone curve frequencies corresponding to small amplitude oscillations. Such variations have a negligible effect on the large amplitude oscillations. It is also found that the effect of increasing (decreasing) the magnitude of the nonlinearity parameter, ϵ, is to increase (decrease) the extent to which the backbone curves lean in Figure 4.2.

Referring to Figure 4.3 it is seen that a more complicated situation exists. Although all backbone curves are softening and exhibit the expected small amplitude behavior, the first backbone curve clearly differs from the rest in that it terminates at a finite

amplitude. This unusual behavior results from the fact that, for the cubic softening nonlinearity, there exists a critical amplitude A_{cr} above which the effective stiffness of the constraint becomes negative. This critical amplitude is found by equating to zero the effective stiffness, C(A)/A, in equation (4.2). For the parameters corresponding to Figure 4.3, one finds

$$A_{cr} = \frac{4}{\sqrt{3}} \tag{4.12}$$

Clearly, as the amplitude of oscillation approaches A_{cr}, the effective stiffness of the constraint approaches zero, causing the backbone curve frequencies to approach the natural frequencies of the unconstrained system [i.e., the zeros of $\kappa_{22}(\omega)$]. This phenomenon is demonstrated in Figure 4.3, where it is noted that the unconstrained natural frequencies are $\omega = 0, 2, 4, 6$, etc.

For oscillation amplitudes larger than A_{cr}, the nonlinear restoring force is negative over most of each cycle of oscillation, which results in a negative effective constraint stiffness. Such negative stiffness characteristics might, for example, be encountered in models which include the destabilizing effects of gravity for large displacements (e.g., the "P-Δ" effect).

Referring to Figure 4.3, it is observed that large amplitude (i.e., $A \cong A_{cr}$) free oscillations represented by the first backbone curve occur at vanishingly small excitation frequencies. At such low frequencies, the shear beam moves essentially as a rigid body.

An analysis of the single-degree-of-freedom system which results by modeling the shear beam as a rigid body has been performed [59]. In that study, the existence of such a critical amplitude was also reported. For low frequency motions with amplitude larger than A_{cr}, the destabilizing effect of the negative restoring force prevents any oscillations by driving the motion increasingly in one direction (i.e., $x \rightarrow \pm\infty$).

Oscillations with amplitude larger than A_{cr} do exist, however, and are represented by the second and successive backbone curves. At these higher frequencies the motion is no longer "quasi-static," and significant deformation in the shear beam is required to produce such oscillations. It is noted from equation (4.2) that as the amplitude of response increases without bound, the effective constraint stiffness approaches negative infinity. Thus, for large oscillations each backbone curve asymptotically approaches the next lower natural frequency of the rigidly constrained system.

The effects of varying the linear spring stiffness, k, and the nonlinearity parameter, ϵ, are the same as described for the hardening system.

4.2.3 Discussion of Forced Oscillations without Viscous Dissipation

The approximate solutions for steady-state forced oscillations of the system with no viscous dissipation (i.e., c = 0) are shown as solid lines in Figures 4.2 and 4.3. It is observed in each figure that the response is separated by the poles of $\kappa_{22}(\omega)$ into distinct regions, each of which contains a single backbone curve and two

separate branches of the solution loci. It is found that the phase lag, φ [defined in equation (2.27)], corresponding to each branch of the solution loci is either zero or π. Furthermore, starting from the origin in each figure and proceeding in the direction of increasing frequency, it is found that, for each successively encountered solution branch, the corresponding phase lag alternates between zero and π, in that order. These observations are in agreement with the predictions given in Chapter III concerning the general structure of the response diagram.

Careful examination of the response reveals that the steady-state amplitude passes through the value A = 1 as the excitation frequency passes through the values $\omega = 1, 3, 5$, etc., which correspond to the poles of $\varkappa_{22}(\omega)$. Such behavior is in agreement with the predictions in Theorem 4 of Chapter III regarding the vibration absorber effect. Applying the theorem to the systems discussed in this section, it is found that as the excitation frequency approaches one of the poles of $\varkappa_{22}(\omega)$, the corresponding response amplitude must approach the level of excitation, which in this case is $z_0 = 1$. Furthermore, the theorem states that this result is independent of the nonlinearity and is therefore independent of k, ϵ, and c.

Referring to Figure 4.2, it is observed that the response amplitude passes through the value A = 0 as the excitation frequency passes through each of the values $\omega = 0, 2, 4, 6$, etc., which correspond to the zeros of $p_2(\omega)$. Identical observations are noted in Figure 4.3. Such behavior is in agreement with the predictions in Theorem 5 of Chapter III concerning the response near the zeros

of $p_2(\omega)$. Furthermore, the theorem predicts that such behavior is independent of the nonlinearity and is therefore independent of k, ϵ, and c.

Referring to Figure 4.3, the branches of the solution loci are observed to cross, while for the hardening system in Figure 4.2 they remain separated. More careful examination of the response reveals that the intersection of each pair of crossing branches lies on a backbone curve at the common amplitude $A = A_{cr}$, as given in (4.12). Furthermore, the frequency at which intersection occurs is one of the values $\omega = 0, 2, 4, 6$, etc., which correspond to the zeros of $p_2(\omega)$. Such behavior again is also in agreement with the predictions in Theorem 5 of Chapter III. In this case, the theorem predicts that as the excitation frequency approaches one of the zeros of $p_2(\omega)$, the corresponding response must approach the backbone curve at the amplitude corresponding to such zeros (i.e., $A = A_{cr}$). An alternate interpretation is that as ω approaches one of the zeros of $p_2(\omega)$, the effective amplitude of excitation vanishes, so that the only possible response is either that of free oscillations or no motion at all, both of which are observed in Figure 4.3.

It is possible to extend the proof of Theorem 3 in Chapter III to the case of a cubic nonlinearity [i.e., $\lim_{A \to \infty} \frac{C(A)}{A}$ is unbounded]. Applying the theorem one then finds that unbounded oscillations occur at each pole of $\kappa_{22}(\omega)$, in the case of either the hardening or softening systems. Thus, as the response amplitude becomes

unbounded, each pair of solution branches in Figures 4.2 and 4.3 must converge onto the backbone curve which separates them. Furthermore, this behavior occurs for all excitation levels, as expected for conservative systems.

4.2.4 Discussion of Forced Oscillations with Viscous Dissipation

Forced oscillations of the cubic hardening system for three different values of excitation are shown in each of Figures 4.4 and 4.5, for respectively different values of viscous dissipation. As predicted in Theorem 4 of Chapter III, it is observed for each curve in each figure that the response amplitude approaches the value $A = z_0$ as the excitation frequency approaches each pole of $\kappa_{22}(\omega)$. These observations are in agreement with the predictions that this feature of the response is independent of the level of viscous dissipation. Furthermore, it is also observed for each curve in each figure that the response amplitude approaches the value $A = 0$ as the excitation frequency approaches each zero of $p_2(\omega)$. These observations are in agreement with the predictions in Theorem 5 of Chapter III, that this feature of the response is not only independent of the level of viscous dissipation, but is also independent of the level of excitation.

Referring to Figure 4.4, it is observed that near the first backbone curve the response for each excitation level is similar in that there are two separate solution branches which continuously converge on the backbone curve as the response amplitude increases. Near the second backbone curve, it is seen that the response for the

two largest excitation levels is qualitatively unchanged, but that for the smallest excitation level the response takes the form of a single solution branch which crosses the backbone curve and displays a peak slightly to the right.

Near the third backbone curve the response is quite interesting. It is seen that for the largest excitation level the response is again qualitatively unchanged, and for the lowest excitation level the response is also qualitatively unchanged, except that the response peak is lower in amplitude and occurs farther to the right of the backbone curve. However, for the intermediate excitation level, it is seen that there exists two disjoint solution branches which each cross the backbone curve. The lower branch displays a peak slightly to the right of the backbone curve, while the upper branch displays a minimum, also to the right. It is the upper branch of this response which is interesting. It can be shown that this branch extends up to unbounded amplitudes. Furthermore, it can be shown that unbounded response exists near each backbone curve for any nonzero excitation level, even though the constraint contains a viscous dissipation element. Such a result is peculiar to this system and is a consequence of the fact that the shear beam is undamped and that the effective stiffness becomes unbounded for large amplitudes. Hence, there also exists a disjoint upper branch corresponding to the response for the lowest excitation level near each of the second and third backbone curves. However, these

branches exist only for amplitudes larger than A = 5, and thus they do not appear in Figure 4.4.

Further examining Figure 4.4, it is observed for the lowest excitation level that the response peaks decrease in amplitude as the excitation frequency is increased. It is also found that the response minima of the corresponding upper branches follow an opposite trend, increasing in amplitude as the excitation frequency is increased. Furthermore, for each level of excitation and viscous dissipation, there exists a critical excitation frequency beyond which only disjoint solution branches which display this behavior are observed. This basic behavior of the response near successive backbone curves is found to characterize the system for all levels of excitation and viscous dissipation.

The effect of varying the level of excitation is readily observed in Figure 4.4. As the level of excitation is increased, it is clear that the level of response increases at all frequencies except the zeros of $p_2(\omega)$. By increasing the level of excitation, it is observed that each response maximum is increased and each response minimum is decreased. Furthermore, for increasing excitation levels, the separation increases between each pair of solution branches which straddle a backbone curve. Finally, increasing the level of excitation causes the critical excitation frequency to increase, so that near any given backbone curve, the disjoint response will become connected for sufficiently large excitation.

Referring to Figure 4.5, which shows the response for a larger level of viscous dissipation, the previous comments concerning the general behavior of the response also apply. Furthermore, by comparing Figures 4.4 and 4.5, the effects of varying the level of viscous dissipation are apparent. A careful comparison reveals that, for a fixed level of excitation, the effect of increasing the level of viscous dissipation is to decrease the amplitude of all response peaks and to increase the amplitude of all response minima. In particular, it is observed for the lowest level of excitation that the response peaks near the second and third backbone curves are decreased in amplitude. For the intermediate level of excitation, it is observed that the response peak near the third backbone curve is decreased in amplitude, and that the response minimum of the corresponding upper branch is increased sufficiently that this branch no longer appears in the figure. Furthermore, near the second backbone curve, it is observed that the response now takes the form of two disjoint solution branches; an upper branch and a lower branch. Thus, by increasing the level of viscous dissipation, the critical excitation frequency (beyond which only disjoint solutions exist) is decreased. For the largest level of excitation in the figure, it is seen that the separation is decreased between each pair of solution branches which straddle a backbone curve. Thus, it is observed that near any given backbone curve, the connected response will separate into two disjoint branches for sufficiently large viscous dissipation.

It is observed in both figures that each local response extremum occurs near, but slightly to the right of, a backbone curve. Furthermore, it is observed in Figure 4.5 that the response near the third backbone curve, for the largest level of excitation, appears to "neck down" toward the right of the backbone curve, even though it remains connected. This behavior is primarily the result of the particular choice of load distribution (e.g., base excitation), although it is also dependent upon the levels of excitation and viscous dissipation. By studying the loci of horizontal tangency [as determined by equation (3.66)] for fixed level of excitation, it can be shown that the effect of increasing the level of viscous dissipation is to lower all frequencies at which response extrema occur for amplitudes larger than $A = z_0$ and to increase such frequencies for lower amplitudes.

Local Response Extrema

Since the existence of local maxima and minima are prominent features of the response from an engineering point of view, it is of practical interest to obtain estimates of these values directly, without having to obtain the entire steady-state solution curve. Applying the approximate methods discussed in Chapter III, lower and upper bounds on the amplitude of each local response extremum in Figures 4.4 and 4.5 are obtained, as well as estimates of the corresponding frequencies. Results of these calculations are shown in Table 4.1 for comparison with the actual amplitudes and frequencies of response extrema.

TABLE 4.1

Comparison of Estimated and Actual Response Extrema
for Forced Oscillations of the Damped Cubic Hardening System

Damping (c)	Excitation (z_0)	Amplitude			Frequency		
		Estimated (Backbone)	Estimated (Horiz. Tan.)	Actual	Estimated (Backbone)	Estimated (Horiz. Tan.)	Actual
0.142	0.5	1.36	1.62	1.48	2.24	2.28	2.26
0.142	0.5	0.570	0.890	0.778	4.10	4.16	4.18
0.142	1.0	1.60	*	2.57	4.14	*	4.24
0.142	1.0	3.70	*	3.07	4.31	*	4.27
0.260	0.5	0.600	0.880	0.774	2.19	2.28	2.29
0.260	0.5	0.302	0.665	0.583	4.10	4.21	4.33
0.260	1.0	1.68	2.91	2.26	2.26	2.41	2.36
0.260	1.0	4.30	3.42	3.96	2.53	2.46	2.52
0.260	1.0	0.635	1.45	1.24	4.11	4.23	4.31

*No intersection.

It is seen that in most cases the estimates provide useful bounds on the amplitude extrema, even for relatively small amplitude response. It is also observed that the variation in the corresponding frequency estimates is smaller for the larger amplitude extrema. This occurs because the loci of horizontal tangency approach the backbone curves as the amplitude of response increases. Finally, it is noted that no estimates of amplitude or frequency are obtained for two cases shown in Table 4.1. In these particular cases, the estimates are not obtainable because the loci of horizontal tangency and the loci of solutions of (3.65b) do not intersect. As noted in the discussion in Chapter III, such intersections do not always exist.

4.3 Steady-State Response to Harmonic Base Excitation of a Uniform Ten-Mass Chainlike Structure with a Bilinear Softening Terminal Constraint

4.3.1 Application of General Formulation

Depicted in Figure 4.6 is an idealized model for the physical system under consideration. The system consists of a uniform ten-mass chainlike structure with one end stress free and the other constrained by a one-dimensional nonlinear structural element. Excitation is provided by an impressed harmonic displacement of the rigid base of the system, to which one end of the nonlinear element is attached. In this case, x measures the relative displacement between the first mass of the chainlike structure and the

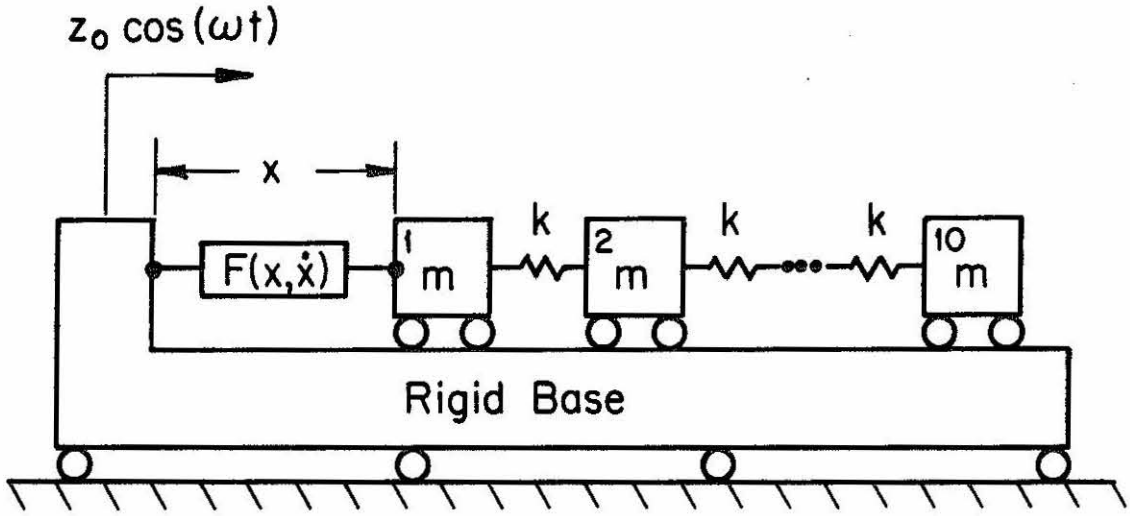

Figure 4.6 - Base Excitation of a Uniform Ten-Mass Chainlike Structure with a Nonlinear Terminal Constraint

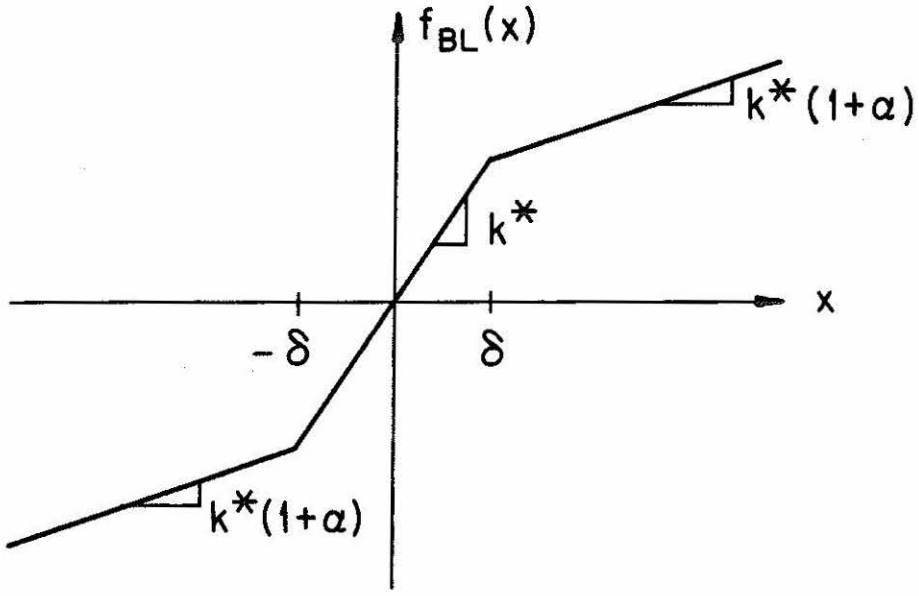

Figure 4.7 - Behavior of the Conservative Bilinear Restoring Force, $f_{BL}(x)$

base of the system. Such a system might be used to model the behavior of a ten-story building with a soft first story.

The nonlinear structural element is assumed to have a restoring force given by

$$F(x, \dot{x}) = f_{BL}(x) + c\dot{x} \tag{4.13}$$

where c is a viscous damping coefficient and $f_{BL}(x)$ is the symmetric bilinear restoring force shown in Figure 4.7. The restoring force may be expressed mathematically as

$$f_{BL}(x) = \begin{cases} k^*x\left[1 + \alpha\left(1 + \frac{\delta}{x}\right)\right] ; & x < -\delta \\ k^*x ; & |x| \leq \delta \\ k^*x\left[1 + \alpha\left(1 - \frac{\delta}{x}\right)\right] ; & x > \delta \end{cases} \tag{4.14}$$

where k* is a linear spring constant, δ is the yield displacement, and α is a (small) nonlinearity parameter, which produces hardening behavior when positive and softening behavior when negative.

Substituting (4.13), (4.14) into (2.31) and using (2.27), one finds that the "equivalent linear stiffness" in this case is given by

$$\frac{C(A)}{A} = \begin{cases} k^* ; & A \leq \delta \\ k^*\left[1 + \alpha\frac{2}{\pi}(\theta^* - \tfrac{1}{2}\sin 2\theta^*)\right] ; & A > \delta \end{cases} \tag{4.15}$$

where

$$\theta^* \equiv \cos^{-1}\left(\frac{\delta}{A}\right) \tag{4.16}$$

The "equivalent linear damping coefficient" is simply the viscous damping coefficient, c. Thus,

$$-\frac{S(A)}{\omega A} = c \tag{4.17}$$

The linear system takes the form of a uniform mass-terminated linear chainlike structure, with attachment point P taken at one end. The complex frequency transfer function $H_{22}(i\omega)$ is the force developed in the chainlike structure at P, in response to an impressed displacement time history $e^{i\omega t}$ applied at P. The force is positive when in the same direction as positive displacement.

If each element of the chainlike structure has mass m and stiffness k, then one finds that

$$H_{22}(i\omega) = -m \frac{\prod_{j=1}^{10} (\omega^2 - \lambda_{zj}\omega_n^2)}{\prod_{k=1}^{9} (\omega^2 - \lambda_{pk}\omega_n^2)} \tag{4.18}$$

where

$$\omega_n^2 = \frac{k}{m}$$

$$\left.\begin{aligned}
\lambda_{z1} &= 0.0 & \lambda_{p1} &= 0.027277 \\
\lambda_{z2} &= 0.097887 & \lambda_{p2} &= 0.24105 \\
\lambda_{z3} &= 0.38197 & \lambda_{p3} &= 0.64544 \\
\lambda_{z4} &= 0.82443 & \lambda_{p4} &= 1.1966 \\
\lambda_{z5} &= 1.3820 & \lambda_{p5} &= 1.8348 \\
\lambda_{z6} &= 2.0000 & \lambda_{p6} &= 2.4910
\end{aligned}\right\} \tag{4.19}$$

$$\left.\begin{aligned} \lambda_{z7} &= 2.6180 & \lambda_{p7} &= 3.0939 \\ \lambda_{z8} &= 3.1756 & \lambda_{p8} &= 3.5783 \\ \lambda_{z9} &= 3.6180 & \lambda_{p9} &= 3.8916 \\ \lambda_{z10} &= 3.9021 \end{aligned}\right\} \text{(4.19, cont.)}$$

Thus, from (2.34), one finds that

$$\left.\begin{aligned} \kappa_{22}(\omega) &= -m \frac{\prod_{j=1}^{10} (\omega^2 - \lambda_{zj}\omega_n^2)}{\prod_{k=1}^{9} (\omega^2 - \lambda_{pk}\omega_n^2)} \\ \gamma_{22}(\omega) &= 0 \end{aligned}\right\} \text{(4.20)}$$

Since the linear system in this case is a mass-terminated linear chainlike structure, and since the generalized loading consists of base excitation only, equations (3.53) may be applied directly to obtain

$$\left.\begin{aligned} p_2(\omega) &= -m \frac{\prod_{j=1}^{10} (\omega^2 - \lambda_{zj}\omega_n^2)}{\prod_{k=1}^{9} (\omega^2 - \lambda_{pk}\omega_n^2)} \\ q_2(\omega) &= 0 \end{aligned}\right\} \text{(4.21)}$$

Thus, $p_2(\omega)$ and $\kappa_{22}(\omega)$ are identical and share the same poles and zeros.

Let

$$\frac{k}{m} = 43.67 \qquad \text{(4.22)}$$

then the poles and zeros of $\kappa_{22}(\omega)$ are readily determined from (4.18) and (4.19) to be

$$\left.\begin{aligned}
\omega_{z1} &= 0.0 & \omega_{p1} &= 1.0914 \\
\omega_{z2} &= 2.0675 & \omega_{p2} &= 3.2445 \\
\omega_{z3} &= 4.0842 & \omega_{p3} &= 5.3091 \\
\omega_{z4} &= 6.0002 & \omega_{p4} &= 7.2288 \\
\omega_{z5} &= 7.7687 & \omega_{p5} &= 8.9513 \\
\omega_{z6} &= 9.3456 & \omega_{p6} &= 10.430 \\
\omega_{z7} &= 10.692 & \omega_{p7} &= 11.624 \\
\omega_{z8} &= 11.776 & \omega_{p8} &= 12.501 \\
\omega_{z9} &= 12.570 & \omega_{p9} &= 13.036 \\
\omega_{z10} &= 13.054
\end{aligned}\right\} \quad (4.23)$$

Substituting (4.15)-(4.17), (4.19)-(4.22) into (3.3) and (3.62), it is found that the approximate steady-state solutions for forced and free oscillations are governed by two complicated transcendental equations. These equations were solved iteratively by digital computation, and the resulting loci of solutions are shown in Figure 4.8. The solid lines represent the approximate solution for forced oscillations, and the broken lines represent the approximate solution for free oscillations (i.e., $c = 0$). The data points represent "exact" solutions and are discussed at the end of this chapter.

Shown in Figure 4.8 are the approximate steady-state solutions for the first three modes of the system, for three different levels of excitation: $z_0 = 0.5,\ 1.0,\ 2.0$. The system is strongly softening with $\alpha = -0.70$ and is viscously dissipative ($c = 0.06$). The

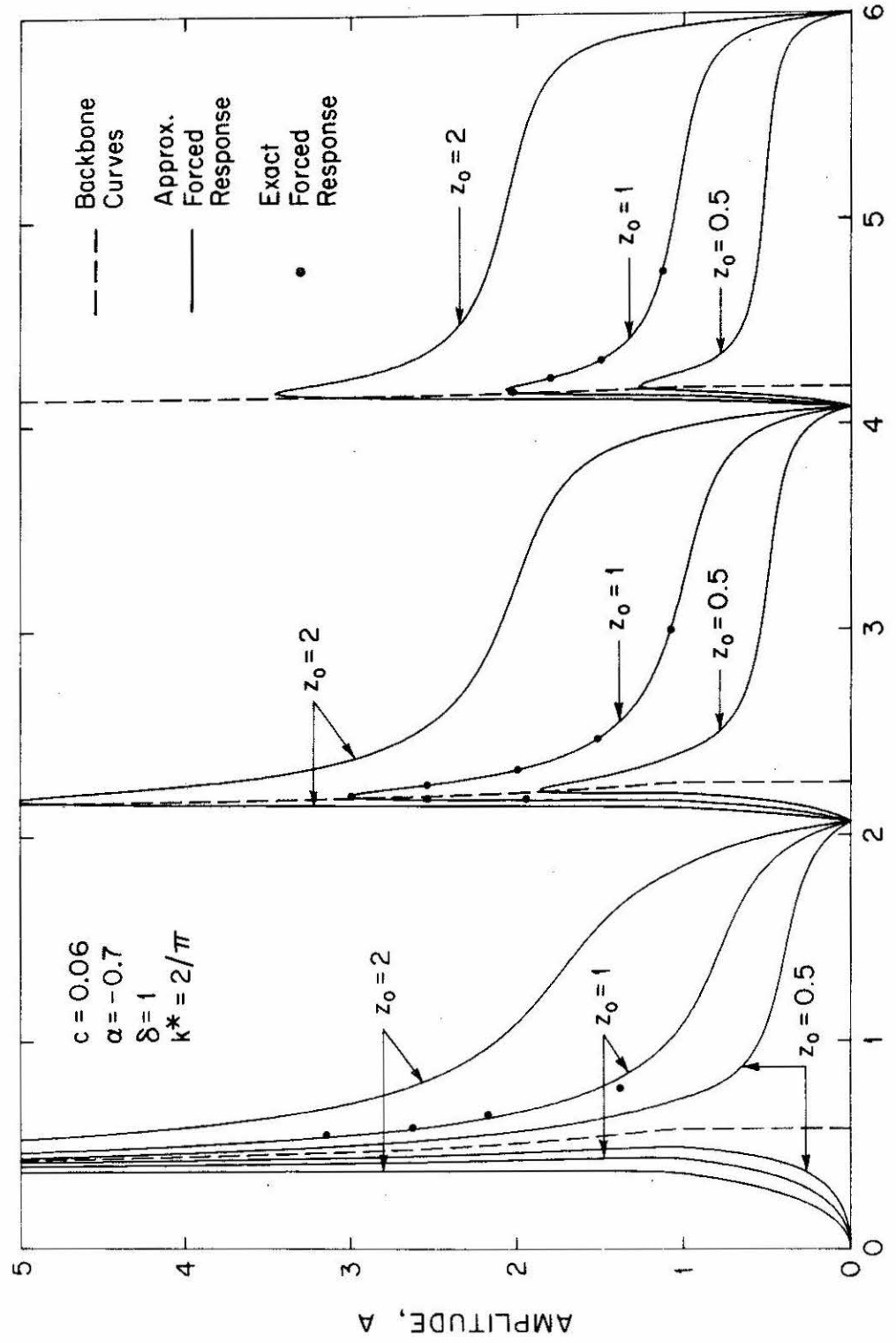

Figure 4.8 - Approximate Steady-State Response for Forced and Free Oscillations of a Chainlike System with a Damped Bilinear Softening Constraint

yield displacement is $\delta = 1$, and the small amplitude constraint stiffness is $k^* = 2/\pi$. The elemental mass of the chainlike system is $m = 0.1458$.

4.3.2 Discussion of Free Oscillations

The approximate steady-state solutions for free oscillations are shown in Figure 4.8 as broken lines. It is observed that each of the three backbone curves exhibits similar behavior. Careful examination of Figure 4.8 reveals that for amplitudes smaller than δ each backbone curve is vertical, and for amplitudes larger than δ each backbone curve leans to the left and asymptotically approaches a vertical line. These observations agree with the predictions in Theorem 1 of Chapter III, since, for $\frac{C(A)}{A}$ as given in (4.15), the derivative $\frac{d}{dA}[C(A)/A]$ is zero for $A < \delta$ and, for $A > \delta$ and $\alpha < 0$, the derivative is negative but increasing toward zero for large amplitudes.

It is further observed that exactly one backbone curve exists in each of the frequency intervals $[0, \omega_{p1})$, $(\omega_{p1}, \omega_{p2})$, and $\omega_{p2}, \omega_{p3})$, where the ω_{pi} are the poles of $\kappa_{22}(\omega)$ as given in equations (4.23). Although Figure 4.8 displays only the first three backbone curves, it can be shown that there exists an additional seven such curves, one in each of the frequency intervals $(\omega_{p3}, \omega_{p4})$, $(\omega_{p4}, \omega_{p5}), \ldots,$ (ω_{p9}, ∞). These observations agree with the predictions in Theorem 2 of Chapter III.

Since the constraint stiffness for small amplitudes $(A < \delta)$ is constant (k^*), the backbone curve frequencies for small amplitudes

approach the natural frequencies of the system with a linear spring constraint of stiffness k*. Furthermore, it can be shown that for large amplitude response ($A \gg \delta$) the equivalent linear constraint stiffness is $k^*(1 + \alpha)$ and that the corresponding backbone frequencies approach the natural frequencies of the system with a linear spring constraint of stiffness $k^*(1 + \alpha)$. Thus, the effect of increasing (decreasing) the parameter k* is to increase (decrease) each of the backbone curve frequencies at each response amplitude. It can also be shown that the effect of increasing (decreasing) the magnitude of the nonlinearity parameter α is to increase (decrease) the separation between the frequency asymptotes for large and small amplitude response of each backbone curve. Clearly, the effect of increasing (decreasing) the yield level δ is to increase (decrease) the amplitude at which each backbone curve first begins to lean.

4.3.3 Discussion of Forced Oscillations with Viscous Dissipation

Forced oscillations of the system with viscous dissipation for three different excitation levels are shown in Figure 4.8. Careful examination of the figure reveals that for each response curve the amplitude approaches the value $A = z_0$ as the excitation frequency approaches each pole of $\varkappa_{22}(\omega)$. These observations are in agreement with the predictions in Theorem 4 of Chapter III. Furthermore, combined with the observations previously noted for the system with cubic nonlinearity, it is seen that these observations are

also in agreement with the predictions that this characteristic of the response is independent of the properties of the nonlinear constraint.

It is further observed that for each response curve the amplitude approaches the value A = 0 as the excitation frequency approaches each zero of $p_2(\omega)$. These observations are in agreement with the predictions in Theorem 5 of Chapter III.

Applying Theorem 3 of Chapter III to this system (noting that $M \rightarrow \infty$ in this case, since the nonlinearity contains viscous dissipation), it is concluded that the response amplitude is bounded for all frequencies and levels of excitation. Thus, each curve in Figure 4.8 has a finite amplitude peak, even though some are too large to appear in the figure. It is observed from the figure that for a fixed excitation level, the amplitude of peak response decreases for peaks near successive backbone curves. This trend is found to characterize the response for all levels of excitation and viscous dissipation. Further examining the amplitude peaks in Figure 4.8, it is observed that each peak occurs slightly to the right of a backbone curve, indicating that the loci of horizontal tangency once again lie to the right of the backbone curves. As previously discussed, this behavior is primarily the result of the choice of load distribution (e.g., base excitation), although it is also affected by the level of excitation and of viscous dissipation.

The approximate methods for estimating the locations of response extrema were not applied to this system, primarily because the functions $\kappa_{22}(\omega)$ and C(A)/A are sufficiently complex in this case that very little computational savings is obtained over that

required for an exact solution. However, from the figure it is clear that at least the lower bound estimates, which are located at the intersections of the response curves with the backbone curves, agree very well with the actual response extrema.

The effect of varying the level of excitation is clearly shown in Figure 4.8. By increasing (decreasing) the level of excitation, the amplitude of response is increased (decreased) at all frequencies except the zeros of $p_2(\omega)$. It is also observed that for response of fixed amplitude near any backbone curve, the effect of increasing (decreasing) the level of excitation is to increase (decrease) the width of the response curve about the locus of horizontal tangency.

4.4 Steady-State Response to a Harmonic Concentrated Load of a Uniform Ten-Mass Chainlike Structure with a Terminal Constraint Exhibiting a Form of Limited Slip

4.4.1 Application of General Formulation

Depicted in Figure 4.9 is an idealized model for the physical system under consideration. The system consists of a uniform ten-mass chainlike structure with one end stress free and the other constrained by a one-dimensional nonlinear structural element. Excitation is provided by a single concentrated harmonic force of amplitude z_0 applied to the first mass of the chainlike structure, which is attached to one end of the nonlinear element. In this case, x measures the absolute displacement of the first mass of the chain-like structure. Such a model might, for example, be used to

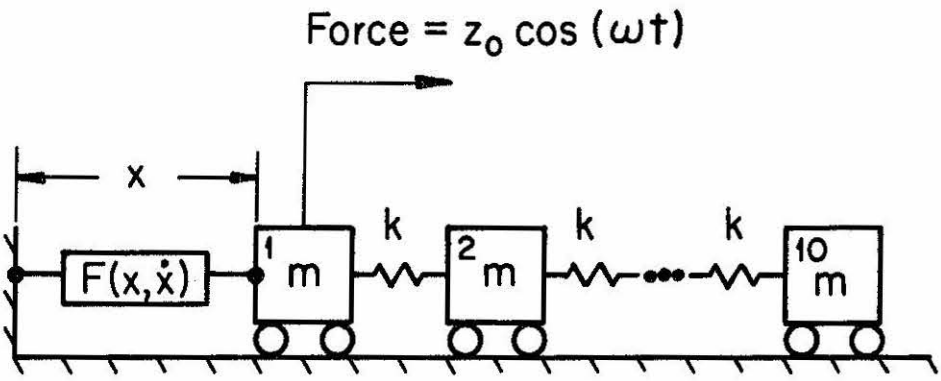

Figure 4.9 - Concentrated Load Excitation of a Uniform Ten-Mass Chainlike Structure with a Nonlinear Terminal Constraint

represent the behavior of a nine-story building mounted on a nonlinear foundation.

The nonlinear structural element is assumed to have a restoring force given by

$$F(x, \dot{x}) = f_{SH}(x, \dot{x}) + c\dot{x} \tag{4.24}$$

where c is a viscous damping coefficient and $f_{SH}(x, \dot{x})$ is the restoring force developed by the structural assemblage shown in Figure 4.10. It can be shown that the restoring force is characterized by the rate-independent hysteresis loop shown in Figure 4.11.

Such a structural nonlinearity displays several important features and has not been previously investigated. From Figure 4.11, it is observed that there are three distinct types of response behavior produced by the structural assemblage for different amplitudes of deformation. For small deformation amplitudes ($A \leq \delta$), the response is linear elastic with stiffness k_E. For moderate amplitudes ($\delta < A \leq \delta + g$), the response is softening, with the familiar elastoplastic behavior. For large amplitudes ($A > \delta + g$), the response again becomes hardening, but remains hysteretic. Such softening-hardening hysteresis loops are frequently encountered in applications involving the large deformations of composite structural systems, where secondary structural elements (e.g., architectural elements) contribute to the structural response only after the primary structural elements have yielded or slipped at the connections. Such composite structural behavior in various forms has also been

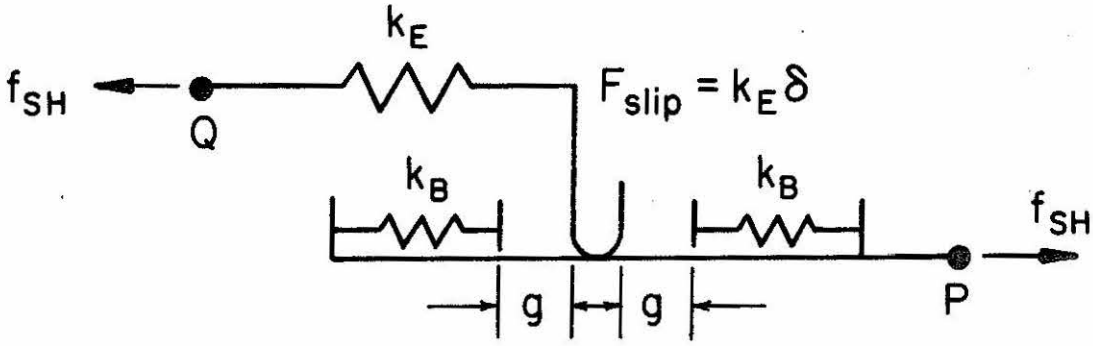

Figure 4.10 - Physical Model for the Softening-Hardening Hysteretic Nonlinearity

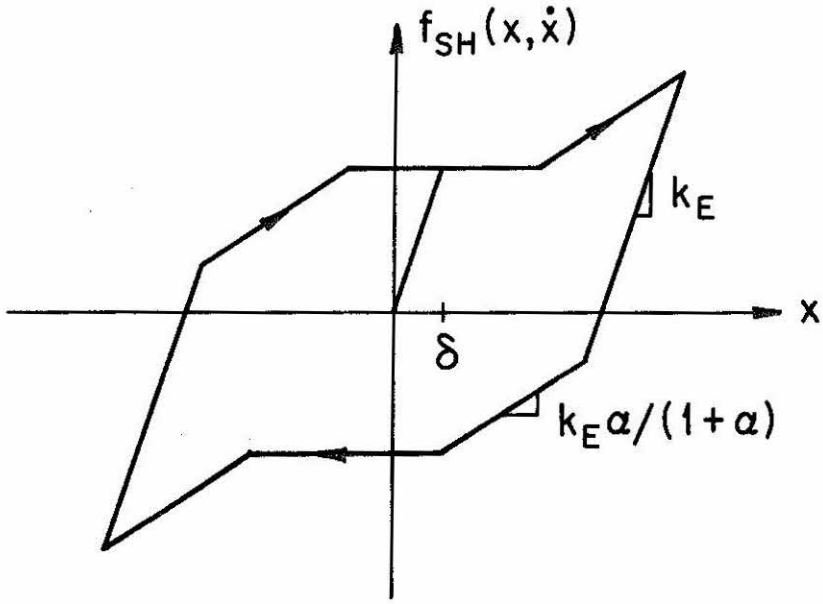

Figure 4.11 - Restoring Force Characteristics of the Softening-Hardening Hysteretic Nonlinearity

considered [60] as a mechanism for intentional energy absorption in structural systems, including entire building structures. Softening-hardening hysteresis loops are also encountered in certain concrete and steel assemblages [61,62].

The nonlinearity presented herein represents the simplest structural model currently available for modeling both the transient and steady-state response of such systems. Since the nonlinear restoring force is derived from a physical model, no arbitrary mathematical assumptions are required to determine its transient behavior.

By varying the "stiffness ratio," α, and "slip level," g, three familiar types of structural response may be obtained. By letting $\alpha \to 0$ or $g \to 0$, the model produces the familiar elastoplastic behavior. By letting $g \to 0$, the model produces bilinear hysteretic behavior, and by letting $\alpha \to 0$, the model produces limited slip behavior [58]. In fact, the model may be viewed as a generalization of the limited slip model obtained by inserting barriers with finite stiffness k_B to limit the slipping behavior in a less abrupt fashion.

Substituting (4.24) into (2.31), and using (2.27) and the properties of the hysteresis loops in Figure 4.11, it can be shown that the "equivalent linear stiffness" of such a nonlinearity is a combination of two terms whose proportion is determined by α. In particular, C(A)/A may be expressed as

$$\frac{C(A)}{A} = \frac{1}{(1+\alpha)} \frac{C_{EP}(A)}{A} + \frac{\alpha}{1+\alpha} \frac{C_{LS}(A)}{A} \qquad (4.25)$$

where $C_{EP}(A)/A$ is the equivalent stiffness of an elastoplastic nonlinearity and $C_{LS}(A)/A$ is the equivalent stiffness of a limited slip nonlinearity. The terms $C_{EP}(A)/A$ and $C_{LS}(A)/A$ may be expressed as

$$\frac{C_{EP}(A)}{A} = \begin{cases} k_E ; & A \le \delta \\ \frac{k_E}{\pi}[\theta_1 - \frac{1}{2}\sin 2\theta_1] ; & A > \delta \\ \theta_1 \equiv \cos^{-1}(1 - \frac{2\delta}{A}) & \cdot \end{cases}$$

$$\frac{C_{LS}(A)}{A} = \begin{cases} k_E ; & A \le \delta \\ \frac{k_E}{\pi}[\theta_1 - \frac{1}{2}\sin 2\theta_1] ; & \delta \le A \le \delta + g \\ \frac{k_E}{\pi}[\pi + (\theta_2 - \frac{1}{2}\sin 2\theta_2) - (\theta_3 - \frac{1}{2}\sin 2\theta_3)] ; & A > \delta + g \\ \theta_1 \equiv \cos^{-1}(1 - \frac{2\delta}{A}); \ \theta_2 \equiv \cos^{-1}(\frac{g-\delta}{A}) ; \ \theta_3 \equiv \cos^{-1}(-\frac{g+\delta}{A}) & \end{cases} \quad (4.26)$$

Similarly, it is found that the "equivalent linear damping coefficient" is composed of the viscous damping coefficient, c, and a similar weighted average of two contributions. In particular, $-S(A)/\omega A$ may be expressed as

$$-\frac{S(A)}{\omega A} = c - \frac{1}{(1+\alpha)}\frac{S_{EP}(A)}{\omega A} - \frac{\alpha}{(1+\alpha)}\frac{S_{LS}(A)}{\omega A} \quad (4.27)$$

where $-S_{EP}(A)/\omega A$ is the equivalent damping coefficient of an elastoplastic system and $-S_{LS}(A)/\omega A$ is the equivalent damping coefficient

of a limited slip system. The terms $-S_{EP}(A)/\omega A$ and $-S_{LS}(A)/\omega A$ may be expressed as

$$\left.\begin{aligned} -\frac{S_{EP}(A)}{\omega A} &= \begin{cases} 0\,; & A \le \delta \\ \frac{4}{\pi}\frac{k_E}{\omega}\left(\frac{\delta}{A}\right)\left(1-\frac{\delta}{A}\right)\,; & A > \delta \end{cases} \\ -\frac{S_{LS}(A)}{\omega A} &= \begin{cases} 0\,; & A \le \delta \\ \frac{4}{\pi}\frac{k_E}{\omega}\left(\frac{\delta}{A}\right)\left(1-\frac{\delta}{A}\right)\,; & \delta \le A \le \delta+g \\ \frac{4}{\pi}\frac{k_E}{\omega}\frac{\delta g}{A^2}\,; & A > \delta+g \end{cases} \end{aligned}\right\} \quad (4.28)$$

The linear system takes the form of a uniform mass-terminated linear chainlike structure, with attachment point P taken at one end. For convenience, all parameters of the linear system are chosen to be identical to those used for the chainlike structure considered in the previous section. Thus, $\kappa_{22}(\omega)$ and $\gamma_{22}(\omega)$ are again given by equations (4.20), with the poles and zeros of $\kappa_{22}(\omega)$ specified by (4.23).

Since the excitation in this case consists of a single concentrated load applied to the mass which moves rigidly with attachment point P, equations (3.45) may be applied directly to obtain

$$\left.\begin{aligned} p_2(\omega) &= 1 \\ q_2(\omega) &= 0 \end{aligned}\right\} \quad (4.29)$$

Substituting (4.25)-(4.29) into (3.3) and (3.62), it is found that the approximate steady-state solutions for forced and free oscillations are governed by two complicated transcendental equations. These equations were solved iteratively by digital computation, and the resulting loci of solutions are shown in Figures 4.12 and 4.13. The solid lines represent the approximate solution for forced oscillations, and the broken lines represent the backbone curves.

Shown in Figure 4.12 are the approximate steady-state solutions for the first three modes of the undamped system (i.e., $c = 0$), for three different levels of excitation: $z_0 = 0.70,\ 0.75,\ 0.80$. The system is strongly nonlinear with slip level $g = 1.5$ and stiffness ratio $\alpha = 4/3$. The yield displacement is $\delta = 1$, and the small amplitude constraint stiffness is $k_E = 1$. The elemental mass of the chainlike system is $m = 0.1458$.

Shown in Figure 4.13 are the approximate steady-state solutions for the first three modes of the system with fixed excitation level ($z_0 = 0.75$), for three different levels of viscous dissipation: $c = 0,\ 0.0081,\ 0.036$. All other parameters are the same as those given for Figure 4.12.

4.4.2 Discussion of Backbone Curves

The approximate steady-state solutions for the backbone curves are shown as broken lines in Figure 4.12. It should be noted that since the nonlinearity is hysteretic, the system is strictly dissipative for response amplitudes larger than $A = \delta$, even though there is no viscous dissipation present (i.e., $c = 0$). Therefore, steady free oscillations do not exist for amplitudes larger than $A = \delta$.

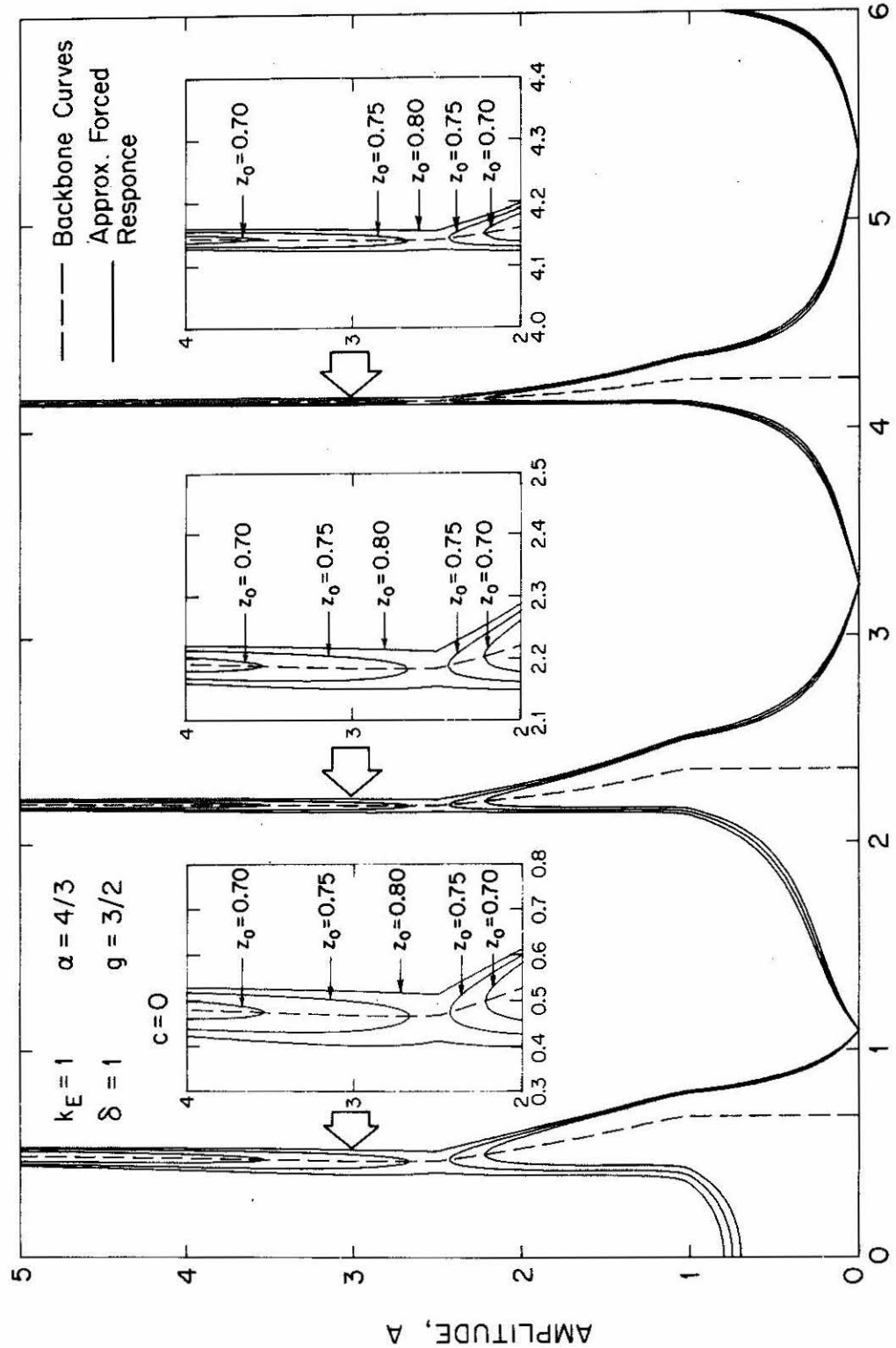

Figure 4.12 - Approximate Steady-State Response to a Harmonic Concentrated Load of a Chainlike System with an Undamped Hysteretic Constraint

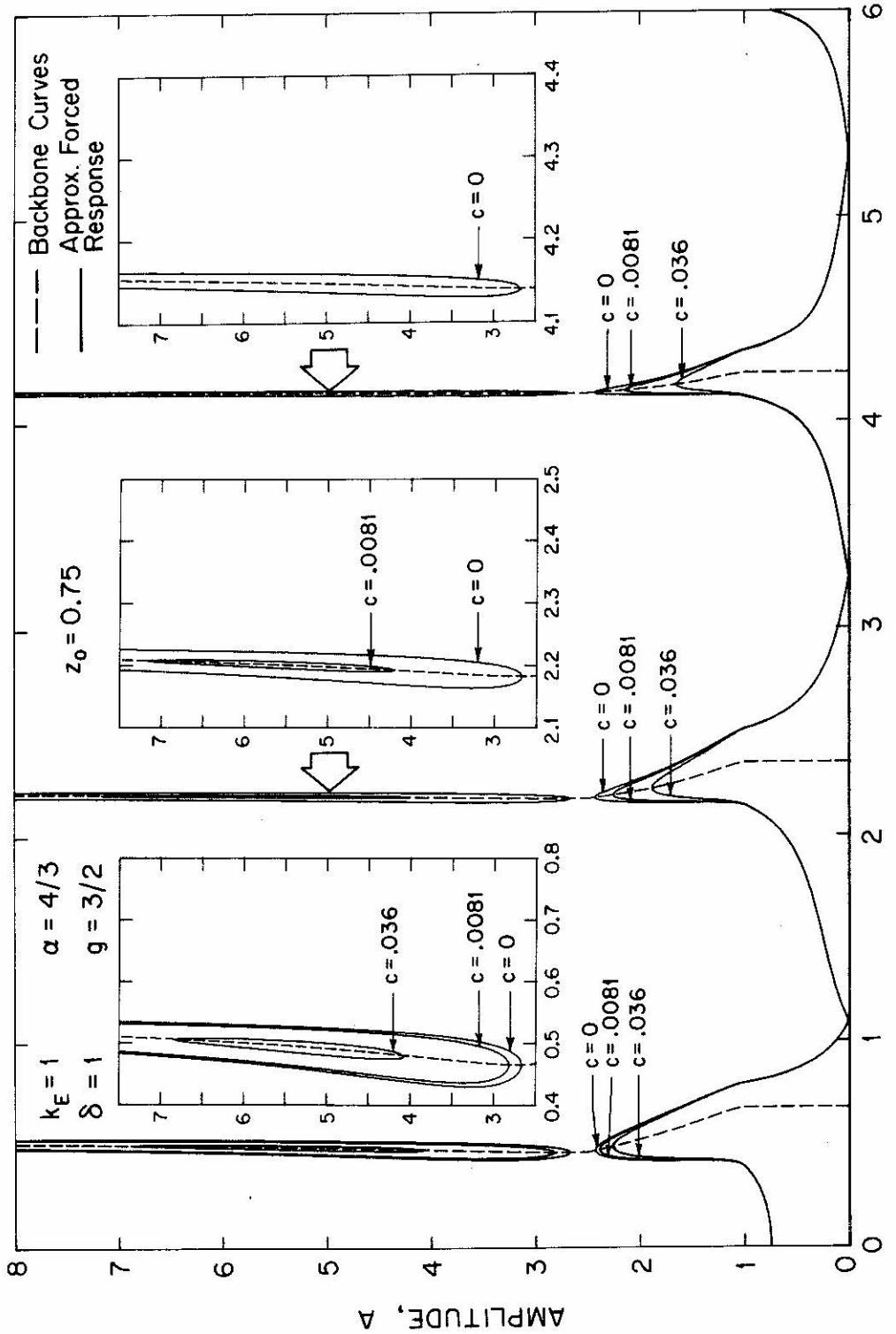

Figure 4.13 - Approximate Steady-State Response to a Harmonic Concentrated Load of a Chainlike System with a Damped Hysteretic Constraint

However, the backbone curves remain worthy of discussion since they also represent the loci of horizontal tangency in this application, due to the particular load distribution involved. This can be verified by substituting (4.29) into (3.64) and comparing with (3.62).

It is observed from Figure 4.12 that each of the three backbone curves exhibits similar behavior. For amplitudes smaller than δ, each backbone curve is vertical since the system response is linear in this range. For amplitudes between δ and $\delta+g$, each backbone curve leans to the left. In this range the response is elastoplastic. For amplitudes larger than $\delta+g$, each backbone curve leans slightly to the right, indicating hardening behavior. It can be shown that these observations agree with the predictions in Theorem 1 of Chapter III by carrying out the required differentiation of $C(A)/A$ as given in (4.25), (4.26).

It is further observed that exactly one backbone curve exists in each of the frequency intervals $[0, \omega_{p1})$, $(\omega_{p1}, \omega_{p2})$, and $(\omega_{p2}, \omega_{p3})$, where the ω_{pi} are the poles of $\kappa_{22}(\omega)$ as given in equations (4.23). Although Figure 4.12 displays only the first three backbone curves, it can be shown that there exists an additional seven such curves, one in each of the frequency intervals $(\omega_{p3}, \omega_{p4})$, $(\omega_{p4}, \omega_{p5}), \ldots,$ (ω_{p9}, ∞). These observations agree with the predictions in Theorem 2 of Chapter III.

As in the case of the system discussed in the previous example, the backbone curve frequencies for small amplitudes approach the natural frequencies of the system with a linear spring constraint of stiffness k_E. Furthermore, it can be shown that for

very large response amplitudes ($A \gg \delta + g$), the equivalent linear constraint stiffness is $k_E\alpha/(1+\alpha)$ and that the corresponding backbone curve frequencies asymptotically approach vertical lines which represent the natural frequencies of the system with linear spring constraint of stiffness $k_E\alpha/(1+\alpha)$. For response amplitudes between these extremes, the parameters δ and g affect the response. Clearly, the effect of increasing (decreasing) the yield level δ is to increase (decrease) the amplitude at which each backbone curve first begins to lean. Similarly, the effect of increasing (decreasing) the slip level g is to increase (decrease) the interval in response amplitudes (δ to $\delta + g$) for which softening behavior is observed. It is also clear that the effect of increasing (decreasing) the stiffness k_E is to shift each entire backbone curve to the right (left) along the frequency axis. Finally, the effect of varying the stiffness ratio α clearly affects only the large amplitude ($A > \delta + g$) response behavior. It can be shown that the effect of increasing (decreasing) α is to increase (decrease) the frequency of each large amplitude asymptote and to increase (decrease) the rate at which each backbone curve approaches its asymptote.

4.4.3 Discussion of Forced Oscillations without Viscous Dissipation

The approximate solutions for steady-state forced oscillations of the system with no viscous dissipation (i.e., $c = 0$) for three different excitation levels are shown as solid lines in Figure 4.12. It is observed for each curve that the response amplitude approaches the value $A = 0$ (rather than $A = z_0$ as in previous examples) as the

excitation frequency approaches each pole of $\alpha_{22}(\omega)$. This behavior is due to the particular load distribution involved and illustrates one of the changes in response which are produced by changes in the load distribution. It can be shown that these observations are in agreement with Theorem 4 of Chapter III, which concerns the vibration absorber effect.

Careful examination of Figure 4.12 reveals that the response displays several interesting characteristics. For example, it is observed for each curve with fixed excitation level that the response extrema occur at the intersections with the backbone curves. Furthermore, the values of each local amplitude maximum and minimum are observed to be identical for response near successive backbone curves. This behavior is observed to be independent of the level of excitation and is not coincidental. Each of these observations is in agreement with the predictions given in Chapter III for systems with load distribution such that $p_2(\omega) = 1$. It can also be shown that the qualitative behavior of the response curves for all excitation frequencies is in agreement with the predictions of Theorem 6 in Chapter III.

Another interesting characteristic of the response is the existence of disconnected response behavior for certain excitation levels. Such behavior is primarily the result of the properties of the nonlinear terminal constraint. As previously discussed, the equivalent linear stiffness and damping coefficients for the nonlinear constraint may be expressed as a weighted average of the corresponding coefficients for an elastoplastic system and a limited slip

system. In particular, as $\alpha \to 0$ the behavior of the nonlinearity approaches that of an elastoplastic system, and as $\alpha \to \infty$ the behavior approaches that of a limited slip system. Thus, the response of the present system displays certain features of the response of each component system. For example, it is well known that for an elastoplastic system there exists a critical excitation level z_{EP} given by

$$z_{EP} = \frac{4}{\pi} k_E^{\delta} \tag{4.30}$$

such that for all excitation levels smaller than z_{EP} the response is strictly bounded and for all larger excitation levels unbounded response exists. Furthermore, no disconnected response exists at any excitation level for an elastoplastic system. It is also well known [58] that for a limited slip system there exists unbounded response for all nonzero excitation levels and that disconnected response exists for all excitation levels smaller than z_{LS} where

$$z_{LS} = \frac{4}{\pi} k_E^{\delta} \left(\frac{g}{\delta + g}\right) \tag{4.31}$$

For the present system, it can be shown by applying Theorem 3 of Chapter III that unbounded response exists for all excitation levels larger than z_{cr} where

$$z_{cr} = \frac{4}{\pi} k_E^{\delta} \frac{1}{(1+\alpha)} \tag{4.32}$$

Evaluating z_{cr} for the parameters used in Figure 4.12, one finds

that $z_{cr} = 0.546$. Therefore, the large amplitude response branches of each curve in Figure 4.12 extend up to unbounded amplitudes.

Furthermore, it can be shown that disconnected response exists for the present system only if two conditions are met. First, the excitation level must be smaller than z_{LS} and, second, the stiffness ratio α must be larger than δ/g. Thus, there exists a critical slip ratio α_{cr} where

$$\alpha_{cr} = \frac{\delta}{g} \tag{4.33}$$

such that for $\alpha > \alpha_{cr}$ there will exist disconnected response for excitation levels between z_{cr} and z_{LS}. For $\alpha < \alpha_{cr}$ there does not exist disconnected response for any excitation level. Evaluating α_{cr} and z_{LS} for the parameters used in Figure 4.12, one finds that $\alpha_{cr} = 0.667$ and that $z_{LS} = 0.764$. Therefore, there exists disconnected response for the two smallest excitation levels and connected response for the largest excitation level, as verified by observation.

Other effects of varying the excitation level are shown in Figure 4.12. It is observed that by increasing the excitation level the response maxima are increased and the response minima are simultaneously decreased. For excitation levels equal to z_{LS}, the response maxima and minima coincide, and for larger excitation levels the response becomes connected. It is also observed that as the excitation level is increased (decreased), the width of the response near each backbone curve is also increased (decreased).

Finally, it can be shown that the approximate methods presented in Chapter III for obtaining upper and lower bounds on the response extrema yield identical estimates in every case. Furthermore, these estimates coincide with the response extrema of the approximate steady-state solutions shown in the figure.

4.4.4 Discussion of Forced Oscillations with Viscous Dissipation

Forced oscillations of the system with fixed excitation level and three different levels of viscous dissipation are shown in Figure 4.13. By comparing curves in the figure, the primary effects of varying the level of viscous dissipation are apparent. It is clear that the changes in response due to viscous dissipation are concentrated near the backbone curves. In particular, it is observed that as the level of viscous dissipation is increased (decreased), the value of each response maximum is decreased (increased). Furthermore, it is observed that for fixed level of viscous dissipation, the attenuation of response maxima increases for response near each successive backbone curve.

The response minima are observed to display precisely the opposite trend. As the level of viscous dissipation is increased (decreased), the value of each response minimum is observed to increase (decrease). Furthermore, this effect becomes more prominent for response near each successive backbone curve.

Careful examination of Figure 4.13 reveals that for fixed levels of excitation and viscous dissipation, disconnected response curves do not exist near the third backbone curve for either of the

nonzero levels of viscous dissipation. Furthermore, it can be shown that for each curve there exists a critical frequency ω_{cr} beyond which disconnected response does not exist. From the figure it is observed that as the level of viscous dissipation is increased (decreased), ω_{cr} is simultaneously decreased (increased). It can also be shown that as the level of viscous dissipation tends to zero, ω_{cr} tends to infinity, and conversely.

Applying Theorem 3 of Chapter III to this system (noting that $M \to \infty$ in this case, since the nonlinearity contains viscous dissipation), it is concluded that the response amplitude is bounded for all frequencies and excitation levels. Thus, the disconnected response curves corresponding to $c = 0.0081$ and $c = 0.0360$ in Figure 4.13 each take the form of a closed loop with a finite maximum amplitude, even though one of these maxima is too large to appear in the figure.

The approximate methods for estimating the locations of response extrema were not applied to this system, because of the complexity of the equations involved. However, from the figure it is clear that at least the lower bound estimates, which are located at the intersections of the response curves and the backbone curves, agree very well with the actual response extrema.

4.5 Comparison of Exact and Approximate Steady-State Solutions

4.5.1 Accuracy of the Approximate Solution for the Continuous System

For the continuous system discussed in Section 4.2, the accuracy of the approximate steady-state solution may be inferred by

comparing exact and approximate solutions at several points in the A, ω plane. "Exact" solution points are generated by using numerical methods to solve the initial value problem obtained by specializing equations (2.24) and specifying appropriate initial conditions.

By applying a modal analysis technique to the uniform shear beam, a representation for the operator $\mathfrak{F}_{22}(\cdot)$ (which is the only such operator involved in the specialized equations) as a superposition of an infinite number of independent modal contributions is obtained. For practical considerations, however, the representation is truncated to include only a finite number of modal contributions. The resulting finite system of coupled ordinary differential equations are then solved by numerical integration after initial conditions are computed from the approximate steady-state solution.

Shown as data points in Figures 4.4 and 4.5 are the resulting "exact" solutions computed for an excitation level of $z_0 = 1$ and for a ten-mode representation of the shear beam. Relatively few data points are shown because of the excessive computing costs involved in finding the numerical steady-state solutions of the required twenty-two order system of ordinary differential equations. It can be seen from the figures that the exact and approximate solutions agree very well for each data point that is shown. In each of Figures 4.4 and 4.5 there is a difference of less than 5% in amplitude and 5% in frequency between the exact solution points and the approximate steady-state solutions.

The effect on the exact solution points of varying the number of modes used to represent the shear beam was investigated for a few of the points shown in the figures. Solution points were computed at a given excitation frequency for equations representing five, ten, and twenty mode approximations of the shear beam. Upon comparing the solution points thus obtained, it was found in each case that the change in steady-state amplitude of the solution points due to increasing the number of modes was smaller than 2%. Furthermore, it was found in each case that as the number of modes was increased, the corresponding solution point amplitudes monotonically approached an amplitude which is in better agreement with the approximate solutions than the solution points shown in the figures.

4.5.2 Accuracy of the Approximate Solution for the Discrete System

For the discrete system discussed in Section 4.3, the accuracy of the steady-state solution may be inferred by comparing exact and approximate solutions at several points in the A, ω plane. "Exact" solution points are generated by using numerical methods to solve the initial value problem consisting of the equations of motion of the ten masses and a set of appropriate initial conditions computed from the approximate steady-state solutions.

Shown as data points in Figure 4.8 are the resulting "exact" solutions computed for an excitation level of $z_0 = 1$. It can be seen from the figure that the exact and approximate solutions are in excellent agreement for each data point near the second and third

backbone curves. Noticeably poorer agreement is observed for points near the first backbone curve, but the overall agreement is still good. For points near the second and third backbone curves, there is a difference of less than 1% in both amplitude and frequency between the exact and approximate solutions. For points near the first backbone curve, there is a difference of less than 9% in amplitude and 6% in frequency between the exact and approximate solutions. It is suspected that the apparent increase in accuracy with increasing frequency is associated with the corresponding increase in magnitude of the viscous damping force relative to the nonlinear force in the constraint. Clearly, as the contribution of the viscous damping force grows relative to that of the nonlinear force, the equivalent linearization approximation becomes more accurate.

V. Summary and Conclusions

Considered in Chapter II is the dynamic response of a general linear system with a one-dimensional nonlinear constraint attached between two arbitrarily chosen points. The dynamic equations for general spatial and temporal load distributions are developed in an operator notation which is valid for both continuous and discrete systems. Symmetry conditions on loading and system configurations are presented under which the nonlinear constraint (1) moves as a rigid body without deformation about the mass center and (2) the mass center remains stationary with all motion occurring as "pure" deformation. In general, however, the response consists both of rigid body motion and pure deformation.

The method of equivalent linearization is used to develop equations which govern the approximate steady-state response to loads with harmonic time dependence. The nonlinear constraint is assumed to consist of rate-independent conservative or hysteretic nonlinearities and may contain a viscous dissipation term.

Considered in detail in Chapter III is the approximate steady-state response of systems with a nonlinear terminal constraint. Several theorems are developed concerning the qualitative response characteristics of a class of undamped linear chainlike structures with a nonlinear terminal constraint. Concerning the free oscillations of such systems, the following conclusions are drawn:

1. Each backbone or resonance curve displays similar "hardening" and/or "softening" behavior which is

determined exclusively by the properties of the nonlinear constraint. (Theorem 1)

2. There exists exactly one backbone curve contained in each non-negative frequency interval which has as an end point at least one member of the set $\Lambda \equiv \{\omega_{pi} | i = 1, 2, 3, \ldots\}$. The set Λ consists of the natural frequencies of the rigidly constrained linear system, but excludes those frequencies for which the attachment point corresponds to a node. (Theorem 2)

Concerning the forced oscillations of undamped linear chain-like structures with a nonlinear terminal constraint, the following conclusions are drawn:

1. If the constraint contains no viscous dissipation, then for sufficiently large excitation levels there may exist unbounded response at one or more frequencies depending upon the properties of the nonlinear constraint and the load distribution. Such unbounded response always occurs on a backbone curve. (Theorem 3)
2. Besides being dependent upon the properties of the linear system and nonlinear constraint, the loci of response extrema are shown to be dependent upon the load distribution. It is shown that the loci of response extrema and the backbone curves do not generally coincide.

Methods for estimating the location of response extrema are presented.

3. At each excitation frequency which is a member of the set Λ, the linear system acts as a "vibration absorber." At such frequencies the amplitude of deformation in the nonlinear constraint is independent of the properties of the nonlinear constraint. (Theorem 4)

4. Depending upon the load distribution and linear system, there may exist excitation frequencies for which the "effective excitation level" vanishes. At such frequencies it is shown that the amplitude of deformation of the nonlinear constraint either vanishes or lies on a backbone curve. (Theorem 5)

5. Special results are obtained for the case in which the load distribution consists of a single concentrated load applied at the point of attachment between the nonlinear constraint and the linear system. It is shown that in the absence of viscous dissipation the loci of response extrema and the backbone curves coincide. Furthermore, the values of the response peaks (and minima) are identical in each "mode." Properties of the nonlinear constraint which determine the existence of disconnected

response curves are presented. Qualitative properties of the entire response curve are presented in Theorem 6.

Of particular interest in engineering applications is the conclusion that the loci of response extrema are at least partially dependent upon the load distribution. Full-scale tests of structures frequently involve the determination of the response to harmonic excitation in order to identify the "effective natural frequencies" of the system. The results of this investigation indicate that particular attention should be given to the load distribution during such tests since, in general, different estimates of the natural frequencies might result from different load distributions.

Presented in Chapter IV are numerical examples of the harmonic response of three structural systems. These examples illustrate the application of the formulation and theorems to various combinations of linear system, nonlinear constraint, and load distribution. The qualitative effects on the response of varying the properties of the system and excitation are studied in each example.

Considered first is the response to harmonic base excitation of a uniform shear beam mounted on a linear-plus-cubic foundation spring. Free and forced oscillations are considered for both hardening and softening systems, with and without viscous dissipation. For the undamped cubic softening system it is shown that there exists a critical amplitude at which each pair of branches of the forced steady-state response intersect and cross on successive

backbone curves. The critical amplitude is that amplitude at which the equivalent linear stiffness of the softening constraint passes through zero. This interesting behavior is shown to be in agreement with the theorems presented in Chapter III.

Forced oscillations of the cubic hardening system with viscous dissipation also display interesting behavior. It is shown that disconnected response curves exist for sufficiently high excitation frequency, for all nonzero levels of viscous dissipation. It is also shown that unbounded response exists at each successive backbone curve, even though the constraint contains a viscous dissipation element. This behavior is a result of the particular properties of the nonlinear constraint and load distribution in this example. The approximate methods are used to estimate the location of the response extrema, and a comparison is made between the estimated and actual extrema as determined by the approximate steady-state response.

Also considered in Chapter IV is the response to harmonic base excitation of an undamped uniform ten-mass chainlike structure with a bilinear softening foundation containing viscous dissipation. Forced oscillations are studied for various levels of excitation, and it is shown that all response amplitudes are bounded and connected. Furthermore, it is shown that the value of the response peaks decreases for response in successively higher "modes."

The final example considered in Chapter IV is the response to a harmonic concentrated load of a uniform ten-mass chainlike

structure with a nonlinear hysteretic foundation. The model for the hysteretic foundation behavior produces rate-independent hysteresis loops which display softening behavior for small amplitudes and hardening behavior for large amplitudes. This model is useful for modeling the large deformations of composite structural systems, where secondary structural elements (e.g., architectural elements) contribute to the response only after the primary structural elements have yielded or slipped at the connections.

The steady-state solution is shown to be characterized by disconnected and unbounded response curves for certain ranges of system parameters and excitation level. When no viscous dissipation is present, it is shown that the values of the response extrema are identical in each mode. Furthermore, the response extrema are shown to occur on the backbone curves. When viscous dissipation is added to the nonlinear foundation, it is shown that all response is bounded and that the disconnected response no longer exists for response in sufficiently high modes. Furthermore, the values of the response peaks decrease for response in successively higher modes.

Also considered in Chapter IV is the accuracy of the approximate steady-state solutions. In several of the examples "exact" solutions are computed by numerical integration of the equations of motion, and a comparison is made between exact and approximate solutions. In most cases it is found that the approximate solutions differ from the exact solutions by less than 5% in both amplitude and frequency. It is also found that excessive computational costs

are involved in determining the exact steady-state response. Thus, the approximate solution technique presented herein provides an attractive and practical method for determining the steady-state response in many engineering applications.

REFERENCES

1. Chopra, A. K., Bertero, V. V., and Mahin, S. A., "Response of the Olive View Medical Center Main Building During the San Fernando Earthquake," Proc. of the Fifth World Conference on Earthquake Engineering, Rome, Italy, 1974, vol. 1, pp. 26-35.

2. Berg, Glen V., and Hanson, Robert D., "Engineering Lessons Taught by Earthquakes," Proc. of the Fifth World Conference on Earthquake Engineering, Rome, Italy, 1974, vol. 1, pp. 82-91.

3. Kunze, W. E., Fintel. M., and Amrhein, J. E., "Skopje Earthquake Damage," Civil Engineering--ASCE, v. 33, no. 12, (December 1963) pp. 56-59.

4. Fintel, M., "The Caracas Earthquake of July 29, 1967," Civil Engineering--ASCE, v. 38, no. 2 (February 1968) pp. 42-46.

5. Jennings, P. C., Editor, "Engineering Features of the San Fernando Earthquake, February 9, 1971," Earthquake Engineering Research Laboratory Report No. EERL 71-02, California Institute of Technology, 1971, Pasadena, California.

6. Martel, R. R., "The Effects of Earthquakes on Buildings with a Flexible First Story," Bull. Seism. Soc. Amer., v. 19, no. 3 (September 1929) pp. 167-178.

7. Green, N. B., "Flexible First Story Construction for Earthquake Resistance," Trans. A.S.C.E., v. 100 (1935) pp. 645-674.

8. Jacobsen, L. S., "Effects of a Flexible First Story in a Building Located on Vibrating Ground," S. Timoshenko 60th Anniversary Volume, New York: The Macmillan Co., 1938, pp. 93-103.

9. Wirsching, P. H., and Yao, J. T. P., "Safety Design Concepts for Seismic Structures," Computers and Structures, v. 3 (1973) pp. 809-826.

10. Williams, J. H., Jr., "Designing Earthquake Resistant Structures," Technology Review, v. 6, no. 1 (1973) pp. 37-43.

11. Fintel, M., and Kahn, R. R., "Shock-Absorbing Soft-Story Concept for Multistory Earthquake Structures," American Concrete Institute Journal, Title No. 66-29 (May 1969) pp. 381-390.

12. Matsushita, K., and Izumi, M., "Application of Input Controlling Mechanisms to Structural Design of a Tall Building," Proc. of the Fifth World Conference on Earthquake Engineering, Rome, Italy, 1974, vol. 2, pp. 2948-2955.

13. Kobori, T., and Minai, R., "Study on Unstationary Vibration of Building Structure with Plastic Deformation of Substructure," Proc. of the Second World Conference on Earthquake Engineering, Tokyo, Japan, 1960, vol. 2, pp. 1085-1104.

14. Crandall, S. H., Lee, S. S., and Williams, J. H., Jr., "Accumulated Slip of a Friction-Controlled Mass Excited by Earthquake Motions," J. Appl. Mech., v. 41, no. 4, Trans ASME (December 1974) pp. 1094-1098.

15. Skinner, R. I., Kelly, J. M., and Heine, A. J., "Energy Absorption Devices for Earthquake Resistant Structures," Proc. of the Fifth World Conference on Earthquake Engineering, Rome, Italy, 1974, vol. 2, pp. 2924-2933.

16. Northwood, T. D., "Isolation of Building Structures from Ground Vibrations," Isolation of Mechanical Vibration, Impact, and Noise, J. C. Snowden, ed., ASME Symposium No. AMD-Vol. 1, 1973.

17. Crocker, R. J., "Construction of the RHM Centre on Resilient Mountings," Insulation (July 1972) pp. 173-178.

18. Chopra, A. K., Clough, D. P., and Clough, R. W., "Earthquake Resistance of Buildings with a 'Soft' First Storey," Earthquake Engrng. and Struct. Dyn., v. 1, no. 4 (April 1973) pp. 347-355.

19. Hudson, D. E., "Equivalent Viscous Friction for Hysteretic Systems with Earthquake Excitation," Proc. of the Third World Conference on Earthquake Engineering, New Zealand, 1965, vol. 1.

20. Jennings, P. C., "Equivalent Viscous Damping for Yielding Structures," J. Engrng. Mech. Div., v. 94, no. EM1, Trans. ASCE (February 1968) pp. 103-116.

21. Giberson, M. F., "The Response of Nonlinear Multi-Story Structures Subjected to Earthquake Excitation," Ph.D. Thesis, California Institute of Technology, 1967.

22. Iwan, W. D., "Response of Multi-Degree-of-Freedom Yielding Systems," J. Engrng. Mech. Div., v. 94, no. EM2, Trans. ASCE (April 1968) pp. 421-437.

23. Iwan, W. D., "Steady-State Response of Yielding Shear Structure," J. Engrng. Mech. Div., v. 96, no. EM6, Trans. ASCE (December 1970) pp. 1209-1228.

24. Berg, G. V., "A Study of the Earthquake Response of Inelastic Systems," Proc. of the 34th Annual Convention of the Structural Engineers Association of California, Coronado, October 7-9, 1965, pp. 63-67.

25. Rosenblueth, E., and Herrera, I., "On a Kind of Hysteretic Damping," J. Engrng. Mech. Div., v. 90, no. EM4, Trans. ASCE (August 1964) pp. 37-48.

26. Jacobsen, L. S., "Damping in Composite Structures," Proc. of the Second World Conference on Earthquake Engineering, Tokyo and Kyoto, Japan, 1960, vol. 2, pp. 1029-1044.

27. Fung, Y. C., Fundamentals of Solid Mechanics, Englewood Cliffs, N. J.: Prentice Hall, 1965, pp. 429-433.

28. Poincaré, H., Les methodes nouvelles de la mechanique céleste, Paris: Gauthier-Villars, 1882.

29. McLachlan, N. W., Ordinary Nonlinear Differential Equations in Engineering and Physical Sciences, London: Oxford University Press, 1956, pp. 87-102.

30. Bogolinbov, N. N., and Mitropolsky, Y. A., Asymptotic Methods in the Theory of Non-Linear Oscillations, New York: Gordon Breach, 1961.

31. Iwan, W. D., "A Generalization of the Method of Equivalent Linearization," Intl. J. of Non-Linear Mech., v. 8 (1973) pp. 279-287.

32. Minorsky, N., Nonlinear Oscillations, Princeton, N. J.: D. Van Nostrand Co., Inc., 1962, pp. 351-353.

33. Patula, E. J., and Iwan, W. D., "On the Validity of Equation Difference Minimization Techniques," Intl. J. of Non-Linear Mech., v. 7, no. 1 (1972) pp. 1-17.

34. Prelewicz, D. A., "Range of Validity of the Method of Averaging," Ph. D. Thesis, California Institute of Technology, June, 1970.

35. Iwan, W. D., "The Dynamic Response of the One-Degree-of-Freedom Bilinear Hysteretic System," Proc. of the Third World Conference on Earthquake Engineering, Auckland and Wellington, New Zealand, 1965, vol. 2, pp. 783-796.

36. Masri, S. F., "Forced Vibration of the Damped Bilinear Hysteretic Oscillator," Proc. of the Seventh U.S. Natl. Congr. of Applied Mechanics, Boulder, Colorado, 1974.

37. Iwan, W. D., and Furuike, D. M., "The Transient and Steady-State Response of a Hereditary System," Intl. J. of Non-Linear Mech., v. 8 (1973) pp. 395-406.

38. Jennings, P. C., "Periodic Response of a General Yielding Structure," J. of the Engrng. Mech. Div., v. 90, no. EM2, Proc. of the American Society of Civil Engineers (April 1964) pp. 131-166.

39. Iwan, W. D., "The Steady-State Response of a Two-Degree-of-Freedom Bilinear Hysteretic System," J. Appl. Mech., v. 32, Series E, no. 1, Trans. ASME (March 1965) pp. 151-156.

40. Caughey, T. K., "Sinusoidal Excitational of a System with Bilinear Hysteresis," J. Appl. Mech., v. 27, Series E, no. 4, Trans. ASME (December 1960) pp. 640-643.

41. Jacobsen, L. S., "Steady Forced Vibration as Influenced by Damping," Transactions of the American Society of Mechanical Engineers, v. 52, Part 1 (1930) pp. APM 169-181.

42. Thomson, W. T., Vibration Theory and Applications, Englewood Cliffs, N.J.: Prentice Hall, 1965.

43. Timoshenko, S., Vibration Problems in Engineering, Princeton, N.J.: D. Van Nostrand Co., Inc., 1955.

44. Iwan, W. D., "A Model for the Dynamic Analysis of Deteriorating Structures," Proc. of the Fifth World Conference on Earthquake Engineering, Rome, Italy, 1974, vol. 2, pp. 1782-1791.

45. Paslay, P. R., and Gurtin, M. E., "The Vibration Response of a Linear Undamped System Resting on a Nonlinear Spring," J. Appl. Mech., v. 27, Trans. ASME (June 1960) pp. 272-274.

46. Dokainish, M. A., and Kumar, R., "Transverse Beam Vibrations - Nonlinear Constraint," J. Engrng. Mech. Div., v. 98, no. EM6, Trans. ASCE (December 1972) pp. 1381-1395.

47. Porter, B., and Billet, R. A., "Harmonic and Subharmonic Vibration of a Continuous System Having Nonlinear Constraint," Intl. J. of Mech. Sci., v. 7 (1965) pp. 431-439.

48. Srinivasan, A. V., "Steady State Response of Beams Supported on Nonlinear Springs," A.I.A.A. Journal, v. 4, no. 10 (October 1966) pp. 1863-1864.

49. Tauchert, T. R., and Ayre, R. S., "Shock Response of a Simple Beam on Nonlinear Supports," J. Engrng. Mech. Div., v. 91, no. EM6, ASCE (1965) pp. 91-109.

50. Lee, Samson Sui-Sun, "Accumulated Slip of a Continuous Structure Driven by Friction under Earthquake Excitation," S. B. and S. M. Thesis, Dept. of Mech. Engrng., M. I. T., May 1974.

51. Iwan, W. D., "Application of Nonlinear Analysis Techniques," in Applied Mechanics in Earthquake Engineering, W. D. Iwan, ed., ASME Symposium, AMD vol. 8, 1974, equation (16), p. 142.

52. Ibid, equations (3), (6), and (7); p. 141.

53. Furuike, Dennis M., "Dynamic Response of Hysteretic Systems with Application to a System Containing Limited Slip," Ph. D. Thesis, California Institute of Technology, Dynamics Lab Report No. DYNL-105, 1971, pp. 56-57.

54. Schwarz, R. J., and Friedland, B., Linear Systems, New York: McGraw-Hill Book Co., 1965, pp. 460-463.

55. Ibid, pp. 215-216.

56. Furuike, op. cit., pp. 72-77.

57. Ibid, pp. 59-60.

58. Iwan, W. D., "Steady-State Dynamic Response of a Limited Slip System," J. Appl. Mech., v. 35, Trans. ASME, v. 90, Series E (June 1968) pp. 322-326.

59. Abramson, H. N., "Response Curves for a System with Softening Restoring Force," J. Appl. Mech., v. 22, no. 3, Trans. ASME, v. 77 (September 1955) pp. 434-435.

60. Matsushita, K., and Izumi, M., "Studies on Mechanisms to Decrease Earthquake Forces Applied to Buildings," Proc. of the Fourth World Conference on Earthquake Engineering, Santiago, Chile, 1969, vol. 2, pp. 117-129.

61. Sozen, M. A., "Hysteresis in Structural Elements," in Applied Mechanics in Earthquake Engineering, W. D. Iwan, ed., ASME Symposium, AMD-vol. 8, 1974, pp. 63-98.

62. Townsend, William H., and Hanson, Robert D., "Hysteresis Loops for Reinforced Concrete Beam-Column Connections," Proc. of the Fifth World Conference on Earthquake Engineering, Rome, Italy, 1974, vol. 1, pp. 1131-1134.

63. Franklin, J. N., Matrix Theory, Englewood Cliffs, N. J.: Prentice-Hall, 1968, Theorem 1, p. 149.

Appendix A

Transfer Function Characteristics of Undamped Linear Chainlike Structures

The purpose of this appendix is to provide the proof of the claimed characteristics of the transfer function $\kappa_{22}(\omega)$ for undamped linear chainlike structures. As shown in the text, $\kappa_{22}(\omega)$ may be expressed as

$$\kappa_{22}(\omega) = -m_1 \frac{\prod_{i=1}^{n} (\omega^2 - \bar{\omega}_{zi}^2)}{\prod_{i=1}^{(n-1)} (\omega^2 - \omega_{pi}^2)} \tag{A1}$$

if attachment point P (see Figure 3.3) has nonzero mass. Alternately, $\kappa_{22}(\omega)$ may be expressed as

$$\kappa_{22}(\omega) = (k_1 + k_2) \frac{\prod_{i=1}^{(n-1)} (\omega^2 - \omega_{zi}^2)}{\prod_{i=1}^{(n-1)} (\omega^2 - \omega_{pi}^2)} \tag{A2}$$

if attachment point P is massless. In both cases, the set $\{\omega_{pi}^2 \mid i = 1, 2, \ldots, n-1\}$ is the set of (n-1) eigenvalues of the matrix Ω_p^2, where

$$\Omega_p^2 \equiv \begin{bmatrix} \frac{(k_2+k_3)}{m_2} & \frac{-k_3}{(m_2m_3)^{\frac{1}{2}}} & & & 0 \\ \frac{-k_3}{(m_2m_3)^{\frac{1}{2}}} & \frac{(k_3+k_4)}{m_3} & & & \\ & & & & \frac{-k_n}{(m_{n-1}m_n)^{\frac{1}{2}}} \\ 0 & & & \frac{-k_n}{(m_{n-1}m_n)^{\frac{1}{2}}} & \frac{(k_n+k_{n+1})}{m_n} \end{bmatrix} \tag{A3}$$

However, for nonzero attachment point mass, the set $\{\bar{\omega}_{zi}^2 \mid i = 1, 2, \ldots, n\}$ is the set of n eigenvalues of the matrix $\bar{\Omega}_z^2$, where

$$\bar{\Omega}_z^2 \equiv \begin{bmatrix} \frac{(k_1+k_2)}{m_1} & \frac{-k_2}{(m_1m_2)^{\frac{1}{2}}} & & & 0 \\ \frac{-k_2}{(m_1m_2)^{\frac{1}{2}}} & \frac{(k_2+k_3)}{m_2} & & & \\ & & & & \frac{-k_n}{(m_{n-1}m_n)^{\frac{1}{2}}} \\ 0 & & & \frac{-k_n}{(m_{n-1}m_n)^{\frac{1}{2}}} & \frac{(k_n+k_{n+1})}{m_n} \end{bmatrix} \tag{A4}$$

For massless attachment point, the set $\{\omega_{zi}^2 \mid i = 1, 2, \ldots, n-1\}$ is the set of (n-1) eigenvalues of the matrix Ω_z^2, where

$$\Omega_z^2 \equiv \begin{bmatrix} \frac{(k_2^*+k_3)}{m_2} & \frac{-k_3}{(m_2m_3)^{\frac{1}{2}}} & & & \mathbf{0} \\ \frac{-k_3}{(m_2m_3)^{\frac{1}{2}}} & \frac{(k_3+k_4)}{m_3} & & & \\ & & & & \frac{-k_n}{(m_{n-1}m_n)^{\frac{1}{2}}} \\ \mathbf{0} & & & \frac{-k_n}{(m_{n-1}m_n)^{\frac{1}{2}}} & \frac{(k_n+k_{n+1})}{m_n} \end{bmatrix} \tag{A5}$$

and where

$$k_2^* \equiv \frac{k_1k_2}{(k_1+k_2)} < k_2 \tag{A6}$$

In Part I, the special properties of the matrices Ω_p^2, $\overline{\Omega}_z^2$, and Ω_z^2 are used to show that

$$\overline{\omega}_{z1}^2 < \omega_{p1}^2 < \overline{\omega}_{z2}^2 < \cdots < \omega_{pn-1}^2 < \overline{\omega}_{zn}^2 \tag{A7}$$

and that

$$\omega_{z1}^2 < \omega_{p1}^2 < \omega_{z2}^2 < \cdots < \omega_{zn-1}^2 < \omega_{pn-1}^2 \tag{A8}$$

Additionally, it is shown that attachment point P cannot correspond to a node for excitation frequencies which correspond to any pole of $\kappa_{22}(\omega)$.

In Part II, the form of $\kappa_{22}(\omega)$ given in (A1) and (A2), and the inequalities (A7) and (A8) are used to show that $\kappa_{22}(\omega)$ is strictly decreasing (increasing) for all positive (negative) ω between poles.

Part I - Relations Between Poles and Zeros of $\kappa_{22}(\omega)$

Note from (A3), (A4), and (A5) that each of the matrices Ω_p^2, $\bar{\Omega}_p^2$, and Ω_z^2 is a real symmetric tridiagonal matrix whose off-diagonal band elements are nonzero. As shown in the following two theorems, these properties are sufficient to guarantee that the resulting eigenvalues are distinct and that every eigenvector has nonzero first and last components.

Theorem A1: (Distinct Eigenvalues)

Every real symmetric tridiagonal matrix with nonzero off-diagonal band elements has distinct real eigenvalues.

proof:

Let B be any real symmetric tridiagonal matrix with nonzero off-diagonal band elements. Then

$$B = \begin{bmatrix} b_{11} & b_{12} & & \\ b_{12} & b_{22} & \ddots & \\ & \ddots & \ddots & b_{n-1,n} \\ 0 & & b_{n-1,n} & b_{nn} \end{bmatrix} \quad ; \text{ where } b_{ij} \neq 0 \; \forall \, i \neq j \qquad \text{(A9)}$$

Since B is real and symmetric, it must be diagonalizable. Hence, B must have a full complement of ordinary eigenvectors. In particular, if B has an eigenvalue with multiplicity α, then corresponding to this eigenvalue there are exactly α linearly independent eigenvectors.

Let β be any eigenvalue of B, and let $\underline{x}$ be an associated eigenvector. Then

$$B\underline{x} = \beta\underline{x}$$

or, in component form

$$\left.\begin{aligned} b_{11}x_1 + b_{12}x_2 &= \beta x_1 \\ b_{12}x_1 + b_{22}x_2 + b_{23}x_3 &= \beta x_2 \\ &\vdots \\ b_{n-1,n}x_{n-1} + b_{nn}x_n &= \beta x_n \end{aligned}\right\} \qquad \text{(A10)}$$

The first (n-1) of eqs. (A10) may be solved for the x_i's to obtain

$$x_i = \frac{|E_{(i-1)}(\beta)|}{\prod_{j=1}^{(i-1)} b_{j,j+1}} x_1 \; ; \quad i = 2, 3, \ldots, n \qquad \text{(A11)}$$

where $E_j(\beta)$ is defined as the $(j \times j)$ principle submatrix of $(\beta I - B)$. That is

$$E_1(\beta) = (\beta - b_{11})$$

$$E_2(\beta) = \begin{bmatrix} (\beta - b_{11}) & -b_{12} \\ -b_{12} & (\beta - b_{22}) \end{bmatrix}$$

$$\vdots$$

etc.

Hence, from (A11) and the fact that $|E_j(\beta)|$ is a single-valued function of β, it is clear that every eigenvector $\underline{x}$ associated with the eigenvalue β admits the representation

$$\left.\begin{aligned} \underline{x} &= \mu \begin{Bmatrix} 1 \\ e_2(\beta) \\ e_3(\beta) \\ \vdots \\ e_n(\beta) \end{Bmatrix} \\ \text{where} \quad e_j(\beta) &\equiv \frac{|E_{j-1}(\beta)|}{\prod_{i=1}^{(j-1)} b_{i,i+1}} \; ; \quad j = 2, 3, \ldots, n \end{aligned}\right\} \quad (A12)$$

and μ is an arbitrary nonzero scalar constant.

Thus, every eigenvector $\underline{x}$ corresponding to β is a scalar multiple of every other eigenvector corresponding to the same β.

Therefore, there exists only one linearly independent eigenvector corresponding to each eigenvalue of B.

But since B must have n linearly independent eigenvectors, it is clear that the multiplicity of each eigenvalue must be identically one. Therefore, every eigenvalue is distinct. Every eigenvalue is also real by well-known theorems, since B is real and symmetric. Q. E. D.

Theorem A2: (Properties of eigenvectors)

If $\underline{x}$ is an eigenvector of any real symmetric $(n \times n)$ tridiagonal matrix with nonzero off-diagonal band elements, then its first component, x_1, and last component, x_n, are nonzero.

proof:

Let B be any real symmetric tridiagonal matrix with nonzero off-diagonal band elements, as given in (A9). Let β be an eigenvalue of B, and let $\underline{x}$ be any associated eigenvector. Then

$$B\underline{x} = \beta\underline{x} \tag{A13}$$

where, by definition of an eigenvector, $\underline{x} \neq \underline{0}$. Writing out (A13) in component form, one obtains (A10). As shown in Theorem A1, each eigenvector $\underline{x}$ determined from (A13) admits the representation given in (A11).

Now, assume that $x_1 \equiv 0$. From (A11) it is found that $\underline{x} \equiv \underline{0}$ then results, which contradicts the assumption that $\underline{x}$ is an eigenvector. Thus, $x_1 \neq 0$.

Clearly, a representation similar to (A11) may be developed which yields $\underline{x}$ in terms of x_n, the last component of $\underline{x}$. The above argument may then be repeated to show that $x_n \neq 0$.

Q. E. D.

Note that Theorem A2 guarantees that attachment point P cannot correspond to a node for any excitation frequency which coincides with any pole ω_{pi} of $\kappa_{22}(\omega)$. Thus, $\kappa_{22}(\omega)$ has an isolated singularity at each of the (n-1) poles $\{\omega_{pi}^2 | i = 1, 2, \ldots, n-1\}$.

Relations Between Poles and Zeros for Systems with Massless Attachment Point

Equation (A8) is established by the following two theorems, which make use of the well-known Courant-Fischer mini-max theorem, and a fundamental theorem of algebraic equations, respectively.

Theorem (A3): (Frequency Inequality)

If $\{\omega_{pi}^2 | i = 1, 2, \ldots, n-1\}$ is the set of eigenvalues of the matrix Ω_p^2 given in (A3), and if $\{\omega_{zi}^2 | i = 1, 2, \ldots, n-1\}$ is the set of eigenvalues of the matrix Ω_z^2 given in (A5), then

$$\omega_{z1}^2 \leq \omega_{p1}^2 \leq \omega_{z2}^2 \leq \omega_{p2}^2 \leq \cdots \leq \omega_{zn-1}^2 \leq \omega_{pn-1}^2 \qquad \text{(A14)}$$

proof:

Note from (A3) and (A5) that

$$\Omega_p^2 = \Omega_z^2 + \Delta \qquad \text{(A15)}$$

where

$$\Delta \equiv \left(\frac{k_2}{m_2}\right)\left(\frac{k_2}{k_1+k_2}\right)\begin{bmatrix} 1 & 0 & & 0 \\ 0 & 0 & & \\ \vdots & & & \vdots \\ 0 & \cdots & & 0 \end{bmatrix} \tag{A16}$$

Note also that since k_1, k_2, and m_2 are each non-negative, Δ is positive semidefinite.

Applying the Courant-Fischer mini-max theorem to Ω_p^2, one finds

$$\omega_{pi}^2 = \max_{\substack{(\underline{y}^k, \underline{y}^k) = 1 \\ k = 1,\ldots,i}} \min_{\substack{(\underline{x}, \underline{y}^k) = 0 \\ k = 1,\ldots,i-1}} \left[\frac{(\underline{x}, \Omega_p^2 \underline{x})}{(\underline{x}, \underline{x})}\right] \tag{A17}$$

Using (A15) in (A17), one obtains

$$\omega_{pi}^2 = \max_{\substack{(\underline{y}^k, \underline{y}^k) = 1 \\ k = 1,\ldots,i}} \min_{\substack{(\underline{x}, \underline{y}^k) = 0 \\ k = 1,\ldots,i-1}} \left[\frac{(\underline{x}, \Omega_z^2 \underline{x})}{(\underline{x}, \underline{x})} + \frac{(\underline{x}, \Delta \underline{x})}{(\underline{x}, \underline{x})}\right] \tag{A18}$$

But since Δ is positive semidefinite

$$\frac{(\underline{x}, \Delta \underline{x})}{(\underline{x}, \underline{x})} \geq 0 \quad \forall \underline{x} \tag{A19}$$

Hence, (A18) and (A19) require that

$$\min_{\substack{(\underline{x}, \underline{y}^k) = 0 \\ k = 1,\ldots, i-1}} \left[\frac{(\underline{x}, \Omega_z^2 \underline{x})}{(\underline{x}, \underline{x})} + \frac{(\underline{x}, \Delta \underline{x})}{(\underline{x}, \underline{x})} \right] \geq \min_{\substack{(\underline{x}, \underline{y}^k) \\ k = 1,\ldots, i-1}} \left[\frac{(\underline{x}, \Omega_z^2 \underline{x})}{(\underline{x}, \underline{x})} \right] \quad \text{(A20)}$$

Thus, (A18) and (A20) require that

$$\omega_{pi}^2 \geq \max_{\substack{(\underline{y}^k, \underline{y}^k) = 1 \\ k = 1, 2, \ldots, i}} \min_{\substack{(\underline{x}, \underline{y}^k) = 0 \\ k = 1,\ldots, i-1}} \left[\frac{(\underline{x}, \Omega_z^2 \underline{x})}{(\underline{x}, \underline{x})} \right] = \omega_{z\,i}^2$$

or

$$\omega_{pi}^2 \geq \omega_{zi}^2 \quad \forall\ i = 1, 2, \ldots, (n-1) \qquad \text{Q. E. D.}$$

Theorem (A4): (Distinct poles and zeros)

If ω_p^2 is any eigenvalue of the matrix Ω_p^2 given in (A3), and if ω_z^2 is any eigenvalue of the matrix Ω_z^2 given in (A5), then

$$\omega_z^2 \neq \omega_p^2 \quad \text{(A21)}$$

proof:

Let $\underline{\varphi}_p$ be the eigenvector of Ω_p^2 corresponding to ω_p^2, and let $\underline{\varphi}_z$ be the eigenvector of Ω_z^2 corresponding to ω_z^2. Then

$$\left.\begin{aligned} \Omega_p^2 \underline{\varphi}_p &= \omega_p^2 \underline{\varphi}_p \\ \Omega_z^2 \underline{\varphi}_z &= \omega_z^2 \underline{\varphi}_z \end{aligned}\right\} \text{(A22)}$$

Let $\underline{\varphi}$ be any (n-1) vector. Then

$$\Omega_p^2 \underline{\varphi} - \Omega_z^2 \underline{\varphi} = \left(\frac{k_2}{m_2}\right) \frac{k_2}{(k_1+k_2)} \varphi_1 \begin{Bmatrix} 1 \\ 0 \\ \vdots \\ 0 \end{Bmatrix} \tag{A23}$$

Let

$$\underline{\delta} \equiv \underline{\varphi}_p - \underline{\varphi}_z \tag{A24}$$

then

$$\Omega_p^2 \underline{\varphi}_p = \Omega_p^2 (\underline{\varphi}_z + \underline{\delta})$$

$$= \Omega_p^2 \underline{\varphi}_z + \Omega_p^2 \underline{\delta}$$

$$= \Omega_z^2 \underline{\varphi}_z + \left(\frac{k_2}{m_2}\right) \frac{k_2}{(k_1+k_2)} \varphi_{z1} \begin{Bmatrix} 1 \\ 0 \\ \vdots \\ 0 \end{Bmatrix} + \Omega_p^2 \underline{\delta}$$

or, using (A22),

$$\omega_p^2 \underline{\varphi}_p = \omega_z^2 \underline{\varphi}_z + \left(\frac{k_2}{m_2}\right) \frac{k_2}{(k_1+k_2)} \varphi_{z1} \begin{Bmatrix} 1 \\ 0 \\ \vdots \\ 0 \end{Bmatrix} + \Omega_p^2 \underline{\delta} \tag{A25}$$

Now, <u>assume</u> that

$$\omega_p^2 = \omega_z^2 = \omega^2 \tag{A26}$$

then (A25) and (A26) imply that

$$\omega^2 \underline{\delta} = \left(\frac{k_2}{m_2}\right) \frac{k_2}{(k_1+k_2)} \varphi_{z1} \begin{Bmatrix} 1 \\ 0 \\ \vdots \\ 0 \end{Bmatrix} + \Omega_p^2 \underline{\delta}$$

or

$$\left[\omega^2 I - \Omega_p^2\right] \underline{\delta} = \left(\frac{k_2}{m_2}\right) \frac{k_2}{(k_1+k_2)} \varphi_{z1} \begin{Bmatrix} 1 \\ 0 \\ \vdots \\ 0 \end{Bmatrix} \qquad \text{(A27)}$$

Note that the vector on the right hand side of (A27) is non-trivial, since φ_{z1} is nonzero by Theorem A2. Note also that, by hypothesis, ω^2 is an eigenvalue of the matrix Ω_p^2 on the left hand side of (A27). Thus, the coefficient matrix is singular, and hence there does not exist a unique vector $\underline{\delta}$ which satisfies (A27). Furthermore, it can be shown that the vector on the right hand side of (A27) is linearly independent of the (n-1) column vectors of the coefficient matrix. Hence, by a fundamental theorem of algebraic equations, there is no vector $\underline{\delta}$ which satisfies (A27). This result is clearly a contradiction of (A24) which defines $\underline{\delta}$ uniquely in terms of the eigenvectors $\underline{\varphi}_p$ and $\underline{\varphi}_z$.

Thus,

$$\omega_z^2 \neq \omega_p^2 \qquad \text{Q. E. D.}$$

Hence, (A14) and (A21) together yield (A8), and the desired relation between poles and zeros of $\kappa_{22}(\omega)$ has been established for the case in which the attachment point is massless.

Relations Between Poles and Zeros for Systems with Nonzero Attachment Point Mass

The following two theorems establish equation (A7) by using an eigenvalue "inclusion principle" which is derived from the Courant-Fischer mini-max theorem, and by using a fundamental theorem of algebraic equations.

Theorem (A5): (Frequency Inequality)

If $\{\omega_{pi}^2 \mid i = 1, 2, \ldots, n-1\}$ is the set of (n-1) eigenvalues of Ω^2_p given in (A3), and if $\{\bar{\omega}_{zi}^2 \mid i = 1, 2, \ldots, n\}$ is the set of n eigenvalues of $\bar{\Omega}_z^2$ given in (A4), then

$$\bar{\omega}_{z1}^2 \leq \omega_{p1}^2 \leq \bar{\omega}_{z2}^2 \leq \cdots \leq \omega_{pn-1}^2 \leq \bar{\omega}_{zn}^2 \tag{A28}$$

proof:

The proof proceeds by direct application of the "inclusion principle," [63] where it is noted that Ω_p^2 is the $(n-1)\times(n-1)$ matrix which remains after deleting the first row and first column of the $n\times n$ matrix $\bar{\Omega}_z^2$. Equation (A28) results directly from application of the referenced theorem. Q. E. D.

Theorem (A6): (Distinct Poles and Zeros)

If ω_p^2 is any eigenvalue of the matrix Ω_p^2 given in (A3), and if $\bar{\omega}_z^2$ is any eigenvalue of the matrix $\bar{\Omega}_z^2$ given in (A4), then

$$\omega_p^2 \neq \bar{\omega}_z^2 \tag{A29}$$

proof:

Let $\underline{\varphi}_p$ be the eigenvector of Ω_p^2 corresponding to ω_p^2, and let $\underline{\varphi}_z$ be the eigenvector of $\bar{\Omega}_z^2$ corresponding to ω_z^2. Then

$$\left.\begin{aligned} \Omega_p^2 \underline{\varphi}_p &= \omega_p^2 \underline{\varphi}_p \\ \bar{\Omega}_z^2 \underline{\varphi}_z &= \bar{\omega}_z^2 \underline{\varphi}_z \end{aligned}\right\} \quad \text{(A30)}$$

Let $\bar{\Omega}_p^2$ be the $n \times n$ matrix formed from Ω_p^2 as follows

$$\bar{\Omega}_p^2 \equiv \left[\begin{array}{c|ccc} 0 & 0 & \cdots & 0 \\ \hline 0 & & & \\ \vdots & & \Omega_p^2 & \\ 0 & & & \end{array}\right] \quad \text{(A31)}$$

and let $\bar{\underline{\varphi}}_p$ be the n vector formed from $\underline{\varphi}_p$ as follows

$$\bar{\underline{\varphi}}_p \equiv \left\{\begin{array}{c} 0 \\ \hline \\ \underline{\varphi}_p \end{array}\right\} \quad \text{(A32)}$$

Let $\underline{\varphi}$ be any n vector. Then, using (A31), (A3), and (A4),

$$\bar{\Omega}_z^2 \underline{\varphi} = \bar{\Omega}_p^2 \underline{\varphi} + \Theta \underline{\varphi}$$

where

$$\Theta \equiv \left[\begin{array}{c|cc} \dfrac{(k_1+k_2)}{m_1} & \dfrac{-k_2}{(m_1m_2)^{\frac{1}{2}}} & 0 \quad 0 \\ \hline \dfrac{-k_2}{(m_1m_2)^{\frac{1}{2}}} & & \\ 0 & \multicolumn{2}{c}{\mathbf{0}} \\ \vdots & & \\ 0 & & \end{array}\right] \tag{A33}$$

Let

$$\underline{\bar{\delta}} \equiv \underline{\bar{\varphi}}_z - \underline{\bar{\varphi}}_p \tag{A34}$$

Then,

$$\begin{aligned} \bar{\Omega}_z^2 \underline{\bar{\varphi}}_z &= \bar{\Omega}_z^2 (\underline{\bar{\varphi}}_p + \underline{\bar{\delta}}) \\ &= \bar{\Omega}_z^2 \underline{\bar{\varphi}}_p + \bar{\Omega}_z^2 \underline{\bar{\delta}} \\ &= \bar{\Omega}_p^2 \underline{\bar{\varphi}}_p + \Theta \underline{\bar{\varphi}}_p + \bar{\Omega}_z^2 \underline{\bar{\delta}} \end{aligned} \tag{A35}$$

But (A30), (A31), and (A32) require that

$$\bar{\Omega}_p^2 \underline{\bar{\varphi}}_p = \omega_p^2 \underline{\bar{\varphi}}_p \tag{A36}$$

and (A32), (A33) require that

$$\Theta \underline{\bar{\varphi}}_p = - \frac{k_2}{(m_1m_2)^{\frac{1}{2}}} \varphi_{p1} \begin{Bmatrix} 1 \\ 0 \\ \vdots \\ 0 \end{Bmatrix} \tag{A37}$$

Thus, (A30), (A35), (A36), and (A37) require that

$$\bar{\omega}_z^2 \underline{\bar{\varphi}}_z = \omega_p^2 \underline{\bar{\varphi}}_p - \frac{k_2}{(m_1 m_2)^{\frac{1}{2}}} \varphi_{p1} \begin{Bmatrix} 1 \\ 0 \\ \vdots \\ 0 \end{Bmatrix} + \bar{\Omega}_z^2 \underline{\bar{\delta}} \tag{A38}$$

Now, assume that

$$\bar{\omega}_z^2 = \omega_p^2 = \omega^2 \tag{A39}$$

Then, (A38), (A39), and (A34) imply that

$$\left[\omega^2 I - \bar{\Omega}_z^2\right] \underline{\bar{\delta}} = - \frac{k_2}{(m_1 m_2)^{\frac{1}{2}}} \varphi_{p1} \begin{Bmatrix} 1 \\ 0 \\ \vdots \\ 0 \end{Bmatrix} \tag{A40}$$

Note that the vector on the right hand side of (A40) is nontrivial, since φ_{p1} is nonzero by Theorem A2. Note also that, by hypothesis, ω^2 is an eigenvalue of $\bar{\Omega}_z^2$, so that the coefficient matrix on the left hand side of (A40) is singular. Thus, there does not exist a unique vector $\underline{\bar{\delta}}$ such that (A40) holds. Furthermore, it can be shown that the vector on the right hand side of (A40) is linearly independent of the (n-1) column vectors of the coefficient matrix. Hence, by a fundamental theorem of algebraic equations, there is no vector $\underline{\bar{\delta}}$ which satisfies (A40) under the assumption (A39). This result is clearly a contradiction of (A34) which defines $\underline{\bar{\delta}}$ uniquely in terms of the eigenvectors $\underline{\varphi}_p$ and $\underline{\bar{\varphi}}_z$. Therefore, it must be concluded that assumption (A39) cannot be valid. Thus

$$\bar{\omega}_z^2 \neq \omega_p^2 \qquad \text{Q. E. D.}$$

Equations (A28) and (A29) taken together yield (A7), the desired relation between poles and zeros of $\kappa_{22}(\omega)$ for the case in which the attachment point has nonzero mass.

Part II - Resulting Properties of $\kappa_{22}(\omega)$

For systems with massless attachment point, the following theorem uses (A2) and (A8) to show that $\kappa_{22}(\omega)$ is strictly decreasing for positive ω.

Theorem (A7)

If $\kappa_{22}(\omega)$ is the transfer function of an undamped linear chain-like structure with massless attachment point, then:

(a) For all positive (negative) ω, $\kappa_{22}(\omega)$ is a strictly decreasing (increasing) function.

(b) $\kappa_{22}(\omega)$ ranges from $\kappa_{22}(0) \geq 0$ to $-\infty$ for $\omega \in [0, \omega_{p1})$

(c) $\kappa_{22}(\omega)$ ranges from $+\infty$ to $-\infty$ for $\omega \in (\omega_{pi-1}, \omega_{pi})$; $i = 2, 3, \ldots, n-1$

(d) $\kappa_{22}(\omega)$ ranges from $+\infty$ to (k_1+k_2) for $\omega \in (\omega_{pn-1}, \infty)$

proof:

Regarding (a): Differentiating (A2) with respect to ω, one finds

$$\frac{d\kappa_{22}(\omega)}{d\omega} = \begin{cases} \dfrac{-2\omega_{zj}}{(\omega_{pj}^2 - \omega_{zj}^2)} \prod_{\substack{i=1 \\ i\neq j}}^{(n-1)} \dfrac{(\omega_{zj}^2 - \omega_{zi}^2)}{(\omega_{zj}^2 - \omega_{pi}^2)}; & \omega = \omega_{zj},\ j = 1,2,\ldots,n-1 \\ 2\omega\kappa_{22}(\omega)\left[\sum_{i=1}^{(n-1)} \dfrac{1}{(\omega^2 - \omega_{zi}^2)} - \sum_{i=1}^{(n-1)} \dfrac{1}{(\omega^2 - \omega_{pi}^2)}\right]; & \omega \neq \omega_{zj},\ j = 1,2,\ldots,n-1 \end{cases} \tag{A41}$$

Equation (A8) together with (A41) require that

$$\left.\frac{d\kappa_{22}(\omega)}{d\omega}\right|_{\omega_{zj}} < 0; \quad \forall\ \omega_{zj} > 0, \quad j = 1, 2, \ldots, n-1 \tag{A42}$$

Note that for all positive $\omega \neq \omega_{zj}$, $j = 1, 2, \ldots, n-1$, and $\omega \neq \omega_{pj}$, $j = 1, 2, \ldots, n-1$, equation (A41) implies that $d\kappa_{22}(\omega)/d\omega = 0$ if and only if:

$$\sum_{i=1}^{(n-1)} \frac{1}{(\omega^2 - \omega_{zi}^2)} = \sum_{i=1}^{(n-1)} \frac{1}{(\omega^2 - \omega_{pi}^2)} \tag{A43}$$

for some ω.

It will now be shown that (A8) is sufficient to guarantee that (A43) cannot hold for any ω.

Let

$$\left.\begin{aligned} x_{zj}(\omega) &\equiv \frac{1}{(\omega^2 - \omega_{zj}^2)}; \quad j = 1, 2, \ldots, n-1 \\ x_{pj}(\omega) &\equiv \frac{1}{(\omega^2 - \omega_{pj}^2)}; \quad j = 1, 2, \ldots, n-1 \end{aligned}\right\} \tag{A44}$$

Using (A44), the condition (A43) now becomes

$$\sum_{i=1}^{n-1} x_{zi}(\omega) = \sum_{i=1}^{n-1} x_{pi}(\omega) \tag{A45}$$

Consider the following exhaustive cases:

1. $\omega^2 \in [0, \omega_{z1}^2)$; or $\omega^2 \in (\omega_{pn-1}^2, \infty)$. Then (A8), (A44) imply

$$0 > x_{pn-1}(\omega) > x_{zn-1}(\omega) > \cdots > x_{p1}(\omega) > x_{z1}(\omega);$$

$$0 < x_{z1}(\omega) < x_{p1}(\omega) < \cdots < x_{zn-1}(\omega) < x_{pn-1}(\omega)$$

Thus,

$$\sum_{i=1}^{n-1} x_{zj}(\omega) < \sum_{j=1}^{n-1} x_{pj}(\omega) \text{ for all such } \omega.$$

2. $\omega^2 \in (\omega_{zj}^2, \omega_{pj}^2)$, $j = 1, \ldots, n-1$; or $\omega^2 \in (\omega_{pj}^2, \omega_{zj+1}^2)$, $j = 1, \ldots, n-2$. Then (A8), (A44) imply

$$x_{zj}(\omega) > x_{pj-1}(\omega) > x_{zj-1}(\omega) > \cdots > x_{p1}(\omega) > x_{z1}(\omega) > 0 > x_{pn-1}(\omega)$$

$$> x_{zn-1}(\omega) > \cdots > x_{zj+1}(\omega) > x_{pj}(\omega);$$

$$x_{pj}(\omega) > x_{zj}(\omega) > x_{pj-1}(\omega) > \cdots > x_{p1}(\omega) > x_{z1}(\omega) > 0 > x_{pn-1}(\omega)$$

$$> x_{zn-1}(\omega) > \cdots > x_{pj+1}(\omega) > x_{zj+1}(\omega)$$

Thus,

$$\sum_{j=1}^{n-1} x_{zj}(\omega) > \sum_{j=1}^{n-1} x_{pj}(\omega); \text{ or } \sum_{j=1}^{n-1} x_{pj}(\omega) > \sum_{j=1}^{n-1} x_{zj}(\omega)$$

for all such ω.

Therefore, since (A43) cannot hold for any such ω, it is concluded that $d\varkappa_{22}(\omega)/d\omega$ cannot change sign in those frequency regions separated by the poles $\{\omega_{pi} | i = 1, 2, \ldots, n-1\}$. However, since $\left.\frac{d\varkappa_{22}}{d\omega}\right|_{\omega_{zj}} < 0$ for all positive ω_{zj}, and from (A8), it is concluded that

$$\frac{d\varkappa_{22}}{d\omega} < 0, \quad \forall\ \omega > 0 \quad \text{and} \quad \omega \in \{\omega_{pi} | i = 1, 2, \ldots, n-1\}$$

Therefore, $\varkappa_{22}(\omega)$ is a strictly decreasing function for all positive ω. Furthermore, since $\varkappa_{22}(\omega)$ is an even function, $d\varkappa_{22}/d\omega > 0$ $\forall\ \omega < 0$ and $\omega \notin \{-\omega_{pi} | i = 1, 2, \ldots, n-1\}$.

Regarding (b): From (A2),

$$\lim_{\omega \to 0} \varkappa_{22}(\omega) = (k_1 + k_2) \prod_{i=1}^{(n-1)} \left(\frac{\omega_{zi}}{\omega_{pi}}\right)^2 \geq 0$$

and $\varkappa_{22}(\omega) \to -\infty$ as $\omega \to \omega_{pi}^-$. Since $\varkappa_{22}(\omega)$ is continuous and strictly decreasing for $\omega \in [0, \omega_{p1})$, the statement is proved.

Regarding (c): From (A2) and (A8), $\varkappa_{22}(\omega) \to +\infty$ as $\omega \to \omega_{pi}^+$, $i = 1, 2, \ldots, n-1$, and $\varkappa_{22}(\omega) \to -\infty$ as $\omega \to \omega_{pi}^-$, $i = 1, 2, \ldots, n-1$. Since $\varkappa_{22}(\omega)$ is continuous and strictly decreasing for $\omega \in (\omega_{pi-1}, \omega_{pi})$, $i = 2, 3, \ldots, n-1$, the statement is proved.

Regarding (d): From (A2) and (A8), $\kappa_{22}(\omega) \rightarrow +\infty$ as $\omega \rightarrow \omega^{+}_{pn-1}$. Furthermore, $\kappa_{22}(\omega) \rightarrow (k_1+k_2)$ as $\omega \rightarrow \infty$. Since $\kappa_{22}(\omega)$ is continuous and strictly decreasing for $\omega \in (\omega_{pn-1}, \infty)$, the statement is proved.

Q. E. D.

The following theorem uses (A1) and (A7) to prove similar results for systems with non-zero attachment point mass.

Theorem (A8)

If $\kappa_{22}(\omega)$ is the transfer function of an undamped linear chain-like structure with nonzero attachment point mass, then:

(a) For all positive (negative) ω, $\kappa_{22}(\omega)$ is a strictly decreasing (increasing) function

(b) $\kappa_{22}(\omega)$ ranges from $\kappa_{22}(0) \geq 0$ to $-\infty$ for $\omega \in [0, \omega_{p1})$

(c) $\kappa_{22}(\omega)$ ranges from $+\infty$ to $-\infty$ for $\omega \in (\omega_{pi-1}, \omega_{pi})$; $i = 2, \ldots, n-1$

(d) $\kappa_{22}(\omega)$ ranges from $+\infty$ to $-\infty$ for $\omega \in (\omega_{pn-1}, \infty)$

proof:

Regarding (a): Differentiating (A1) with respect to ω, one finds

$$\frac{d\kappa_{22}(\omega)}{d\omega} = \begin{cases} -m_1 2\bar{\omega}_{zj} \dfrac{\prod\limits_{\substack{i=1 \\ i\neq j}}^{n} (\bar{\omega}_{zj}^2 - \bar{\omega}_{zi}^2)}{\prod\limits_{i=1}^{n-1} (\bar{\omega}_{zj}^2 - \omega_{pi}^2)} ; & \omega = \bar{\omega}_{zj},\ j = 1,2,\ldots,n \\ 2\omega\kappa_{22}(\omega)\left[\sum\limits_{i=1}^{n} \dfrac{1}{(\omega^2 - \bar{\omega}_{zi}^2)} - \sum\limits_{i=1}^{n-1} \dfrac{1}{(\omega^2 - \omega_{pi}^2)}\right] ; & \omega \neq \bar{\omega}_{zj},\ j = 1,2,\ldots,n \end{cases} \tag{A46}$$

Equation (A7) together with (A46) requires that

$$\left.\frac{d\kappa_{22}(\omega)}{d\omega}\right|_{\omega_{zj}} < 0 \ ; \ \forall\ \omega_{zj} > 0,\ j = 1, 2, \ldots, n \tag{A47}$$

Note that for all positive $\omega \neq \bar{\omega}_{zj}$, $j = 1, 2, \ldots, n$, and $\omega \neq \omega_{pj}$, $j = 1, 2, \ldots, n-1$, equation (A46) implies that $d\kappa_{22}(\omega)/d\omega = 0$ if and only if

$$\sum_{i=1}^{n} \frac{1}{(\omega^2 - \bar{\omega}_{zi}^2)} = \sum_{i=1}^{n-1} \frac{1}{(\omega^2 - \omega_{pi}^2)} \tag{A48}$$

for some ω.

It will now be shown that (A7) is sufficient to guarantee that (A48) cannot hold for any ω. Let

$$\left.\begin{aligned} \bar{x}_{zj}(\omega) &\equiv \frac{1}{(\omega^2 - \bar{\omega}_{zj}^2)}; \quad j = 1, 2, \ldots, n \\ x_{pj}(\omega) &\equiv \frac{1}{(\omega^2 - \omega_{pj}^2)}; \quad j = 1, 2, \ldots, n-1 \end{aligned}\right\} \tag{A49}$$

Using (A49), the condition (A48) now becomes

$$\sum_{i=1}^{n} \bar{x}_{zi}(\omega) = \sum_{i=1}^{n} x_{pi}(\omega) \tag{A50}$$

Consider the following exhaustive cases:

1. $\omega^2 \in [0, \omega^2_{E1})$; or $\omega^2 \in (\omega_{pn-1}, \infty)$. Then (A7), (A49) imply

$$0 > \bar{x}_{zn}(\omega) > x_{pn-1}(\omega) > \cdots > x_{p1}(\omega) > \bar{x}_{z1}(\omega) ;$$

$$0 < \bar{x}_{z1}(\omega) < x_{p1}(\omega) < \cdots < x_{pn-1}(\omega) < \bar{x}_{zn}(\omega)$$

Thus,

$$\sum_{i=1}^{n-1} x_{pi}(\omega) > \sum_{i=1}^{n} \bar{x}_{zi}(\omega); \text{ or } \sum_{i=1}^{n-1} x_{pi}(\omega) < \sum_{i=1}^{n} \bar{x}_{zi}(\omega) \text{ for all such } \omega.$$

2. $\omega^2 \in (\bar{\omega}^2_{zj}, \omega^2_{pj})$, $j = 1, \ldots, n-1$; or $\omega^2 \in (\omega^2_{pj}, \bar{\omega}^2_{zj+1})$, $j = 1, \ldots, n-1$.
Then (A7), (A49) imply:

$$\bar{x}_{zj}(\omega) > x_{pj-1}(\omega) > \bar{x}_{zj-1}(\omega) > \cdots > x_{p1}(\omega) > \bar{x}_{z1}(\omega) > 0 > \bar{x}_{zn}(\omega)$$

$$> x_{pn-1}(\omega) > \cdots > \bar{x}_{zj+1}(\omega) > x_{pj}(\omega);$$

$$x_{pj}(\omega) > \bar{x}_{zj}(\omega) > x_{pj-1}(\omega) > \cdots > x_{p1}(\omega) > \bar{x}_{z1}(\omega) > 0 > \bar{x}_{zn}(\omega)$$

$$> x_{pn-1}(\omega) > \cdots > x_{pj+1}(\omega) > \bar{x}_{zj+1}(\omega)$$

Thus,

$$\sum_{j=1}^{n} \bar{x}_{zj}(\omega) > \sum_{j=1}^{n-1} x_{pj}(\omega); \text{ or } \sum_{j=1}^{n-1} x_{pj}(\omega) > \sum_{j=1}^{n} \bar{x}_{zj}(\omega)$$

for all such ω.

Therefore, since (A48) cannot hold for any such ω, it is concluded that $d\kappa_{22}(\omega)/d\omega$ cannot change sign in those frequency regions separated by the poles $\{\omega_{pi} | i = 1, \ldots, n-1\}$. However, since $\left.\frac{d\kappa_{22}}{d\omega}\right|_{\omega_{zj}} < 0$ for all positive $\bar{\omega}_{zj}$, and from (A7), it is concluded that

$$\frac{d\kappa_{22}(\omega)}{d\omega} < 0, \quad \forall \text{ positive } \omega \notin \{\omega_{pi} | i = 1, \ldots, n-1\}$$

Therefore, $\kappa_{22}(\omega)$ is a strictly decreasing function for all positive ω. Furthermore, since $\kappa_{22}(\omega)$ is an even function, $d\kappa_{22}(\omega)/d\omega > 0$ for all negative $\omega \notin \{-\omega_{pi} | i = 1, 2, \ldots, n-1\}$.

Regarding (b): From (A1),

$$\lim_{\omega \to 0} \kappa_{22}(\omega) = m_1 \frac{\prod_{i=1}^{n} \bar{\omega}_{zi}^2}{\prod_{i=1}^{n-1} \omega_{pi}^2} \geq 0$$

and $\kappa_{22}(\omega) \to -\infty$ as $\omega \to \omega_{pi}^-$. Since $\kappa_{22}(\omega)$ is continuous and strictly decreasing for $\omega \in [0, \omega_{p1})$, the statement is proved.

Regarding (c): From (A1) and (A7), $\kappa_{22}(\omega) \to +\infty$ as $\omega \to \omega_{pi}^+$, $i = 1, 2, \ldots, n-1$, and $\kappa_{22}(\omega) \to -\infty$ as $\omega \to \omega_{pi}^-$, $i = 1, 2, \ldots, n-1$. Since $\kappa_{22}(\omega)$ is continuous and strictly decreasing for $\omega \in (\omega_{pi-1}, \omega_{pi})$, $i = 2, 3, \ldots, n-1$, the statement is proved.

Regarding (d): From (A1) and (A7), $\varkappa_{22}(\omega) \to +\infty$ as $\omega \to \omega^{+}_{pn-1}$ and $\varkappa_{22}(\omega) \sim -m_1\omega^2$ as $\omega \to +\infty$. Therefore, $\varkappa_{22}(\omega) \to -\infty$ as $\omega \to +\infty$. Since $\varkappa_{22}(\omega)$ is continuous and strictly decreasing for $\omega \in (\omega_{pn-1}, \infty)$, the statement is proved. Q. E. D.